AR-001-672

DEPARTMENT OF DEFENCE

DEFENCE SCIENCE AND TECHNOLOGY ORGANISATION

ADVANCED ENGINEERING LABORATORY

TECHNICAL REPORT

AEL-0039-TR

FEASIBILITY STUDY ON A LOW POWER VERTICAL AXIS WIND-POWERED GENERATOR

W.R. Crook, T. Puust, M.L. Robinson
and L.J. Vencel

S U M M A R Y

This paper describes investigations carried out to establish a design concept for a 1 kW wind-powered generator suitable for use as an alternative power source in isolated locations. Design criteria include high power to weight ratio, simplicity of assembly and potential for fixed, mobile or portable applications. The report proposes a suitable configuration using a Darrieus straight blade rotor with a microprocessor based control system and provides information on the power output to be expected in different wind environments.

TABLE OF CONTENTS

LIST OF TABLES

LIST OF FIGURES

AEL-0039-TR

LIST OF APPENDICES

1. INTRODUCTION

This paper covers feasibility studies carried out in the twelve month period to September 1978 of a low power wind-powered generator system suitable for use in isolated locations.

For the purpose of the study a design concept has been formulated for an experimental system capable of producing a nominal 1 kW of electrical power in average (7.5 m/s) wind conditions (see Section 3). The design is based on using a Darrieus straight blade rotor of fixed blade pitch with a small Savonius rotor for starting, and the system has been developed to permit operation at variable speed or constant speed using a load matching control system based on a microprocessor.

Sections 4 to 9 cover the investigations into the aerodynamic performance of the Darrieus rotor, structural design of the turbine and tower, mechanical design of the turbine main shaft arrangement, electrical system, energy production and capital cost considerations.

This design concept is in line with low power wind-powered generator development activity recommended by the National Energy Advisory Committee(ref.1).   In general terms the system formulated offers promise as an alternative power source for isolated areas and a means of conserving oil fuels.

2. REQUIREMENT

This feasibility study has been initiated under task DST/212 in response to interest expressed by Army in power sources of low acoustic and IR signature and the need for small quantities of silently generated power(ref.2).

3. WIND-POWERED GENERATOR DESIGN CONCEPT

3.1 Design objectives

In investigating the design of wind-powered generators in general and the 1 kW machine in particular, it was necessary to lay down certain general design guidelines.   The design aims chosen and listed in Table 1 are based on the ABCA Paper entitled "Concept Paper, Electrical Power Sources for 1986 and beyond" contained in reference 2.

TABLE 1. DESIGN GUIDELINES

(a) Capable of operation as a self contained unit in isolated areas.
(b) Capable of operation as an unattended unit.
(c) High efficiency.
(d) High reliability.
(e) Simple to maintain.
(f) Rugged and weatherproof.

TABLE 1(CONTD.).

> (g) Low noise and IR signature.
>
> (h) Lightweight, easy to erect and dismantle.
>
> (i) Potential for fixed, mobile or portable applications.
>
> (j) Low cost.

It was also necessary to stipulate wind conditions for optimal design, in particular, a mean wind speed for rotor design (see Section 4), a maximum wind speed for operation (see Appendix II) and a wind speed limit for equipment survival when in the parked mode.   The various figures are shown in Table 2. The limit for survival chosen for the experimental wind-powered generator design is taken from data for southern Australia for a 50-year return period (ref.3).   This limit also applies to the whole of Australia, but for a reduced, 25-year, return period (see Appendix III).

TABLE 2.   DESIGN WIND CONDITIONS

Description	Wind speed (m/s)
Mean wind speed for rotor design optimisation	7.5
Maximum wind speed for operation	13.5
Wind speed limit for survival with rotor in the parked condition	42

3.2 Design considerations

3.2.1 Main power element selection

The Darrieus vertical axis straight blade rotor* was selected as the main power element for the system because of its promise of high performance combined with simplicity and low cost.   A minimum number of two blades was chosen because, provided that the total blade area is optimised, the power output of a Darrieus rotor is largely independent of the number of blades. The Darrieus rotor was invented by G.J.M. Darrieus, a Frenchman, in 1925 and patented in 1931.   In the 1960's the idea was developed by Messrs South, Rangi and Templin of the National Aeronautical Establishment and the National Research Council of Canada.   More recently, Shankar(ref.4) and Warne and Calnan(ref.5) have drawn attention to the potential of the fixed pitch, fixed chord, straight blade vertical axis rotor configuration.

---

* The term 'rotor' refers to the power producing elements.   For the Darrieus rotor these are the two vertical blades and for the Savonius rotor, the semi circular cylindrical panels.

3.2.2 Characteristics of Darrieus machine

The Darrieus vertical axis wind turbine* is a high speed machine with a
high energy conversion efficiency comparable with the most efficient
horizontal axis propeller-type turbines. The machine is insensitive to
wind direction and thus no yaw mechanism is required. The configuration
is inherently simple, either a fixed pitch curved blade in the form of a
troposkien** or a vertical straight blade arrangement with either fixed
pitch blades, as adopted, or adjustable pitch blades. Troposkien and
straight blade rotor concepts are shown in figure 1.

3.2.3 Blade configuration

In the straight blade configuration, the concept starts off with an inherent
aerodynamic advantage over the troposkien configuration as both blade
efficiency and configuration efficiency are higher. The straight blade
configuration is also attractive as it simplifies packing, transport, assembly
and has potential for portable applications. The straight blade is economic
to fabricate as an extrusion. The troposkien blade shape, whilst difficult
to manufacture, has the advantage that bending stresses arising from
centrifugal forces are negligible and tie rods and braces may not be required.

3.2.4 Auxiliary starting

Since a Darrieus rotor is not self starting some form of auxiliary starting
device is required. A small Savonius rotor mounted on the Darrieus rotor
shaft provides a simple and economic means of starting the turbine.

3.2.5 Load matching

To ensure a high efficiency there is a need for the turbine and load
characteristics to be matched. In addition, some form of turbine speed
control is required to limit centrifugal induced loads in the blades.

Both requirements can be resolved by a control system based on a micro-
processor which regulates the speed and provides a means of optimising the
matching of turbine and electrical load characteristics at all wind speeds,
to utilise almost all the power available from the turbine at any time
within the operational design limits.

3.2.6 Overspeed control

To avoid destructive overspeeding of the turbine in the event of a control
system or mechanical transmission failure, spoilers, which deploy
automatically at a predetermined rotational speed, are incorporated in the
Darrieus rotor blades.

---

* The term turbine is used here to describe the Darrieus rotor assembly
  and therefore includes a central tube, horizontal spars, tie rods and
  braces. Normally the term turbine will also include the Savonius
  rotor assembly, which is used for starting.

** A troposkien is defined as the shape assumed by a perfectly flexible
  cable of uniform density and cross section when its ends are attached
  to two points on a vertical axis and the cable is spun at a constant
  angular velocity about the axis.

3.3 Description

3.3.1 Concept

The wind-powered generator concept thus consists of a Darrieus two blade rotor with a small Savonius rotor as starter, an alternator, a micro-processor based control system and a guyed tubular tower (figure 1). The Darrieus rotor is fitted with spoilers to limit speed in the event of a system failure. The turbine is provided with a hydraulically operated emergency brake and a positive mechanical lock for parking. A conventional alternator can be coupled to the turbine via a speed increaser unit as illustrated. Alternatively, a low speed alternator may be directly coupled to reduce mechanical losses and improve overall efficiency.

3.3.2 Leading particulars

The leading particulars for the wind-powered generator concept are summarised in Table 3.

TABLE 3.   WIND-POWERED GENERATOR CONCEPT LEADING PARTICULARS

Characteristic	Value
(a) Darrieus rotor	
rotor diameter	3660 mm
blade length	3660 mm
number of blades	2
blade profile	NACA 0012 * aerofoil section
blade chord	180 mm
rotor shaft nominal power output at mean wind speed ($V\infty$ = 7.5 m/s)	1.5 kW
rotor shaft net power output, allowing for windage losses	1.3 kW
rotor speed at mean wind speed	180 r/min
rotor maximum speed	300 r/min
turbine mass including Savonius rotor	85 kg
(b) Savonius rotor	
rotor diameter	1220 mm
rotor height	896 mm
number of buckets	2
radius of each bucket	352 mm
(c) Alternator	
Nominal power output at mean wind speed	1 kW
(d) Tower	
height, allowing for nominal turbine height 10 m	9.4 m
mass	385 kg

* see reference 6

TWO
BLADES

Preferred:
STRAIGHT BLADE
ROTOR FORM

TROPOSKIEN ROTOR
FORM

SWEPT AREA

SWEPT VOLUME

ROTOR CONCEPTS

SAVONIUS
ROTOR

DARRIEUS ROTOR

HYDRAULIC OPERATED
EMERGENCY BRAKE &
MECHANICAL LOCK
FOR PARKING

SPEED INCREASER

GUYS

ALTERNATOR

10 m

TUBULAR
COLUMN

BASE
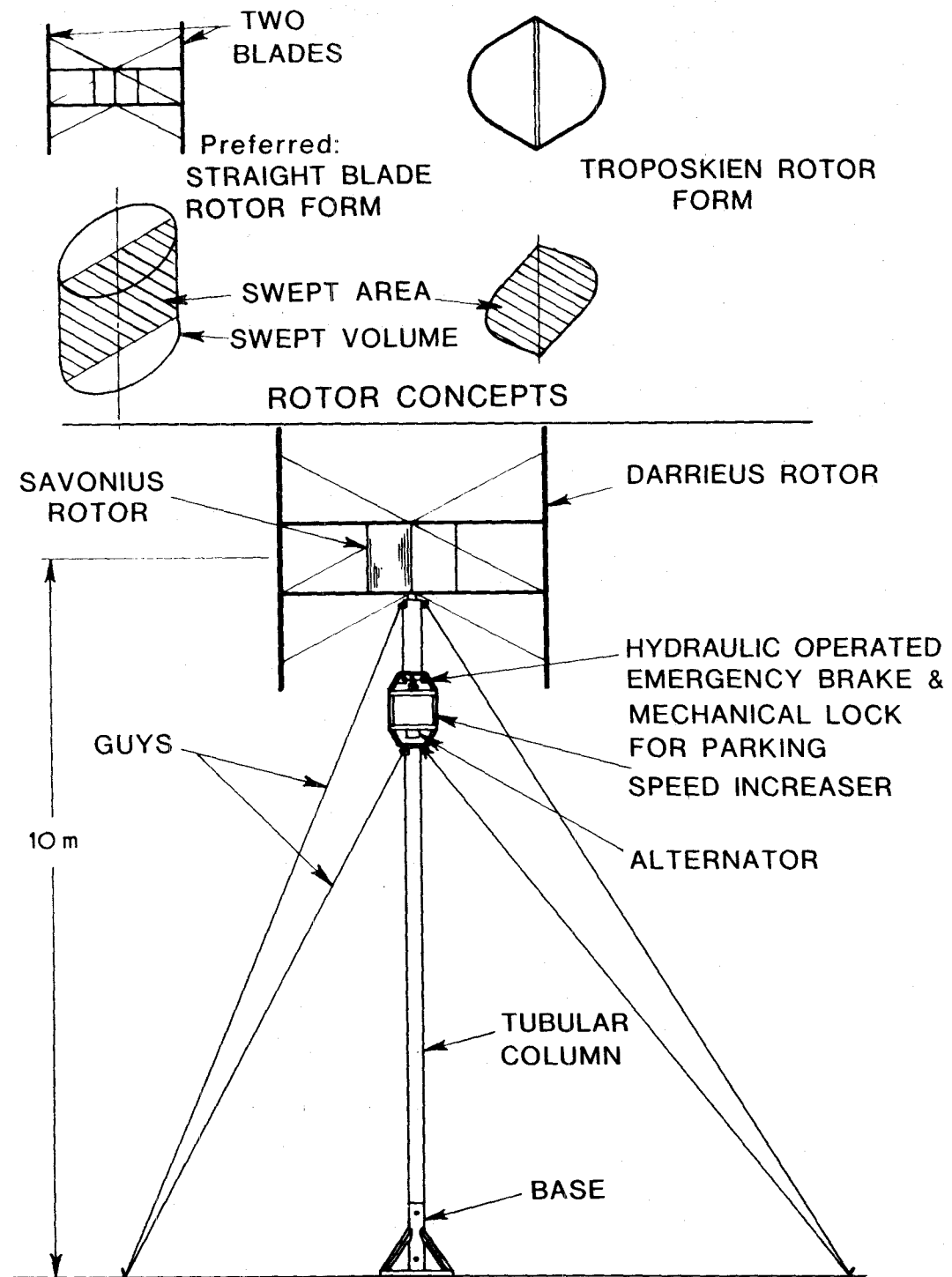
Figure 1.   AEL wind-powered generator concept

4. AERODYNAMIC PERFORMANCE

4.1 Wind speed

To establish the basic dimensions of a wind turbine, the wind speed corresponding to a nominal power output must be specified. In the absence of comprehensive wind information for the continent of Australia, the data of Mullett(ref.7) for the southern region of South Australia were reviewed, and a mean annual wind speed of 7.5 m/s at a height of 10 m above ground level was adopted for the present design.

On the basis that 1 kW of electrical power is required from the wind-powered generator at the mean wind speed and allowing 0.5 kW for mechanical and electrical power losses, the nominal mechanical power output of the turbine is 1.5 kW. A power output well in excess of the nominal value will be possible at wind speeds greater than 7.5 m/s provided that the turbine has the structural capacity to withstand the increased wind loadings and to operate at rotational speeds in excess of 180 r/min, the theoretical speed for maximum power output at the mean annual wind speed.

4.2 Darrieus rotor

In reference 4, Shankar gives details of a method for predicting the aerodynamic performance of a Darrieus rotor, and his results show reasonable agreement with available experimental data. A convenient method of character-ising the performance of a wind turbine is the plot of power coefficient* C_{P_O}

as a function of the speed ratio μ_O as shown in figure 2(a), where

$$C_{P_O} = \frac{\text{power (W)}}{k \; \frac{1}{2} \; \rho \; V_\infty^3 \; A_O} , \tag{1}$$

and

$$\mu_O = \frac{R_O \Omega}{V_\infty} .$$

In these equations,

A_O is the rotor swept area**, m^2 ,

R_O is the radius of the rotor, m,

V_∞ is the freestream wind speed, m/s,

ρ is the air density, kg/m^3 and

Ω is the angular velocity, rad/s.

---

* The subscript 'o' is used to distinguish variables relating specifically to the Darrieus rotor.

** A blade of a Darrieus rotor sweeps out a volume known as the "swept" volume which is symmetrical about and includes the axis of rotation. The area common to this volume and a plane including the axis of rotation is known as the "swept" area (figure 1).

The Betz factor k represents the proportion of incident kinetic energy flux which can theoretically be extracted from a streamtube of area A_o, and has the numerical value 16/27 or 0.593. The present definition of the power coefficient follows that of Shankar, but the Betz factor is omitted by most authors leading to a coefficient 0.593 times the present value.

An important parameter influencing Darrieus rotor performance is the solidity* σ which is defined herein as:

$$\sigma = Nc/R_o,$$

where N is the number of blades and c is the blade chord.

Shankar's analysis indicates that an optimum value of solidity for a straight blade rotor is about 0.2, for which the maximum power coefficient C_{P_o} is 0.72 in the absence of structural windage and frictional losses.

Substituting the value of C_{P_o} of 0.72 in equation (1) in conjunction with the nominal power and mean wind speed, the swept area A_o is established as 13.4 m^2. By choosing the blade length L_o equal to the rotor diameter D_o to achieve satisfactory proportions, $L_o = D_o = 3660$ mm. Finally, the blade chord of 180 mm is derived from the solidity relationship, thus completing the basic dimensional specification of the Darrieus rotor.

Subsequently, the performance analysis was programmed on the DRCS 370/3033 computer using the lift and drag coefficient data for a NACA 0012 aerofoil section specified in reference 6. The basic result of the analysis is the Darrieus rotor power coefficient which is shown as a function of the speed ratio μ_o in figure 2(a). From the non-dimensional data in figure 2(a), the mean power and torque of the Darrieus rotor can be computed as required for a range of wind and rotational speeds. The performance analysis also yields the mean streamwise drag force or thrust on the Darrieus rotor, the instant- aneous torque and power of the rotor, and the fluctuating force components acting on the rotor blades.

The aerodynamic performance aspects of the Darrieus rotor are covered comprehensively in Appendix I, Sections I.1 to I.4.

4.3 Savonius rotor

A Savonius rotor is incorporated into the turbine design as a starting unit, because a Darrieus rotor is not always capable of self starting. A classical design of Savonius rotor is used, and the dimensions are included in Table 3. The performance data for the Savonius rotor were taken from Newman(ref.8) and modified to account for operation of the Savonius rotor in the induced velocity field of the Darrieus rotor to give the power coefficient shown in figure 2(b). Although the positive power contribution of the Savonius rotor is small compared with the maximum power output of the Darrieus rotor, nevertheless the Savonius rotor provides the low-speed torque necessary for reliable starting of the turbine.

---

* Solidity is a measure of the ratio of total blade planform area to the swept area A_o. Some authors have used Nc/D_o and others the actual ratio of total blade planform area to swept area.

(a) Darrieus rotor

(b) Savonius rotor

(c) Windage losses

$$\text{SPEED RATIO}, \mu_0 = R_0\, \Omega / V_\infty$$
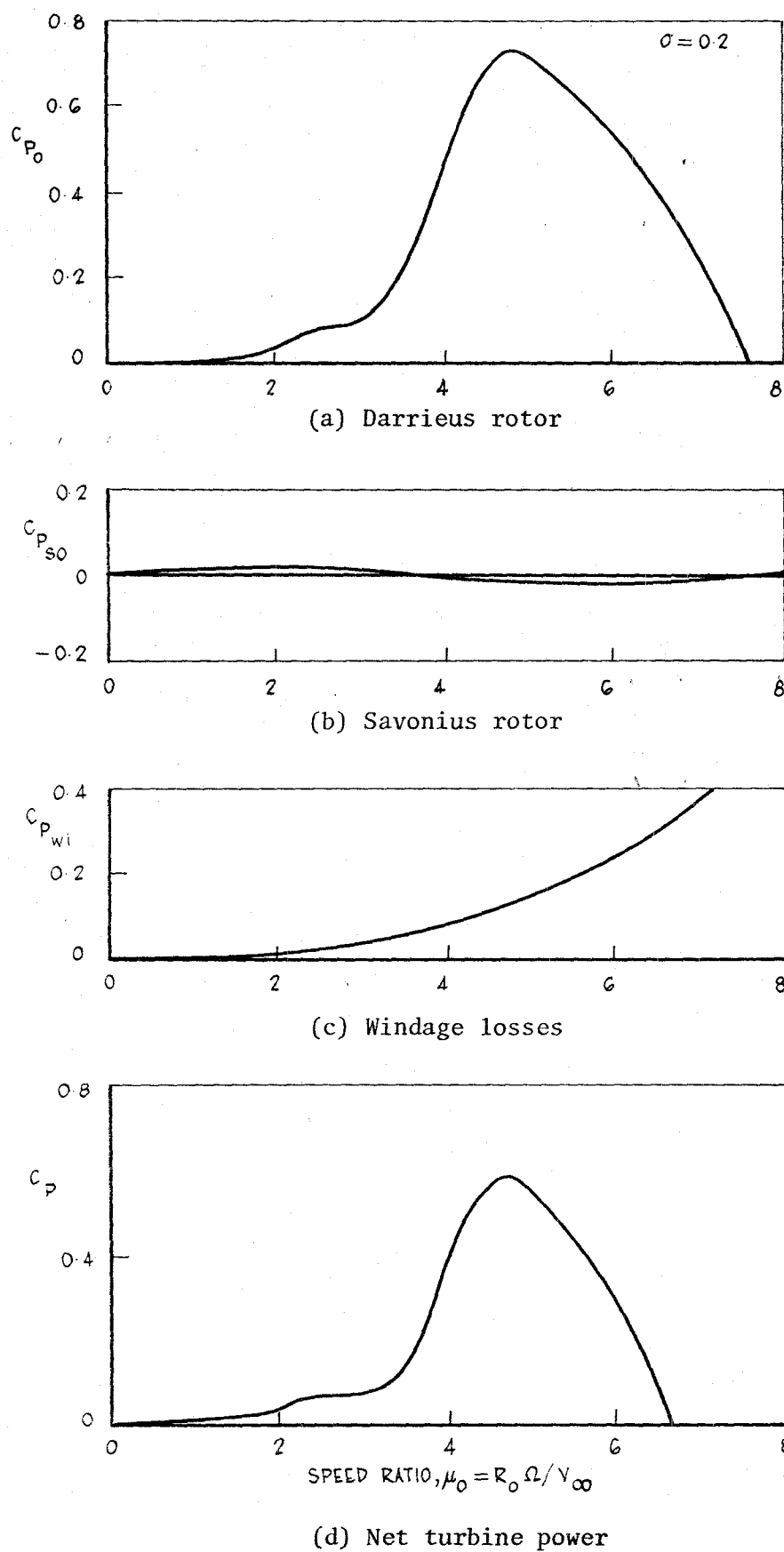
(d) Net turbine power

Figure 2.   AEL wind-powered generator - turbine power coefficients

The full performance analysis of the Savonius rotor is given in Section I.5 of Appendix I.

4.4 Aerodynamic power losses

Non-power producing structural elements of the turbine such as spars, tie rods and braces cause energy losses through windage, and this aspect is considered in Section I.6 of Appendix I. The windage power loss coefficient calculated according to the analysis of Section I.6 is shown in figure 2(c). At the maximum power condition, the losses represent 16% of the power output of the Darrieus rotor. Such losses, which occur even with relatively low drag or streamlined structural elements, demonstrate the need to minimise both the number and drag of rotating structural elements.

4.5 Spoilers

A brief analysis of a spoiler concept to prevent overspeeding of the rotor is given in Section I.7 of Appendix I. The analysis shows that two spoilers, each 523 mm spanwise length and 75 mm chord and located at a radius of 1830 mm are capable of absorbing the maximum power output of the Darrieus rotor at a speed of 250 r/min. The spoilers, which deploy through 60° under the action of centrifugal force as the maximum speed is approached, retract automatically when the speed decreases below a threshold level. Each spoiler is mounted as a trailing edge flap at the mid-span of each Darrieus rotor aerofoil blade.

4.6 Net power and torque of turbine

The net power output of the wind turbine has been obtained by adding the power contributions of the Darrieus and Savonius rotors and subtracting the windage losses. The net power coefficient so derived is shown in figure 2(d) as a function of speed ratio μ_o, and reaches a maximum value of 0.59 at $\mu_o = 4.7$. Power and torque calculated from the net power coefficient curve are shown in figures 3 and 4 for a range of wind and rotational speeds. The maximum net power available from the turbine at the mean wind speed of 7.5 m/s is 1.3 kW which occurs at a rotational speed of 180 r/min. Largely because of windage losses, the desired nominal power of 1.5 kW is not achieved at the mean wind speed, but at the marginally higher wind speed of 7.9 m/s.

Inspection of the power and torque curves in figures 3 and 4 reveals the need for careful consideration of load regulation to match the operating condition of the turbine. For example, if the turbine is operating at 190 r/min near maximum power at a wind speed of 7.5 m/s, an increase in wind speed to 9 m/s will cause an increase in torque and the system will accelerate to a higher rotational speed. However, if the wind speed increases suddenly to 10.5 m/s, the rotor torque decreases and the turbine will slow down unless the load is reduced. The load regulation aspect is considered in Section 7.

4.7 Normal operation - variable speed maximum power mode

The power output of a Darrieus wind turbine is conveniently regulated by using the load to control the rotational speed in relation to the wind speed. The maximum shaft power output of the turbine excluding mechanical friction and transmission losses is shown in figure 5(a) as a function of wind speed by the curve labelled variable speed-maximum power mode. To achieve maximum power, the rotational speed of the turbine must be controlled as a linear function of wind speed according to the maximum power mode curve shown in figure 5(b). The maximum power available varies from less than a kilowatt at wind speeds below 6.8 m/s to a potential value in excess of 10 kW at the high (and infrequent) wind speed of 15 m/s.
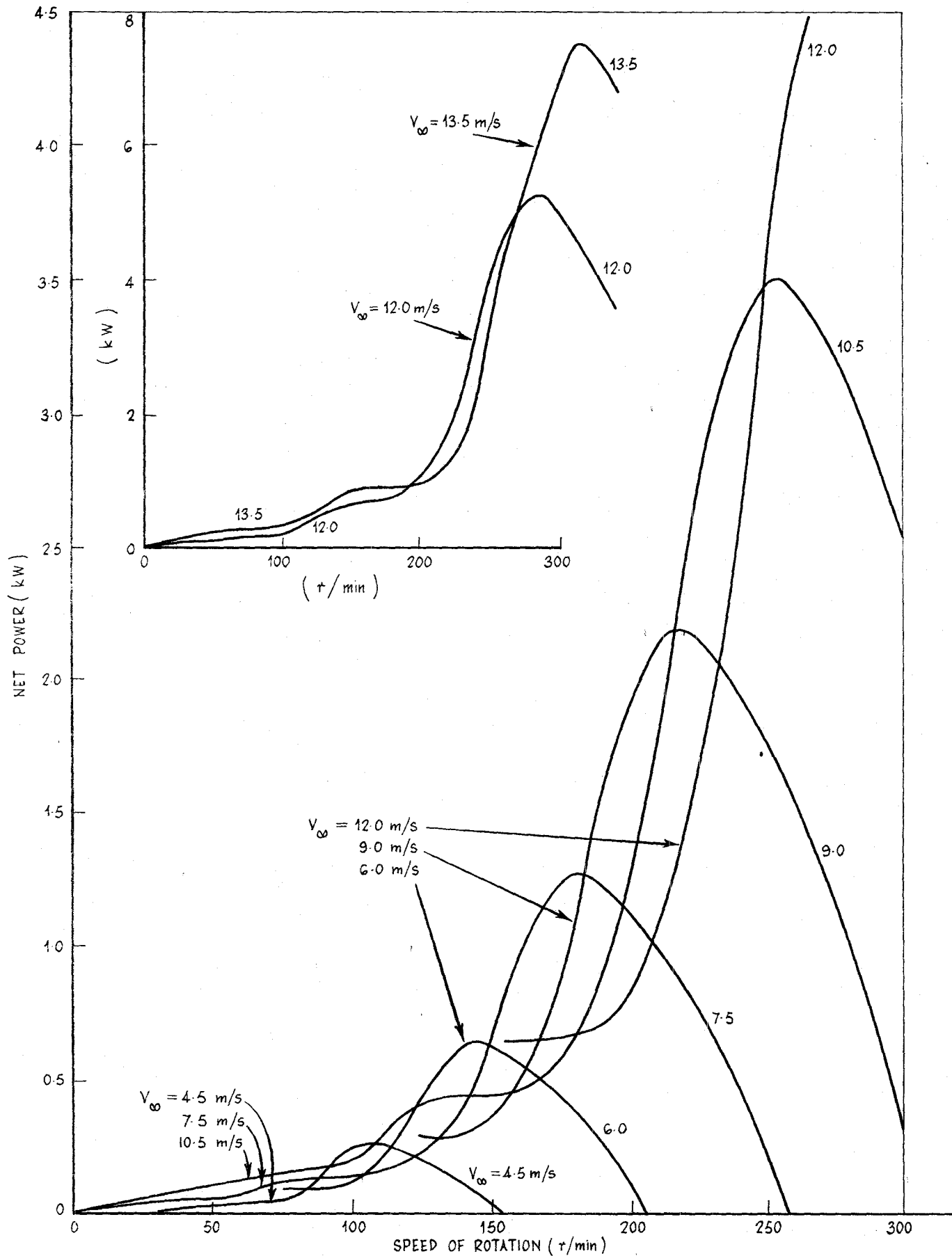
Figure 3.   AEL wind-powered generator - variation of net power output
of turbine with wind speed and rotational speed
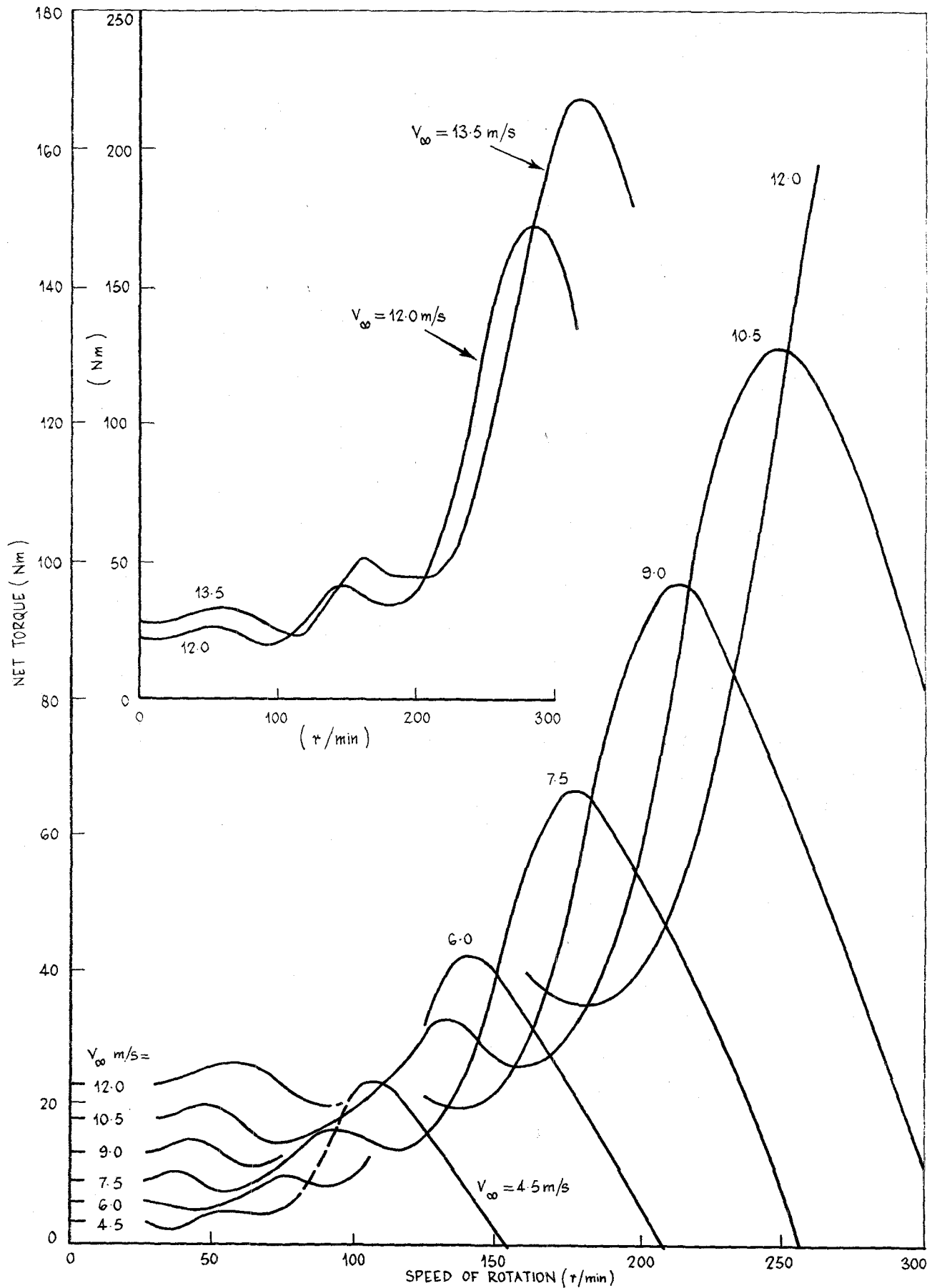
Figure 4.   AEL wind-powered generator - variation of net torque of
            turbine with wind speed and rotational speed
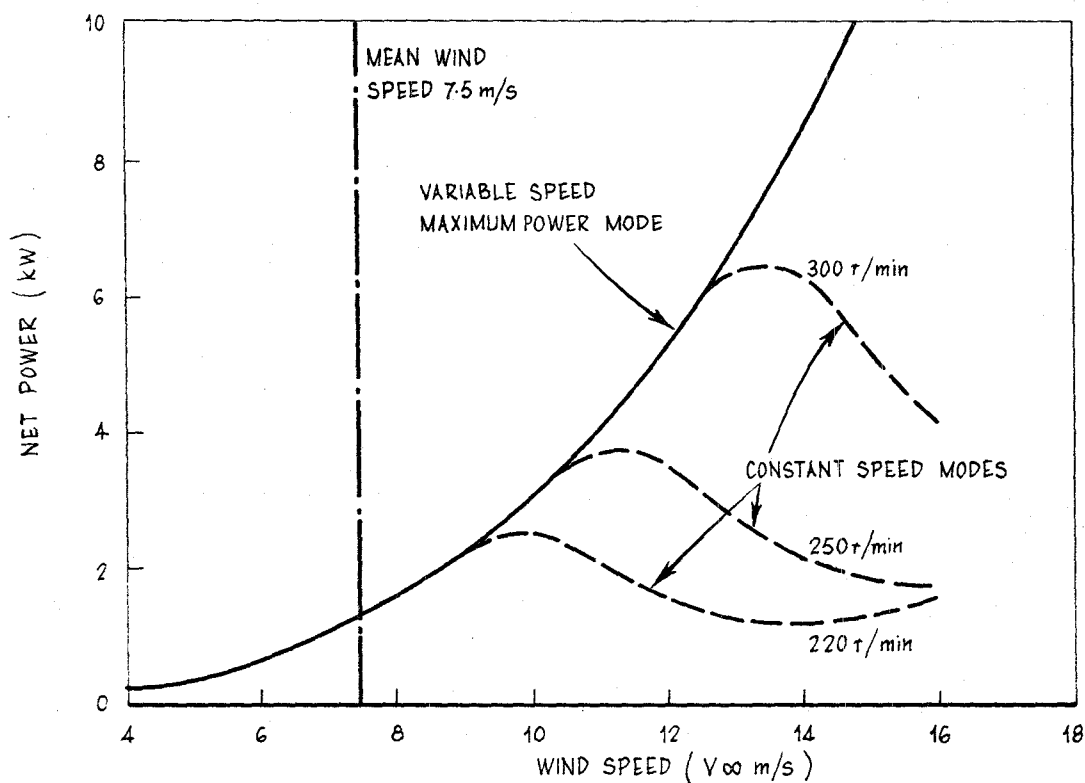
(a)   Turbine power
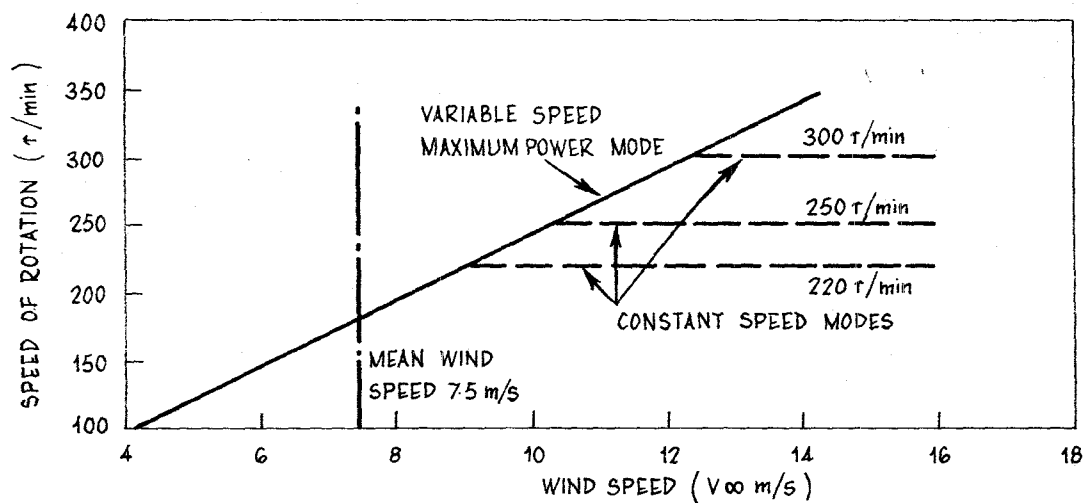
(b)   Turbine speed of rotation

Figure 5.   AEL wind-powered generator operating modes

The variable speed-maximum power mode maximises the energy production of a wind-powered generating system over the full range of wind speeds. It is generally used in small to moderate-sized autonomous windpower systems over the lower wind speed range in which structural, drive system or alternator capacity restrictions do not apply.

In practice the power capacity of an autonomous windpower system will usually be limited by either the permissible rotational speed of the turbine or the continuous input power capacity of the alternator or electrical generator. The maximum permissible rotational speed of a Darrieus turbine and the corresponding power output are fixed by the structural design. The alternator capacity will be specified on the basis of the power requirement, and will be influenced by the turbine power output and the operating mode used.

4.8 Constant speed mode

In the higher wind speed regime, the constant speed mode of operation is applicable to windpower systems of the type under consideration. In this mode the control system regulates the load to maintain a constant rotational speed irrespective of wind speed.

As the turbine structure is designed to operate at a maximum rotational speed of 300 r/min, this is the upper speed limit for power rating purposes. The maximum wind speed for normal operation of the turbine in power production is 13.5 m/s; at higher wind speeds it is proposed to reduce the turbine speed to a safe, low level by applying an excess electrical load, by deploying aerodynamic spoilers or by applying a mechanical brake.

Figure 5(a) shows that the rated shaft power output of the turbine at 300 r/min is 6.4 kW, which is achieved at a wind speed of 13.5 m/s. If the rotational speed of the turbine is limited to 250 r/min, the power and wind speed are 3.7 kW and 11.2 m/s respectively; for low power applications, at a rotational speed of 220 r/min the turbine produces 2.5 kW at a wind speed of 10.0 m/s.

The power figures given above represent the power that, in the absence of friction, is transferred to the alternator at each stated speed of rotation. Therefore, operation of the wind-powered generating system at 250 r/min requires an alternator capable of absorbing 3.7 kW, whereas operation at 300 r/min requires an alternator capacity of 6.4 kW.

In the constant speed mode, the turbine power characteristics (figure 5(a)) are such that the power output falls for wind speeds in excess of the value corresponding to maximum (rated) power. To maximise energy production over a period of time, the rated speed of rotation will need to be chosen with due regard for the turbine characteristics in relation to the wind distribution at the turbine site. For example, if the relative frequency of strong winds is high, the rated speed of rotation should be correspondingly high within the limits imposed by the turbine structure and the alternator capacity.

Consideration of the electrical power generating capacity of the system is deferred to Section 7, following a discussion of alternators and load matching.

<center>5. TURBINE DESIGN</center>

5.1 Design criteria

Criteria for the turbine design are based on the results of investigations on aerodynamic performance (Section 4) and blade strength (Appendix II) and relate to the normal modes of operation as defined and survival in the parked condition.

(a) The Darrieus rotor diameter is 3660 mm and it is fitted with two straight blades which conform to NACA 0012 symmetrical aerofoil profile. Blade chord is 180 mm and constant along the whole length. Blade length is 3660 mm. For the Savonius rotor the diameter is 1220 mm, height is 896 mm and the radius of each of the two buckets is 352 mm.

(b) Operating speed for the turbine at 7.5 m/s mean wind speed is 180 r/min.

(c) Operating speed for the turbine at 11.2 m/s rated wind speed is 250 r/min.

(d) Operating speed for the turbine at 13.5 m/s furling wind speed is 300 r/min.

(e) In the parked condition, the turbine should survive wind speeds up to 42 m/s.

(f) Cut-in wind speed for the turbine is 5.5 m/s.

(g) Blade natural frequencies should be high enough to avoid resonances with aerodynamic force impulses which occur twice in each revolution of the rotor.

5.2 Turbine design configuration

The configuration is optimised to meet the following particular objectives:-

(a) to minimise blade stresses in response to load inputs, mainly centrifugal in nature.

(b) to minimise induced aerodynamic drag.

(c) to minimise the bending moment which occurs at the turbine/tower interface.

(d) to provide adequate stiffness so that structural resonance conditions are avoided in operation.

The preferred configuration is shown in figure 6. The blades are attached to the central steel tube by two main spars and four radial tie rods. The unsupported blade span lengths have been chosen so that the maximum positive and negative stresses induced by centrifugal effects during operation are equalised at minimum level. The spars are made from the same low drag extruded section as the blades. The tie rods are of streamline section in material type 316 stainless steel. The Savonius rotor, in addition to acting as a starter for the rotor system, provides structural support to the Darrieus rotor and together with the wire braces reduces spar deflection in the parked condition. Earlier configurations are shown in figure 6 insets (a) and (b). Example (a) has excessive spar drag and excessive bending moment at the turbine/ tower interface. Example (b) has excessive stresses in the blades.
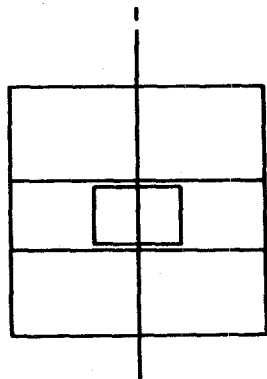
(a) Early configuration-two vertical blades, four horizontal spars
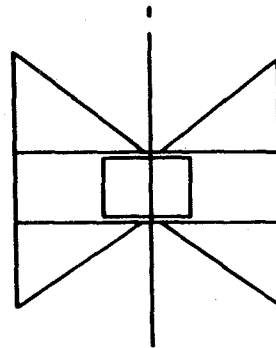
(b) Early configuration-two vertical blades, two horizontal spars, four diagonal tie rods
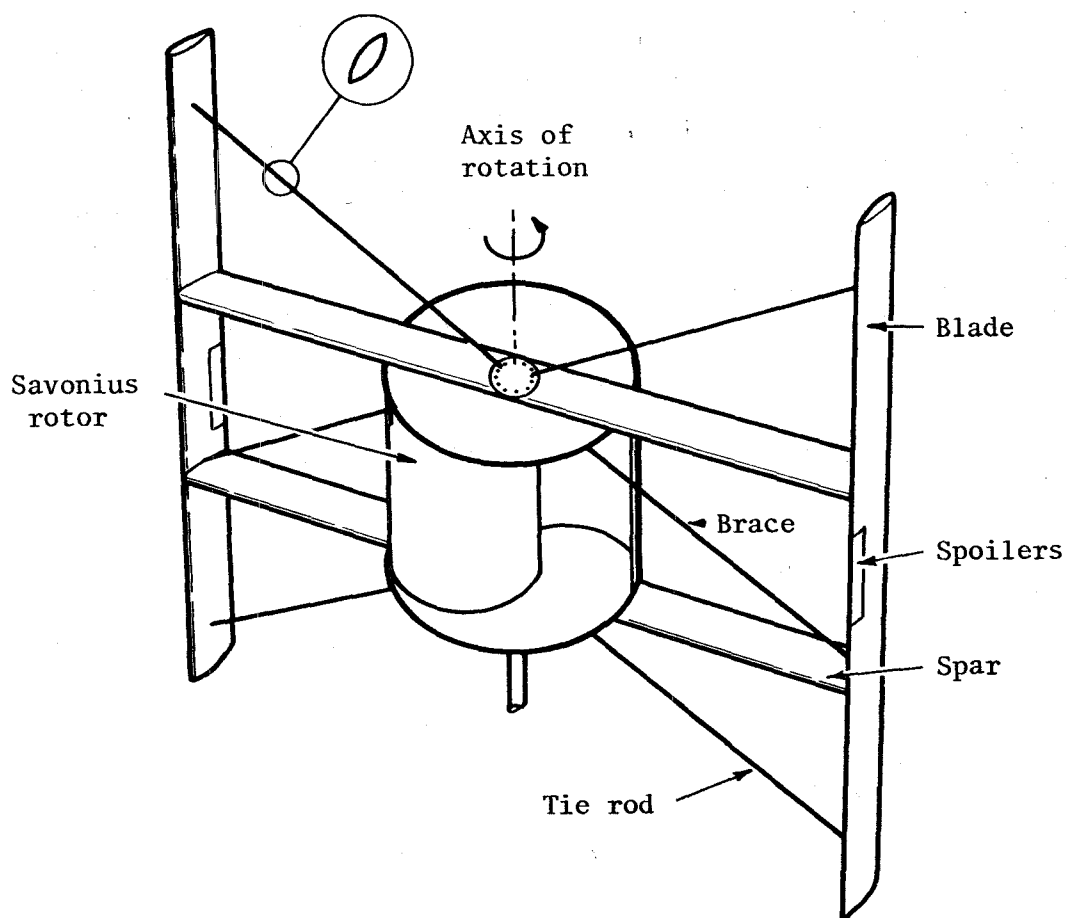
Figure 6.   AEL wind-powered generator - turbine concept

5.3 Blade design

Straight blades offer promise of high performance at low cost provided that centrifugal induced stresses can be contained within safe limits. Blade section is therefore optimised:-

(a) to conform with aerodynamic profile requirements.

(b) to have structural capabilities to resist the bending stresses due to centrifugal loads and sufficient rigidity to avoid flutter, induced by aerodynamic loads.

(c) to meet formability and rotor assembly requirements.

The initial blade section considered is shown in figure 7 inset (a). The section is a hollow extrusion of minimum wall thickness to limit blade mass and is provided with a single web to maintain the required profile. For this size of section the extrusion process limits minimum wall thickness to 2 mm. Sample lengths have been manufactured in aluminium alloy to specification 6063 - T6 with yield strength 172 MPa and ultimate strength 206 MPa, for evaluation. Measurements of profile show a minor degree of belling in the rear section and material strength and section properties limit the safe operation speed of this blade to 250 r/min.

An improved section is shown in figure 7. Blade profile conforms to NACA 0012 symmetrical aerofoil shape with chord length 180 mm and wall thickness 2 mm as before. Two webs are provided to maintain profile over the whole surface and improve structural form to resist the bending loads. An important feature also, is that the rear web provides an integrated structural interface which facilitates installation of the spoiler units. The double webbed section can be supplied in aluminium alloy to specification 6061 - T6, a higher strength material, with yield strength 241 MPa and ultimate strength 262 MPa. With these improvements, it is possible to operate safely at speeds up to 300 r/min in wind speeds up to 13.5 m/s.

For the improved section, die development cost would be $2300 approximately and the cost of each blade length (3660 mm) as extruded $30 approximately, at current 1980 prices, subject to compliance with manufacturers minimum quantity requirements. The difference in extrusion cost for the two sections is in the order of 10%.
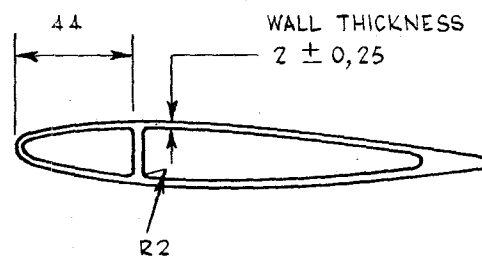
(a) Early blade section
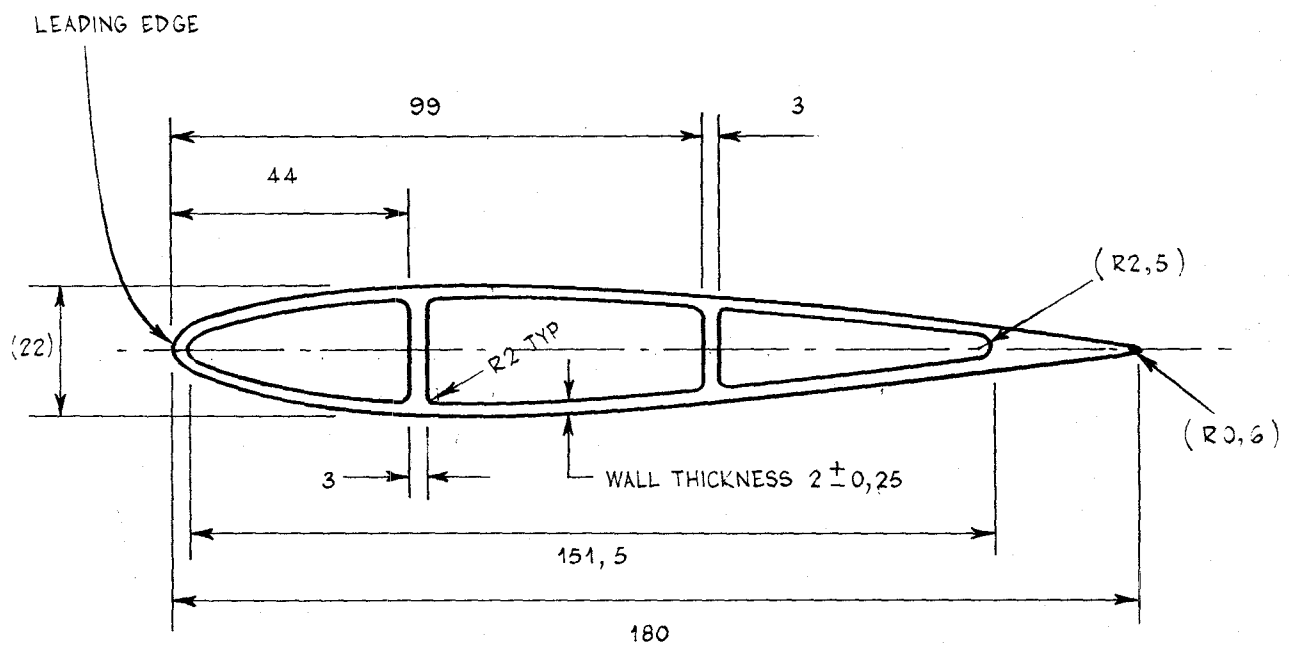
Figure 7.   AEL wind-powered generator - Darrieus rotor blade section

5.4 Turbine mass

In the above considerations, turbine mass and in particular blade mass has been minimised to limit centrifugal induced loads occurring in turbine rotation and to conform to the wind powered generator guidelines Table 1 requirement of low weight for ease of handling in the field.   The resultant turbine mass of 85 kg is detailed in Table 4.

TABLE 4.   MASS ESTIMATE OF TURBINE INCLUDING THE SAVONIUS STARTER

Component	Mass (kg)
two blades less fittings	16.4
blade fittings	2
two main spars	16.4
two centre hubs	3.2
spar fittings	2
steel centre tube	21
four struts and two braces	4
Savonius rotor	20
Total	85

5.5 Turbine construction

Using the precision made extruded section for both blades and spars, construction techniques have been developed accordingly.   Each of the blades is fitted with inserts profiled on a numerically controlled machine and riveted in place to act as strong points for attaching the blades to the spars and braces (figure 8).   The spars are riveted onto machined centre hubs and fitted with profiled inserts and end fittings for attaching the Savonius rotor and the Darrieus blades respectively.   Permanent joints are riveted while joints which may need to be made in the field are bolted.   Attachment of the streamline section tie rods and the circular section wire braces completes the assembly.

For transport, the turbine may be disassembled and packaged in two crates, one containing the Savonius rotor and the centre tube and the other containing the blades, spars and tie rods for the Darrieus rotor.   Field assembly and erection of the turbine and tower is described in Section 6.

BRACE

FILLING BLOCK

SPAR CONNECTION
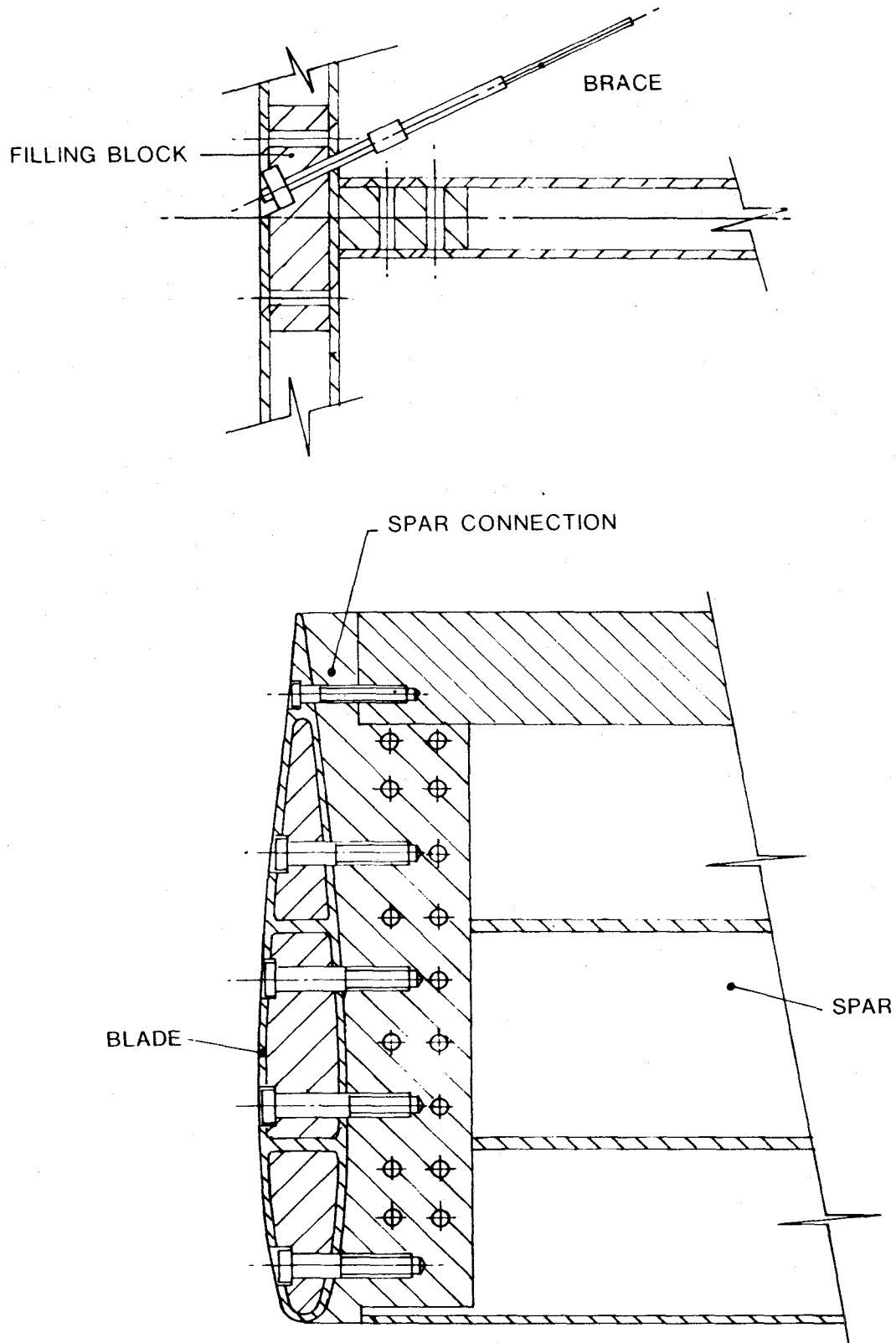
BLADE

SPAR

Figure 8.   AEL wind-powered generator - blade-spar joint

6. TOWER DESIGN

6.1 Design criteria

Criteria for the tower design are based on the results of investigations on aerodynamic performance (Section 4) and turbine design (Section 5). The relevant requirements are as follows.

(a) Tower height should be such that the turbine is 10 m above ground level, 10 m being the datum for the mean wind speed of 7.5 m/s.

(b) The tower needs to be strong enough to withstand the maximum combined loads occurring in operation and comprising:-

    (1) the weight of the turbine and main shaft arrangement.

    (2) the unsteady torsional and bending loads arising from aerodynamic loads on the blades.

    (3) loads due to wind speeds up to 13.5 m/s.

Additionally the tower must withstand the maximum combined loads likely to occur while the turbine is in the parked condition and comprising:-

    (1) the weight of the turbine and main shaft arrangement.

    (2) loads due to wind speeds up to 42 m/s.

(c) The tower needs to be stiff enough in bending to avoid resonance with unsteady normal loads induced in the blades at frequencies up to 10 Hz corresponding to a rotor speed of 300 r/min.

(d) The tower needs to be stiff enough in torsion to avoid resonance with the unsteady torque loads induced in the rotor at frequencies up to 10 Hz corresponding to a rotor speed of 300 r/min.

(e) The tower should be as light as possible.

(f) The tower should be easy to assemble.

6.2 Tower design configuration

To conform with the design guidelines, the tower should be light weight, easy to erect and dismantle, and have potential for fixed, mobile or portable applications. Design of the head of the tower is dictated by the design of the turbine (Section 5) and mainshaft two bearing support assembly (Appendix III), and influenced by the choice of location of the alternator unit (Section 7).

In evaluating light weight tower designs, reference was made to studies by Reuter of Sandia on towers for a troposkien type Darrieus wind turbine(ref.9). Reuter shows that for specified torsional and bending stiffness values, a truss type tower will provide a lighter weight structure than a tower of tubular form, while for a specified axial stiffness value a tubular section will be the most weight effective.

These results indicate that in the case of a free standing tower configuration, where loads are predominantly in bending and torsion, a truss type tower is the most weight effective, while for a guyed tower, where loads are predominantly axial, a tubular section tower is the most weight effective.

For preliminary tests on the wind-powered generator system it is proposed to mount the main shaft arrangement into an existing rigid truss type free standing tower, bolted to a concrete base for stability.   The installation is described in Section 9.

While the free standing tower concept is satisfactory for fixed installations, the massive base which is needed for stability makes it an unacceptable concept for field use in terms of the design guidelines, which accent ease of erection and mobility.

The preferred configuration, utilising a tubular guyed tower is shown in figure 9.   This configuration conforms closely with the design guidelines as it requires only minimum site preparation, is easy to assemble and erect and has potential for mobile applications.

The steel tower is assembled from four sections, the turbine main shaft assembly with tubular housing, an alternator mounting frame fabricated from three equispaced tubes with end plates and intermediate stiffening rings, the main tubular column and a base unit with pivot.   On installation, the tower is supported by six steel guy wires, three from the top of the main shaft assembly and three from the top of the main tubular column.   With this arrangement, the principal loads in the upper portion of the tower are in the axial and sideways directions.   The side loads are reacted by the guys. The main tubular column is subject to axial and torsion loads, the latter being due to the turbine and applied through the mainshaft and alternator unit.

A formal design analysis of the tower is not considered here but a preliminary analysis of the loads acting on the main column shows that standard galvanised mild steel water pipe 155 mm O D x 5 mm wall thickness is suitable for this section of the tower.   The pipe is obtainable in lengths of 6.5 m which is ideally suited to the requirement.   Guys of 8 mm diameter, of 7 x 7 galvanised wire rope would be suitable.

6.3   Tower mass

The estimated mass of the guyed tower including the turbine main shaft assembly but excluding the alternator and speed increaser unit is shown in Table 5.

TABLE 5.   MASS ESTIMATE OF THE TOWER

Component	Mass (kg)
Main shaft main bearing assembly	60
Main shaft housing	50
Disc brake assembly	20
Alternator mounting frame	40
Tubular main column	125
Base	50
Guys	25
Stakes	15
Total	385

Main Bearing
Assy.

Brake with
Mechanical Lock
for Parking

Coupling

Alternator
Mounting
Frame

Speed Increaser

Alternator

Tubular
Column

Tube
(155 OD x 5 Wall)

Pivot

Base
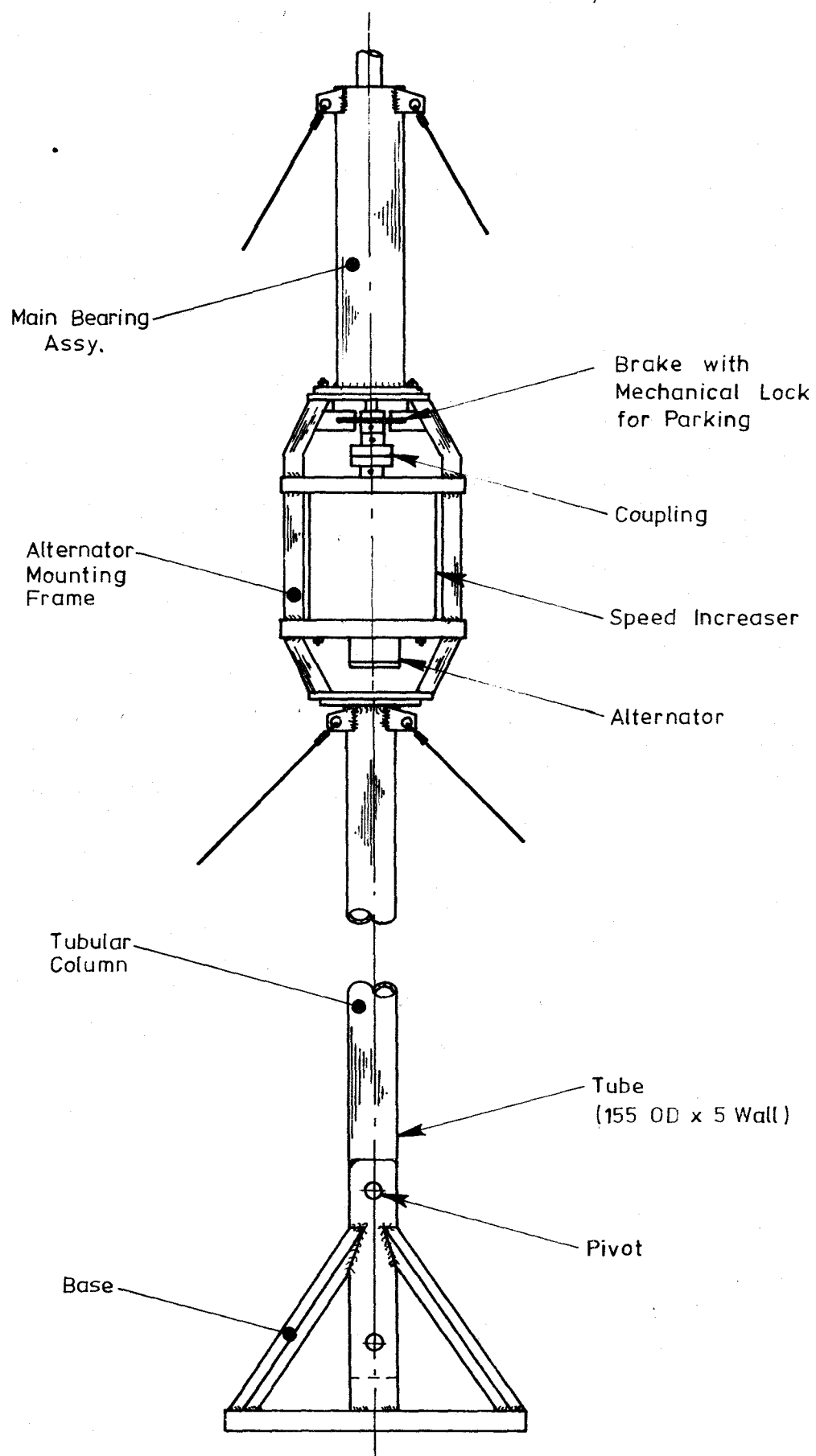
Figure 9.   AEL wind-powered generator - tower concept
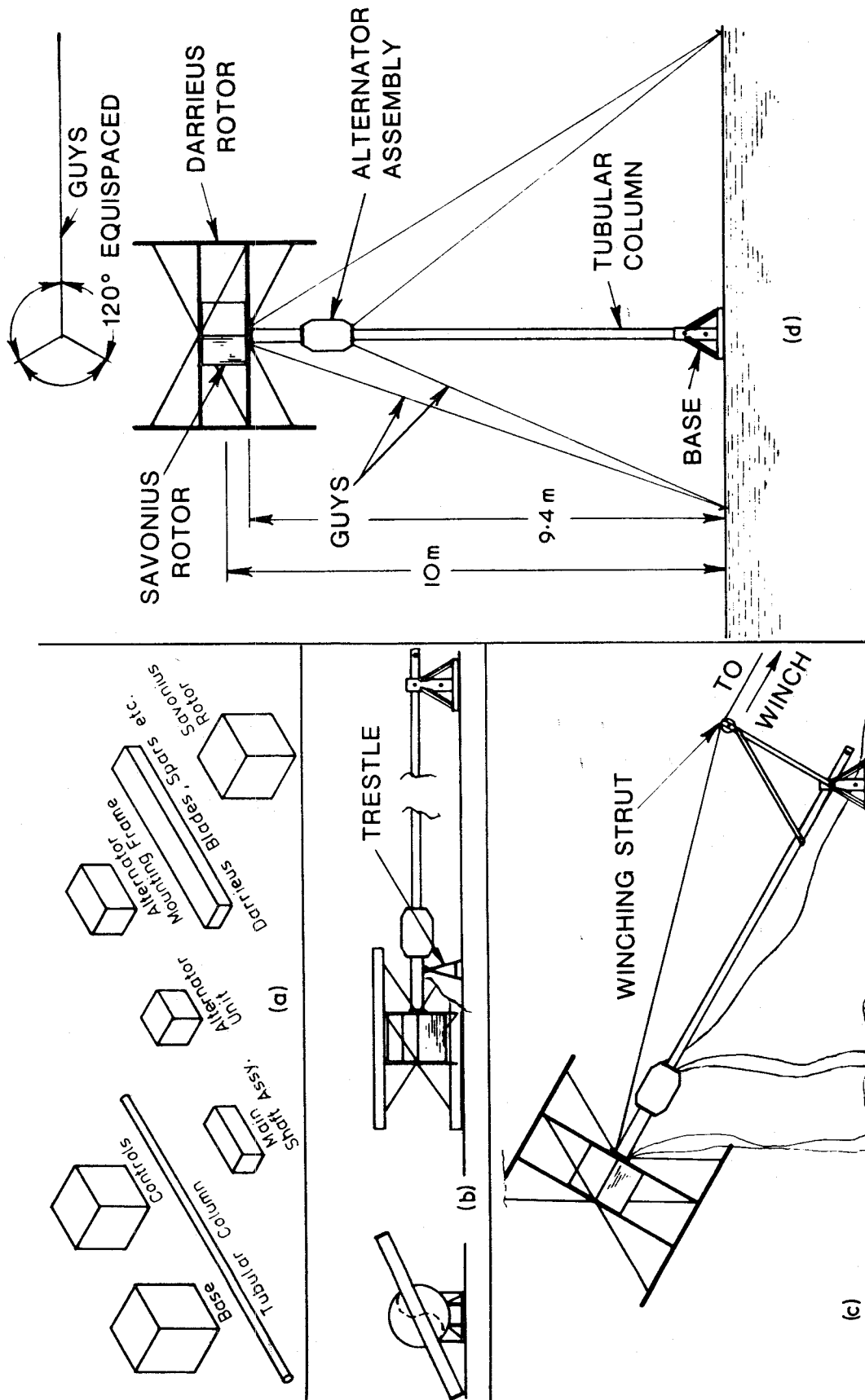
Figure 10. AEL wind-powered generator - assembly and erection

6.4 Assembly and erection

After transport to the site in boxes, the system can be fully assembled on the ground before being raised to the vertical position by using simple erection gear.   No crane is required.   The process is illustrated in figure 10(a) to (d).

(a) Figure 10(a), the nominated units are suitably boxed and transported to the site by truck or helicopter.

(b) Figure 10(b), after bolting the base to pins set in the ground, the main column, alternator frame, main shaft assembly and turbine are assembled in sequence with the aid of trestle supports.

(c) Figure 10(c), using a jury structure and tackle or winch gear, the system is raised to the vertical position.

(d) Figure 10(d), when the system is upright, a lock pin is inserted at the base of the main column.   Then the six guy wires, attached to steel stakes driven into the ground, are adjusted for operational use and the erection gear is removed.

7. ELECTRICAL SYSTEM

7.1 Turbine load

7.1.1 Introduction

The load on a turbine generally consists of a mechanical to electrical power converter, followed by an electrical energy storage system and/or an electrical load.   For the experimental wind generator system (see figure 11) an alternator was selected as the power converter and the electrical load will consist of storage batteries in conjunction with a shunt regulator which is capable of absorbing all of the power generated by the turbine when required.

7.1.2 Alternator selection

The design guidelines outlined in Section 3.1 have an important bearing in the selection of a suitable alternator.   Any choice will involve some compromise and the most desirable alternator criteria can only be determined when taken in the context of the complete turbine system.   In particular, the size and weight of the alternator will generally increase with an increase in efficiency but an increase in alternator efficiency implies a reduced turbine size.   A compromise will have to be reached between high efficiency and a compact light weight unit.

The other main criteria to consider are cost, reliability and the coupling requirements to the turbine.

(a) In the first instance, the experimental system (see figure 11) would be connected to a standard Bosch 28 V, 35 A alternator.   This unit was selected because it is reliable and readily available.   The characteristics of the alternator have been measured and can serve as a useful standard in measuring the performance characteristics of the system as a whole.   The efficiency of the alternator is * 50% nominal and this is believed to be typical of most automotive

---

* Bosch alternator efficiency:- Measurements show that efficiency varies over the range 40 to 60% as a function of speed and power output.
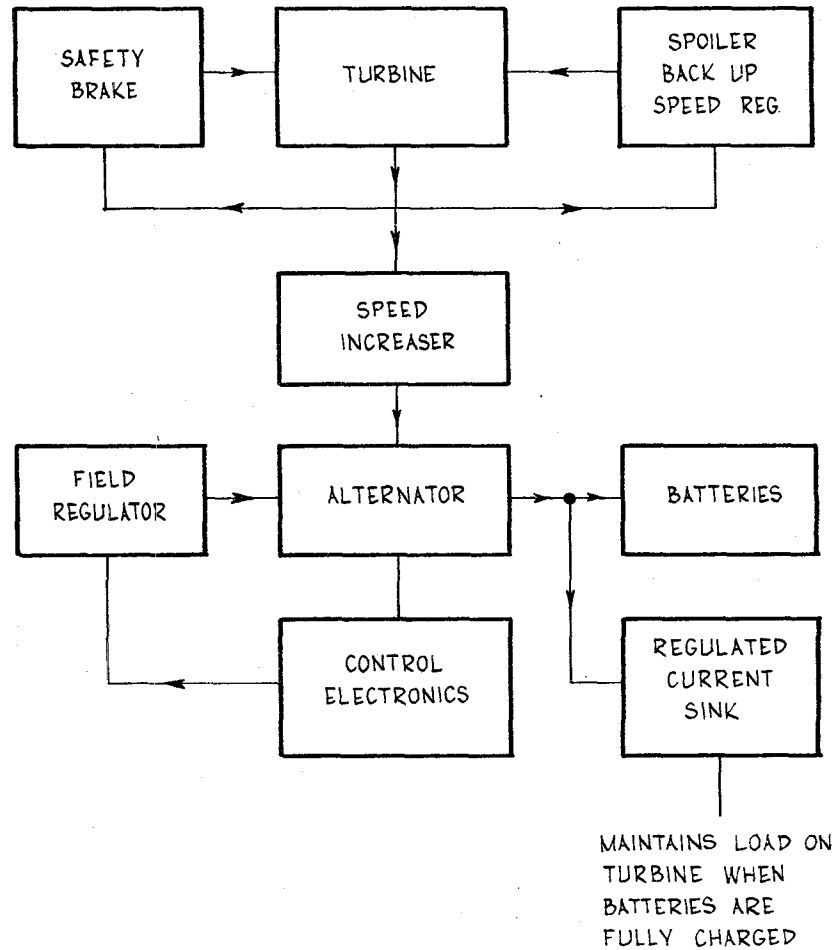
Figure 11. AEL wind-powered generator - basic system configuration

units.   In coupling the Bosch alternator to the turbine there is
a need to use a speed increaser.   Load lines for the alternator,
using various ratios, were plotted and from this information the
ratio 20:1 was selected as being the most appropriate.

(b) Commercial alternators

A limited market survey has been made into the availability of
other commercial alternators with various output, efficiency, weight
and speed combinations so that an optimum selection can be made
for the wind turbine/alternator system.   The survey indicates
that commercial low power alternators can have an efficiency of 70%.

(c) Special alternator

An examination has been made of the design characteristics required
for a special purpose alternator suitable for direct drive from the
turbine shaft.   Emphasis has been given to achieving high efficiency
as this has the effect of increasing electrical power output for a
given turbine size.   The electrical efficiency of the proposed
alternator is estimated to be 75%.   With the elimination of the
speed increaser, system overall mechanical efficiency should change
from an estimated 90% to 96%.   This low speed alternator is expected
to have a continuous power input rating of 4.5 kW and an estimated
short term rating in excess of 6.4 kW.

7.1.3 Mass of alternator

The estimated mass of the commerical alternator with speed increaser or
alternatively the direct coupled alternator is 100 kg.

7.2 Load matching

7.2.1 Introduction

Load matching is necessary for maximum utilisation of the energy which the
turbine is capable of generating at any given wind speed within the design
range of wind speeds.

Using an unregulated system as commonly found in commercial trucks, matching
between the turbine output characteristics and the load line is poor and a
significant loss in turbine power output results.   This aspect is discussed
further in paragraph 7.2.2 (a) below.

The load that the alternator presents to the turbine can be regulated by
controlling the field current if the output voltage of the alternator is
held constant by the electrical load.   There are a number of modes of
operation which must be met by the matching system.

7.2.2 Modes of operation

(a) Variable speed operation

Figure 12 shows a family of turbine torque versus turbine speed
characteristics at various wind speeds.   A locus of maximum power
is drawn through this family of curves to indicate the load torque
versus speed characteristic which would ideally match this turbine.
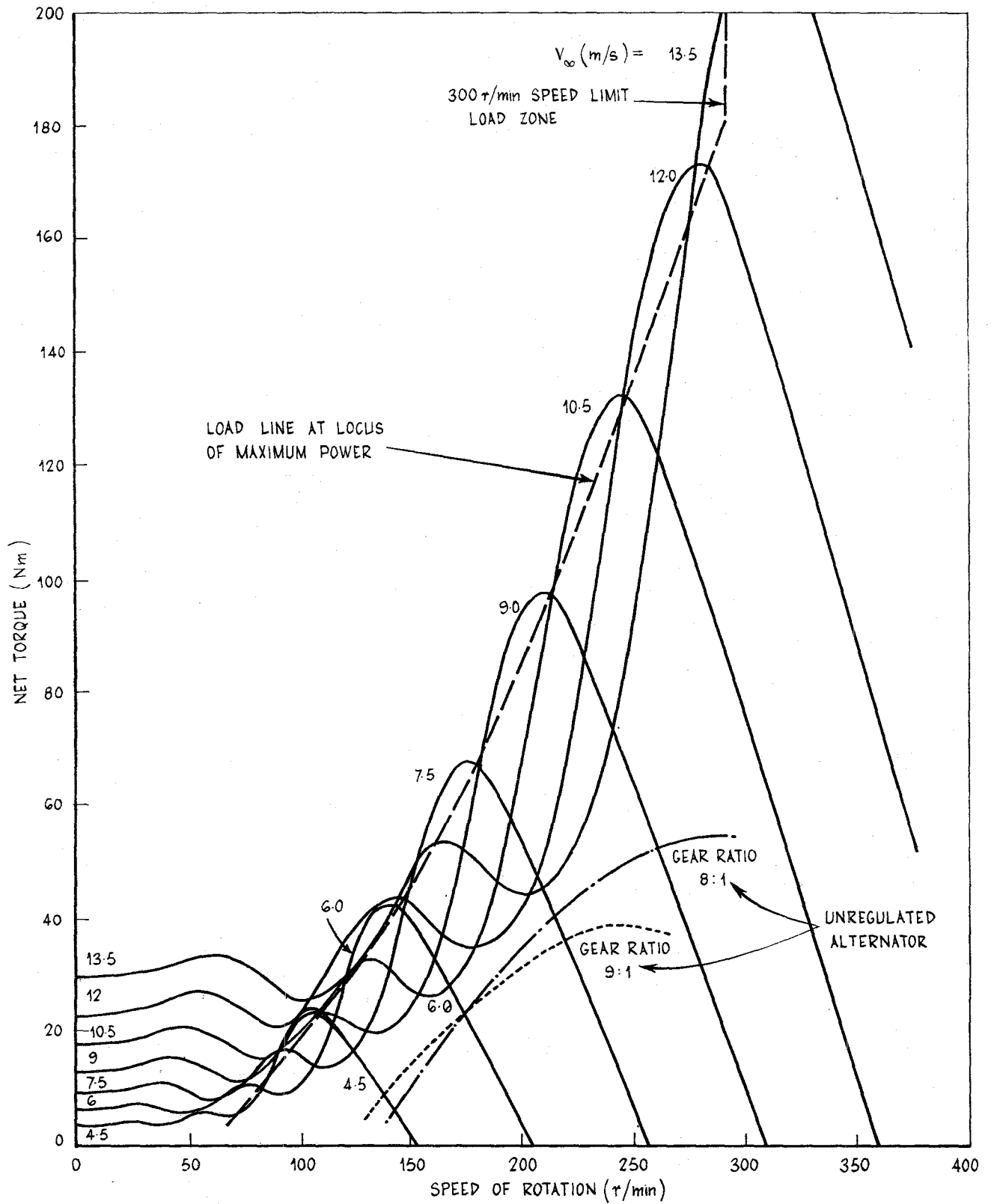
Figure 12. AEL wind-powered generator - theoretical curves for
composite Darrieus and Savonius turbine torque speed
characteristics

This ideal characteristic can be programmed into a function generator (such as a digital read only memory) and a turbine speed signal used to generate the correct alternator field current at all points throughout the working range.

It is apparent from an inspection of figure 12 that operation along the ideal load line presents control problems during large wind transients, because, at any given turbine speed, the turbine output torque is decreased for both increasing and decreasing wind speeds. A technique is proposed for accommodating this behaviour and this is discussed in Section 7.3.

The disadvantage of operating the turbine into an unregulated alternator is illustrated in figure 12 by the two load line examples drawn in for gear ratios of 8:1 and 9:1. To ensure inherently stable operation at all times, the load line must not enclose any of the turbine torque versus speed characteristic troughs. These load lines were derived for an optimum combination of fixed field current and gear ratio over the required operating range.

It would be possible to design an alternator with inherent characteristics which would improve the matching efficiency, when compared with unregulated load lines shown, but because the load line must not enclose the troughs in the turbine torque/speed characteristics, the matching is still well below the optimum which can be achieved with a regulated system. Therefore maximum power cannot be extracted from the turbine with an unregulated system.

(b) Constant speed operation

Figure 12 also shows the variable speed load line termination in a vertical section at a turbine speed of 300 r/min which is the maximum estimated operating speed for the turbine. When the preset constant speed is reached, the control of the alternator changes from the maximum power locus to the vertical section, where the loading is varied to maintain this maximum speed. In this mode, a maximum turbine output of 6.4 kW is achieved at the maximum operational wind speed of 13.5 m/s.

(c) Idle speed operation

There is a requirement for a third mode which can be defined as the idle speed mode. This is a constant speed mode operating at a very low turbine speed and is activated when the turbine is running at its maximum speed and the wind speed has increased beyond the safety limit. This idle speed is maintained until the wind speed has dropped back to a safe operating level.

7.2.3 Voltage regulation

The load that the alternator presents to the turbine can be controlled as a function of speed and field current in the manner proposed only if the output voltage is held constant. This requirement can be met with a shunt regulator which is connected in parallel to the electrical load and any batteries which are being charged by the system. In the presence of high wind power, the regulator must be capable of absorbing all of the generated power if the electrical load is absent, removed temporarily or reduced. This is the system designed for the experimental wind generator.

7.3 Load control

7.3.1 Functions

The main functions of the control systems are to regulate the load so that the maximum power is extracted from the turbine over the spectrum of wind speeds, and to ensure that stable and safe operation is maintained in a changing wind environment. The only state variable input to the control system is the rotational speed which is monitored at frequent intervals (Appendix IV). By analysing the characteristics of turbine speed changes, the control system determines whether the wind speed has increased or decreased and initiates appropriate corrections to the alternator field current to match the load to the turbine.

7.3.2 Turbine characteristics

The family of turbine torque versus speed characteristics for various wind speeds is un-nested as shown in figure 12. This means that the output torque does not continue to increase with increases in either turbine speed or wind speed alone. In the steady-state condition, the control system regulates the alternator field current to apply a load that varies with rotational speed along the maximum power locus.

To illustrate the function of the control system, suppose the turbine is operating on the maximum power locus at 180 r/min at a wind speed of 7.5 m/s. If the wind drops to 6 m/s the turbine torque drops and the turbine decelerates. From the nature of the speed change, the control system detects that the wind speed has decreased and causes the load torque to be reduced in such a manner to enable a stable operating point to be reached at the new wind speed.

If the wind speed increases suddenly to 10.5 m/s, the turbine torque decreases to a level given by the intersection of the 180 r/min constant speed line with the torque curve corresponding to 10.5 m/s wind speed. Since the load torque is unchanged initially, the turbine decelerates in a characteristic manner. The nature of the speed change enables the control system to detect that the wind speed has increased and to take corrective action. Load torque is initially decreased to enable the turbine to increase speed, and is then progressively increased as the turbine accelerates to a new operating point at a wind speed of 10.5 m/s.

7.3.3 Constant speed operation

The alternator and the electrical load can be used to vary the load torque to maintain any constant operating speed, particularly when the design speed limit is reached. As a back up, spoilers on the turbine blades and an emergency brake are fitted.

7.3.4 Mass of control unit

Estimated mass of the electronic control unit is 25 kg.

7.4 Electrical power output

7.4.1 Introduction

The electrical power output of the system is dependent on turbine power output for the particular operating conditions, the effectiveness of the turbine load matching system, the mechanical efficiency of the system and

the electrical efficiency of the alternator. Figures for turbine power
output have been established in Section 4, while matching and efficiency
have been discussed earlier in this Section.

7.4.2 Rated power output

Actual net electrical power outputs for the system when operating with the
various types of alternators at mean wind speeds of 7.5 m/s and 11.2 m/s
and turbine speeds of 180 r/min and 250 r/min are compared in Table 6.

TABLE 6. WIND-POWERED GENERATOR MAXIMUM ELECTRICAL POWER OUTPUT AT
          WIND SPEEDS OF 7.5 m/s AND 11.2 m/s

Alternator type	System mechanical efficiency (%)	Wind speed (m/s)	Turbine speed (r/min)	Turbine output (kW)	Net electrical power output (kW)
Bosch automotive machine (efficiency 50%)	90	7.5 11.2	180 250	1.3 3.7	0.6 beyond rated capacity
Commercial machine (efficiency 70%)	90	7.5 11.2	180 250	1.3 3.7	0.8 2.3
Special low speed machine (efficiency 75%)	96	7.5 11.2	180 250	1.3 3.7	1.0 2.7

(a) Using the Bosch machine, system operation is restricted to the rated
     capacity of the alternator ie 1 kW electrical output. Also, as
     system mechanical efficiency is 90% and alternator electrical
     efficiency is 50%, losses are significant and at a wind speed of
     7.5 m/s the net electrical output is 0.6 kW.

(b) For commercial alternators, with system mechanical efficiency 90%
     and alternator electrical efficiency 70%, electrical output is 0.8 kW
     at 7.5 m/s and 2.3 kW at 11.2 m/s wind speed.

(c) With the direct coupled low speed alternator, system mechanical
     efficiency rises to an estimated 96%, alternator electrical
     efficiency is 75% and electrical output is 1 kW at 7.5 m/s and
     2.7 kW at 11.2 m/s wind speed.

Figure 13. AEL wind powered generator electrical power output

7.4.3 Electrical power output - unrestricted

The variable speed maximum power output curve in figure 13 shows the electrical power output from the wind generating system under conditions of optimal load matching, with alternator efficiency 75% and system mechanical efficiency 96%. The curve applies where no rotational speed limit is imposed.

The curves shown for the constant speed mode show the electrical power output for constant speeds of 220, 250 and 300 r/min for optimal matching of the load to the turbine. At the maximum operating conditions of 300 r/min and wind speed 13.5 m/s the electrical power output is 4.6 kW.

8. ENERGY PRODUCTION

8.1 Nature of power source

The function of the wind-powered generating system is to produce energy from a highly variable power source, the wind.   The value of the system for energy production depends not only on the power conversion efficiency, which was discussed in Section 7.2, but on the efficacy with which the system harnesses the energy available over the spectrum of wind speeds.   The energy production involves the summation of power produced from a highly variable source over a period of time.

An energy storage facility is needed if a continuous supply of power is required from the wind-powered system.   The storage capacity can be determined from an assessment of the power characteristics of the turbine system, the wind speed statistics for the turbine site and the expected power demand.   The storage capacity is also influenced by the choice of rated speed of the turbine, since this has a large influence on the contribution of the relatively low frequency strong winds to energy production.

8.2 Energy distribution

An example of a wind speed distribution is shown in figure 14(a).   The profile corresponds to a mean annual wind speed of 7.5 m/s and is based on the 'wind structure' diagram of Mullett(ref.7).   A power distribution can be derived from the wind speed distribution since power is proportional to the cube of the wind speed.

Using the turbine maximum shaft power output curve in figure 5(a) and assuming a speed limit of 300 r/min, the statistical energy density has been calculated as a function of wind speed and is shown in figure 14(b).   The values plotted are time averages for a unit range of wind speed.   The area under the curve represents the total energy available from the turbine over the range of wind speeds under consideration.   It should be noted that the results in figure 14(b) correspond to the shaft power of the turbine;   any losses arising from load matching, friction, the alternator and other sources are excluded.

8.3 Energy at high wind speeds

Although the relative frequency of winds in excess of 10 m/s is low for the wind speed data shown in figure 14(a), the energy supplies at these wind speeds is considerable as shown in figure 14(b).   As figure 5(a) shows, there is a need for the turbine to operate at relatively high rotational speeds to harness the energy available in strong winds.   By extracting the energy in strong winds, a high proportion of the total energy is generated over relatively short periods of time.   Therefore, in the absence of a standby power source, the energy storage system must have adequate capacity to store this energy to cover periods of low energy production in light winds.

8.4 Regulated and unregulated load matching

The upper curve in figure 14(b) can be interpreted as the energy transferred to the alternator, neglecting friction, where the load is regulated in an optimal fashion to utilise the maximum turbine power output at all wind speeds. The assumed turbine speed limit is 300 r/min.

The lower curve in the figure represents the energy transferred to the alternator with an unregulated load comprising an optimally-matched constant-field alternator (see Section 7.2). The considerable energy gain of the regulated system over the unregulated system is considered to amply justify the additional cost and complexity of the control system.

8.5 Mean power output

If the energy distribution curve shown for optimum load matching in figure 14(b) is integrated over the operational wind speed range, the energy output is 150 kWh per 100 hours, or a mean power of 1.5 kW. This figure assumes a maximum turbine power of 6.4 kW and a maximum speed of 300 r/min.

Provided that the efficiency of the combined stages between the turbine and the load exceeds 67%, the wind-powered system has the potential for delivering 1 kW continuously when a suitable storage system is used. The combined efficiency figure includes the storage system and the probable need for an inverter, and will depend on the requirements of the load, namely the duty cycle, AC or DC, maximum power, and frequency and waveform for AC applications.
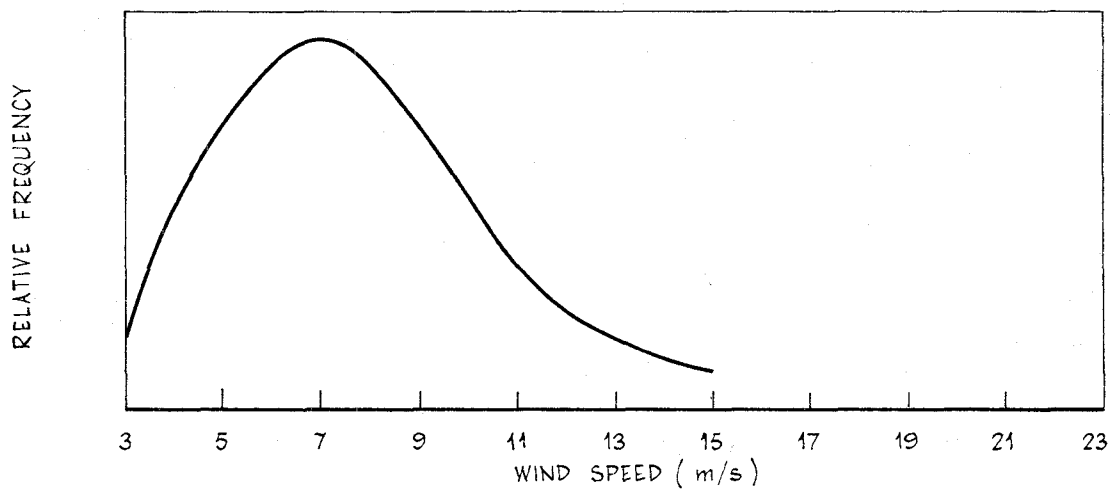
(a) Frequency distribution of wind speed
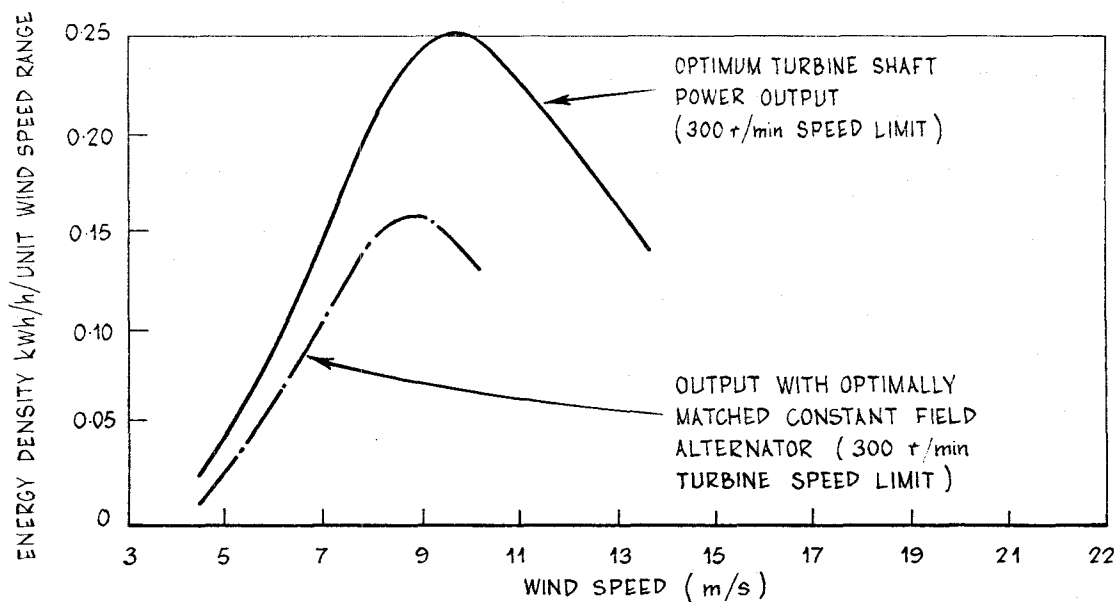
(b)   Energy density distribution

Figure 14.   AEL wind-powered generator - system energy conversion
efficiency characteristics

9. COST CONSIDERATIONS

The capital cost of a low power wind generator may be expressed in dollars per kilowatt electrical output.

The capital cost of a Dunlite horizontal axis wind generator with a rated electrical output of 2 kW at a wind speed of 12.9 m/s and using a 3962 mm (13 ft) diameter propeller mounted on a 12192 mm (40 ft) high tower is $6 000 or $3 000 per kilowatt electrical output (1981 prices).

The AEL concept as described has a rated electrical output of up to 2.7 kW at a wind speed of 11.2 m/s with a turbine of 3660 mm diameter and 3660 mm blade length and it possesses a number of features which make it attractive as an alternative low power source.

  (1)   The turbine is rugged and simple being constructed from lightweight straight sections which can be extruded from aluminium alloy at low cost.

  (2)   The turbine blades are rigidly attached to the supporting structure ie the blades are non-pivoting.

  (3)   The turbine can be coupled directly to a low speed alternator. Thus the usual speed increaser can be eliminated and therefore transmission losses are significantly reduced.

  (4)   The control system based on the microprocessor provides a means of continuously modifying the load torque applied to the turbine. The system ensures that the alternator load characteristic is optimally matched to the turbine torque-rotational speed curves for various wind speeds throughout the whole range of operation.

  (5)   In summary it can be said that the system is simple and rugged and offers promise of high performance at moderate cost.

10. PERFORMANCE TEST AND EVALUATION MODEL

A model of the wind-powered generator system has been constructed by the students of the AEL Apprentice Training School, Salisbury, South Australia, as an exercise, so that the experimental system may be evaluated.

For preliminary tests, the turbine is mounted on a rigid free standing tower which is anchored to a concrete base.

Figure 15 shows the test model in course of installation at the test site.

11. SUMMARY OF RESULTS

  (1)   Operating within guidelines (see Table 1) based on the ABCA Paper entitled "Concept Paper, Electrical Power Sources for 1986 and beyond" (ref.2) a design concept has been produced for a 1 kW wind-powered generator suitable for use in isolated locations. Design criteria include high power to weight ratio, simplicity of assembly and potential for fixed, mobile or portable applications. The concept features a Darrieus straight blade rotor, an alternator and a control system which optimises the power coupling from turbine to load at all wind speeds within the design envelope.

(2) The Darrieus turbine has been designed to operate efficiently at wind
     speeds up to 13.5 m/s. To meet the latter requirement the turbine
     structure has been designed to permit continuous operation at speeds up
     to 300 r/min to take full advantage of the increased energy available at
     the higher wind speeds.

(3) The turbine is capable of producing a maximum shaft power output of
     1.3 kW at 180 r/min at a wind speed of 7.5 m/s and a maximum shaft power
     output of 6.4 kW at 300 r/min at a wind speed of 13.5 m/s.

(4) Net electrical power outputs for the system when operating with the
     various types of alternators at mean wind speeds of 7.5 m/s and 11.2 m/s
     and turbine speeds of 180 r/min and 250 r/min are as follows:-

     (a) Using the Bosch machine, system operation is restricted to the
          rated capacity of the alternator ie 1 kW electrical output.
          Also, as system mechanical efficiency is 90% and alternator
          electrical efficiency is 50%, losses are significant and at a
          wind speed of 7.5 m/s the net electrical output is 0.6 kW.

     (b) For commercial alternators, with system mechanical efficiency
          90% and alternator electrical efficiency 70%, electrical output
          is 0.8 kW at 7.5 m/s and 2.3 kW at 11.2 m/s wind speed.

     (c) With the direct coupled low speed alternator, system mechanical
          efficiency rises to an estimated 96%, alternator electrical
          efficiency is 75% and electrical output is 1 kW at 7.5 m/s and
          2.7 kW at 11.2 m/s wind speed.

(5) Using the microprocessor based control system to provide optimum
     matching by regulating turbine speed, it is possible to achieve a very
     high utilisation of the energy output from the turbine. This effect is
     particularly significant at the higher wind speeds where the matching
     cannot normally be achieved with an unregulated system. If the wind
     energy distribution curve is integrated over the whole range of wind
     speeds up to 13.5 m/s, the system has the potential of delivering 1 kW
     of electrical power continuously when combined with a suitable storage
     system.

(6) Independent starting capability is provided by a small Savonius rotor of
     1.06 m^2 swept area which represents 7.92% of the Darrieus rotor swept
     area. The Savonius rotor should accelerate the Darrieus rotor to a
     speed ratio of 1 within 2 min at a wind speed of 7.5 m/s.

(7) Structural computations confirm that the Darrieus rotor is capable of
     operating safely at speeds up to 300 r/min with wind speeds up to 13.5 m/s.
     The major source of induced stress in the structure is centrifugal force
     and the computed factor of safety for the rotor blades is 2.7, based on
     the yield strength of the material. Stresses due to aerodynamic
     fluctuating loads are low by comparison, representing 2% of the induced
     stress due to centrifugal effects.
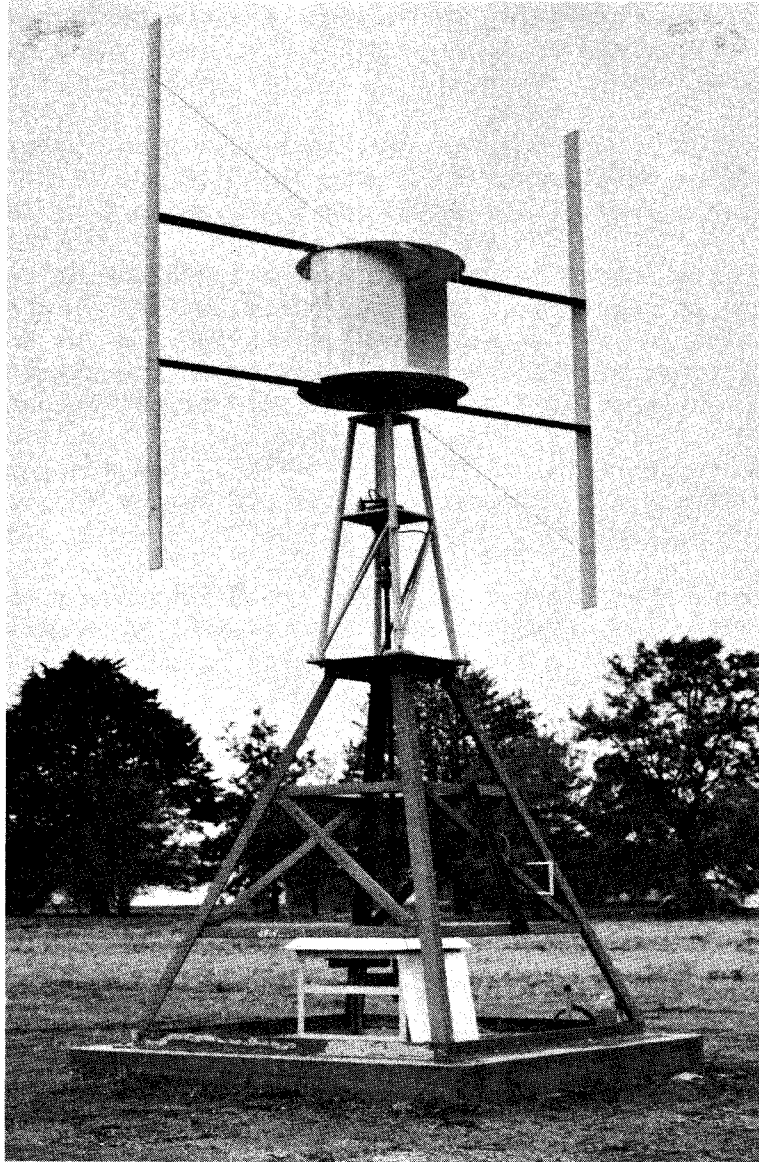
Figure 15. AEL wind-powered generator - performance test and evaluation model

(8)   Aerodynamic spoilers are feasible as a safeguard to limit rotor speed in
      the event of an electrical or transmission system failure. Alternatively
      or as a further safeguard, a hydraulic disc brake system can be fitted to
      operate at a predetermined speed.

(9)   Structural components can be scaled and the system adapted to suit low
      power or high power output requirements.

(10) The straight blade configuration is practicable to fabricate as an
      extrusion in aluminium alloy, specification 6061 - T6 in the section
      shown.

(11) The Darrieus rotor with straight blade configuration and essentially
      light weight sections is simple to pack, transport and assemble. When
      combined with the Savonius rotor and light weight tubular guyed tower,
      the resultant assembly is easy to erect in the field and has potential
      for fixed, mobile or portable applications.

(12) Total mass of the system is 600 kg approximately which includes turbine
      85 kg, tower 385 kg, alternator 100 kg and control unit 25 kg.

12. CONCLUSIONS

(1)   This study establishes a design concept for a nominal 1 kW wind-powered
      generator for use as an alternative power source for isolated locations.
      The system utilises a Darrieus straight blade rotor with matched load
      and a microprocessor based control system.

(2)   The optimally matched load results in a system of superior efficiency
      and higher power output relative to conventional wind-powered generator
      systems of comparable size using fixed or stepped loads.

(3)   The design configuration is easy to assemble and erect and has potential
      for fixed, mobile or portable applications.

(4)   The system has a number of design features which can be expected to make
      the system very competitive on cost with horizontal axis systems.

(5)   The components and method of assembly can be expected to provide a
      reliable and low maintenance system.

(6)   The design configuration can be scaled to produce lower or higher
      powers.

13. RECOMMENDATIONS

It is recommended that the work involved in carrying out this study and in
constructing the test and evaluation model be recognised and supported by the
initiation of a follow-on programme to evaluate performance at component and
system level.

Accordingly the plan should include:-

    (a)   evaluation of turbine structural performance

    (b)   evaluation of turbine aerodynamic performance

    (c)   development and test of spoiler units

    (d)   evaluation of alternator performance

    (e)   optimisation and evaluation of electrical control

    (f)   development and test of the guyed tubular tower

Once these initial objectives have been achieved, it is desirable that the wind-powered generator be deployed in the field for an extended period for evaluation of overall performance.

14. ACKNOWLEDGEMENT

NOTATION

A   swept area

C_P mean power coefficient, $= \dfrac{\text{power}}{k\ \frac{1}{2}\ \rho\ V_\infty^3\ A_o}$

C_P' mean power coefficient based on local velocity,

$$= \frac{\text{power}}{k\ \frac{1}{2}\ \rho\ V^3\ A_o}$$

$C_{P\,\phi}$ blade power coefficient at angle ϕ,

$$= \frac{\text{power }(\phi)/\text{blade}}{k\ \frac{1}{2}\ V_\infty^3\ A_o}$$

C_T mean thrust coefficient,

$$= \frac{\text{thrust}}{\frac{1}{2}\ \rho\ V_\infty^2\ A_o}$$

C_T' mean thrust coefficient based on local velocity,

$$= \frac{\text{thrust}}{\frac{1}{2}\ \rho\ V^2\ A_o}$$

$C_{Q\,\phi}$ blade torque coefficient at angle ϕ,

$$= \frac{\text{torque }(\phi)/\text{blade}}{\frac{1}{2}\ \rho\ V_\infty^2\ A_o\ R_o}$$

D   diameter, also drag

F_N normal force on blade

F_T tangential or thrust force on blade

F_1 lift force on blade element

F_d drag force on blade element (or spoiler)

F_n normal force on blade element

F_t tangential or thrust force on blade element

I   polar moment of inertia of rotor

L   length; also lift

N   number of blades; also speed of rotation, r/min

Q   torque

R   radius

T   thrust

U	resultant wind speed, figure I.2
V	local wind speed at rotor, figure I.5
V_1	wind speed downstream from rotor, figure I.5
V_∞	freestream wind speed
c	aerofoil chord; also reference dimension for lift and drag coefficient
c_{1a}	lift curve slope, dc_1/da
c_1	blade lift coefficient, $= \dfrac{\text{lift}}{\frac{1}{2}\rho U^2 c}$
$c_{1_{max}}$	maximum lift coefficient
c_d	drag coefficient, $= \dfrac{\text{drag}}{\frac{1}{2}\rho U^2 c}$
c_{d_o}	blade drag coefficient at zero lift
c_n	normal force coefficient, equation (I.4)
c_t	tangential or thrust force coefficient, equation (I.4)
h	displacement of trailing edge of spoiler normal to chordwise axis of aerofoil
i_f	interference factor for spar-aerofoil junction
k	Betz factor, $= \dfrac{16}{27}$
1	spanwise length
t_1	time to accelerate to $\mu_0 = 1$
Ω	angular velocity of rotation
Ω_1	angular velocity of rotation corresponding to $\mu_0 = 1$
a	angle of attack; also angular acceleration
β	inclination of spar, tie rod or brace to horizontal plane
μ	speed ratio, $= R\Omega/V_\infty$
μ'	local speed ratio, $= R\Omega/V$
ρ	air density
σ	rotor solidity, $= Nc/R_o$
ϕ	azimuth angle, figure I.2

Subscripts

o   Darrieus rotor

s   Savonius rotor

sp   spoiler

w   windage

wi   windage including interference effects

Superscript

i   initial or starting condition

REFERENCES

No.	Author	Title
1	National Energy Advisory Committee (NEAC)	"Proposal for a Research and Development Program for Energy". NEAC Report No.3, December 1977
2	US Army Mobility and Equipment Research and Development Command	"Memorandum for Record". American British Canadian and Australian Fifth Meeting of the Quadripartite Working Group on Electrical Power Sources (Fort Belvoir Virginia USA) 5 to 11 May 1976
3	Standards Association of Australia (SAA)	"SAA Loading Code-Wind Forces". Australian Standard 1170 Part 2, 1975
4	Shankar, P.N.	"On the Aerodynamic Performance of a Class of Vertical Shaft Windmills". Proc. Roy. Soc. London, A349, 35-51, 1976
5	Warne, D.F. and Calnan, P.G.	"Generation of Electricity from the Wind". Proc. IEE Vol.124, No.11R, November 1977
6	Abbott, I.H. and von Doenhoff, A.E.	"Theory of Wing Sections". Dover, New York, 1958
7	Mullett, L.F.	"Surveying for Wind Power in Australia". Journal, Institution of Engineers Aust. March 1957
8	Newman, B.G.	"Measurements on a Savonius Rotor with Variable Gap". Proceedings of Symposium - Wind Energy: Achievements and Potential, University of Sherbrooke, May 1974
9	Reuter, R.C.	"Tower Analysis". Proceedings of the Vertical Axis Wind Turbine Technology Workshop, Albuquerque, New Mexico, SAND 76-5586, 18 to 20 May, 1976
10	Diesendorf, M.	"Recent Scandinavian R and D in Wind Electric Power-Implications for Australia". Search Vol.10, No.5, pp.165 to 173, May 1979
11	Wilson, R.E., Lissaman, P.B.S., and Walker, S.N.	"Aerodynamic Performance of Wind Turbines". Oregon State University Report NSF/RA-760228, June 1976
12	Hoerner, S.F.	"Fluid-Dynamic Drag". New Jersey, USA, Published by the Author, 2nd edition, 1965

No.	Author	Title
13	-	"The Structural Members Users Group Ltd. Programs". University of Virginia Station, Charlottesville Virginia, 22903
14	Feltz, L.V. and Blackwell, B.F.	"An Investigation of Rotation Induced Stresses of Straight and of Curved Vertical-Axis Wind Turbine Blades". Sandia Laboratories, Albuquerque, New Mexico, SAND 74-0379, March 1975
15	Spotts, M.F.	"Design of Machine Elements". Prentice-Hall, Inc. Englewood Cliffs, N.J. 3rd edition, 1961
16	Faires, V.M.	"Design of Machine Elements". The Macmillan Company, New York, 4th edition, 1966
17	Maleev, V.L.	"Machine Design". Internation Textbook Co. Scranton, Pennsylvannia, 9th edition, December 1949
18	FAG	"FAG Ball Bearings". "FAG Roller Bearings". Catalogue 41000 E issued by Bearing Service Co. of Aust. Pty. Ltd., 1966
19	SKF	"Ball and Roller Bearings". Catalogue No.2403 E, issued by the SKF Ball Bearing Co. (Australia) Pty. Ltd., 1962

APPENDIX I

AERODYNAMIC PERFORMANCE ANALYSIS

I.1 Basic considerations

The primary power producing component of the wind turbine is the Darrieus
rotor which, in aerodynamic terms, comprises the aerofoil blades which are
capable of extracting energy from the wind.   The other portions of the turbine
structure such as horizontal spars of aerofoil form or otherwise, tie rods
and braces generally do not contribute useful power and are not part of the
Darrieus rotor in the performance analysis.   The power loss or windage
arising from the motion of these components relative to the local wind is
computed as a separate item to be subtracted from the power produced by the
Darrieus rotor.   In the case of a Darrieus rotor of troposkien form, there
may be no rotating structural elements other than the curved power-producing
aerofoil blades which then constitute the total Darrieus rotor.

The Darrieus rotor is not generally self-starting as explained in Section I.2,
and some means of accelerating the rotor to a threshold rotational speed
relative to wind speed is required.   Because the present study is concerned
with a power generating system for remote areas, a self-starting wind-driven
Savonius rotor is preferred to an electrical starting system.   The swept
area of a suitable Savonius rotor was estimated initially to be about 10% of
the Darrieus rotor swept area, and on this basis it is assumed in the
performance analysis that the operation of the Darrieus rotor is relatively
unaffected by the presence of the Savonius rotor.   However, the Savonius
rotor operates in the induced velocity field of the Darrieus rotor, and so
its characteristics differ from those pertaining to free air conditions.
In terms of the combined power output of the Darrieus and Savonius rotors,
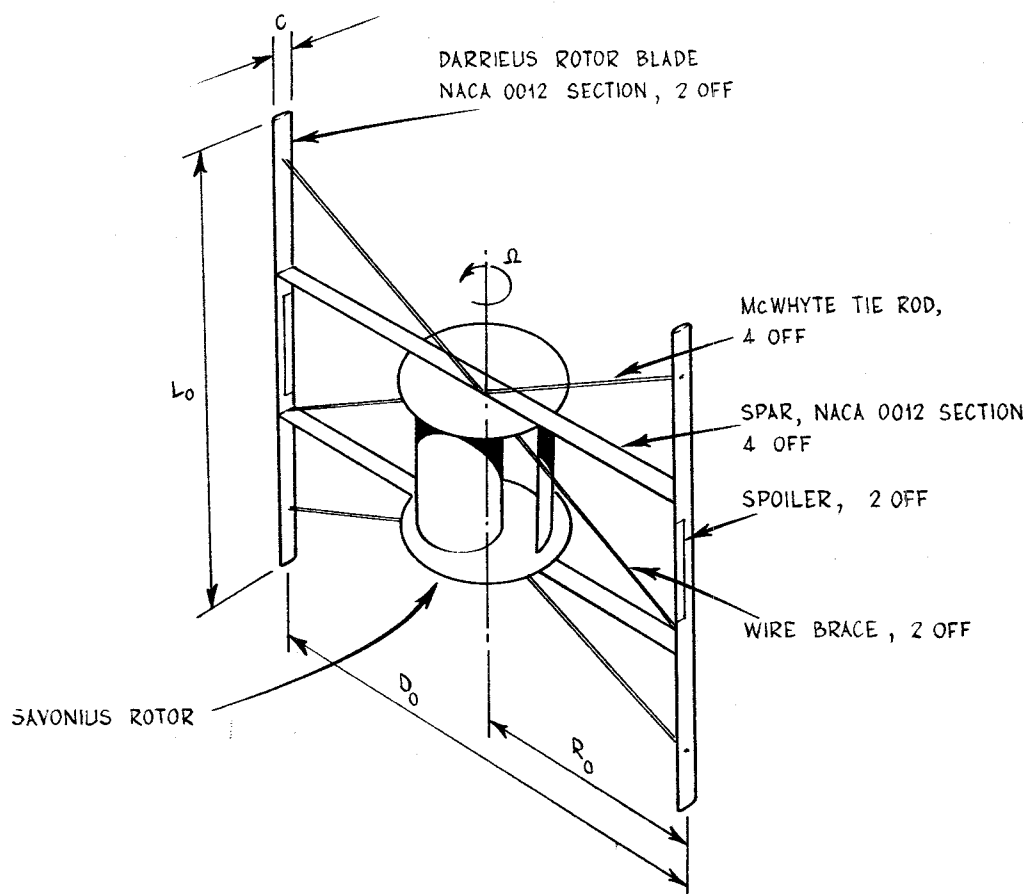the assumptions above are not likely to result in excessive errors.

Figure I.1   Turbine scheme

Summing up, for the purposes of performance calculations the turbine will be considered to comprise the following:

    (a) A Darrieus rotor consisting of aerofoil blades operating free of structural and Savonius rotor interference;

    (b) A conventional Savonius rotor operating in the induced velocity field of the Darrieus rotor;

    (c) All rotating structural elements subject to windage, operating in the induced velocity field of the Darrieus rotor.

A diagram of the turbine showing the principal components and notation is given in figure I.1.

I.2 Principle of operation of Darrieus rotor

The Darrieus rotor operates on the principle that a lifting surface operating efficiently at a high lift to drag ratio produces a force component acting in the forward direction along the aerofoil axis.   Consider an element of an aerofoil blade located at a radius R_o from the axis of rotation as shown in figure I.2. Designating the angular velocity by Ω, the absolute speed of the blade is given by $R_o \Omega$, and this is taken to be large compared with the local wind speed V.   By combining the blade velocity $R_o \Omega$ and wind velocity V in a vector diagram, it is seen that the blade element operates in a resultant wind velocity U at an angle of attack α.   A lift force F_1 and a drag force F_d are produced normal to and in the direction of U respectively.   As can be seen in figure I.2, the lift force produces a counter-clockwise torque which acts to sustain the rotation whilst the drag force produces a torque which opposes rotation.   Provided that the lift to drag ratio L/D is sufficiently large, the net result is a torque which maintains the rotation continuously.

The mechanism of production of the driving torque may be seen more clearly if the lift and drag forces are resolved in the radial and tangential directions as shown in figure I.2.   Over a full angular cycle of 2π rad, the normal force F_n produces no useful torque.   However, in the efficient lifting regime of the aerofoil, a tangential forward-acting force F_t is generated, and it is this force which provides the driving torque necessary to maintain the motion and produce useful power.

For cases where $R_o \Omega$ is large compared to V, the aerofoil element operates in an unstalled condition for all values of azimuthal angle ϕ, developing lift and drag forces as shown for four values of ϕ in figure I.3.   When the aerofoil blade speed approaches the magnitude of the local wind speed, the aerofoil element operates in a stalled condition at a high angle of attack for a proportion of each rotational cycle as shown in figure I.4.   Under these circumstances, the lift to drag ratio of the aerofoil is relatively low and the tangential force opposes the rotation for a range of azimuthal angles. As the blade speed decreases further relative to wind speed, the aerofoil element becomes more severely stalled over a greater range of azimuthal angles and thus negligible torque is available for starting.

As the rotational speed increases, the ratio of aerofoil blade velocity to local wind speed $R_o \Omega /V$ becomes large, perhaps in excess of 10, and by referring back to figure I.3 it can be seen that the angle of attack becomes smaller at all azimuthal angles ϕ.   The aerofoil element therefore operates at decreasing lift levels in conjunction with a declining lift to drag ratio.
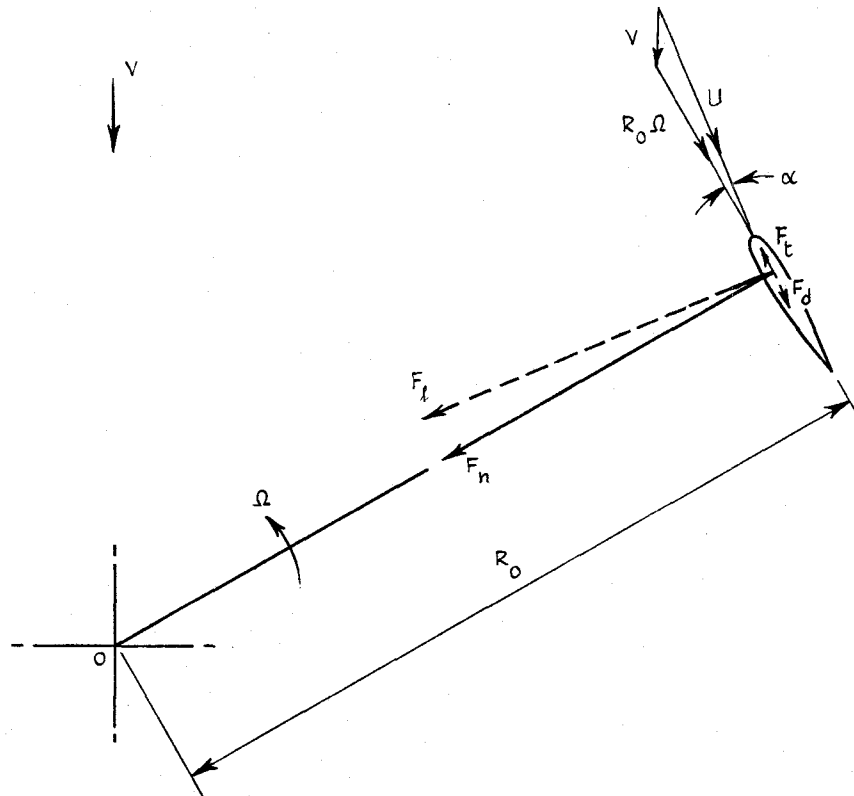
Figure I.2   Operating principle of Darrieus rotor
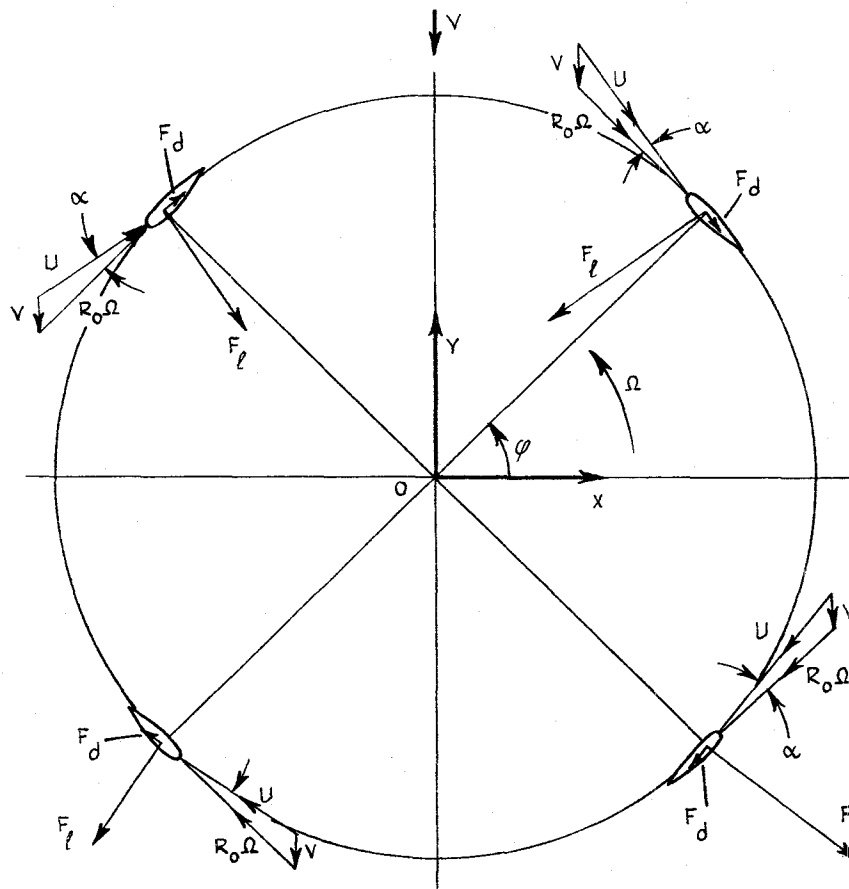
Figure I.3   Forces on blade element, $R_o \Omega \gg V$

Therefore, the power output decreases as rotational speed increases beyond a threshold value.

This effect is shown by recourse to an elementary analysis as follows:

$$F_t = F_1 \sin a - F_d \cos a \qquad (I.1)$$

where F_t, F_1 and F_d are the tangential, lift and drag forces acting on a blade element and a is the angle of attack. For $a \leqslant 0.15$ rad, $F_1 \propto c_{1a} \cdot a$, $\sin a \approx a$ and $\cos a \approx 1$, where c_{1a} is the lift curve slope of the aerofoil blade and a is in radians. From equation (I.1),

$$F_t \propto c_{1a} \cdot a \left(a - \frac{1}{(L/D)} \right) \qquad (I.2)$$
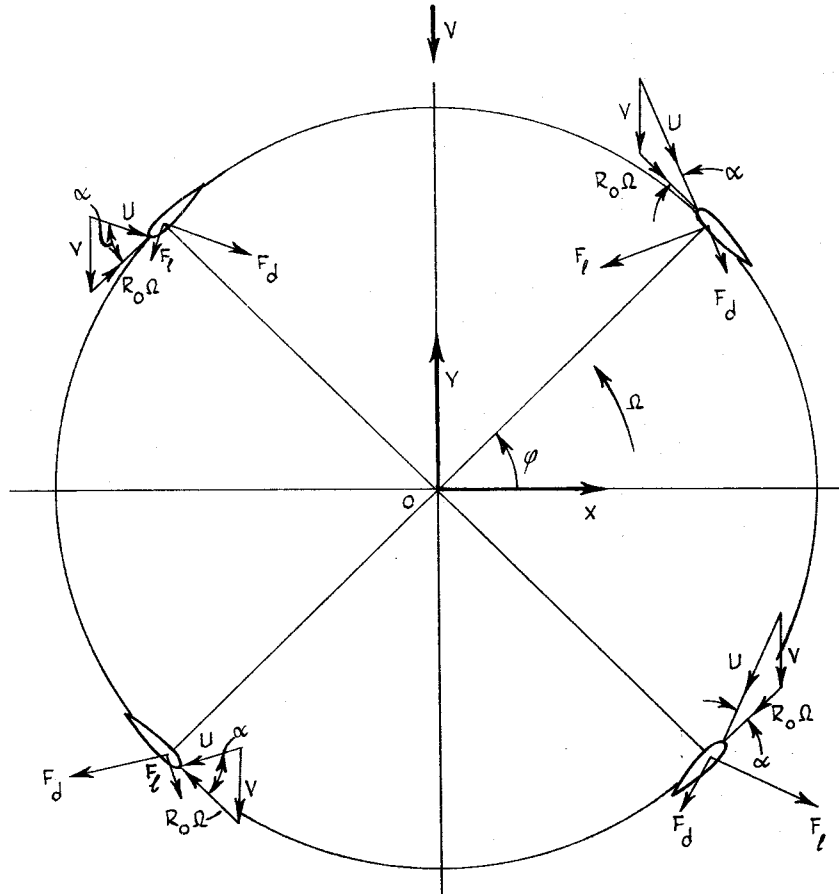
Figure I.4　　Forces on blade element, $R_o \, \Omega \approx V$

where L/D is the lift to drag ratio.   Since the power output is directly related to F_t, as u decreases the power output declines and becomes zero when $u = \frac{1}{(L/D)}$. The significance of both a and the lift to drag ratio in relation to F_t and hence power output is clearly seen in equation (I.2) which shows that an efficient aerofoil for a Darrieus rotor will combine a high lift curve slope c_{1a} with a high lift to drag ratio peaking at a relatively high angle of attack.

I.3 Derivation of rotor size

The design specification called for a nominal electrical power output of 1 kW without reference to a load factor or wind speed characteristics.   It was assumed in the early phase of the work that an efficiency of conversion from mechanical to electrical energy of about 70% could be achieved with a suitable alternator.   Making a small allowance for other losses of about 5% of the mechanical power, a nominal turbine power output of 1.5 kW was taken as the design goal.

To convert this power output figure to a set of rotor dimensions requires consideration of the performance characteristics of a Darrieus rotor together with wind speed data for the chosen site.   To simplify blade manufacture, an early decision was made to use two straight blades as the power-producing elements of the rotor.   For good proportions, a blade length L_o to diameter D_o ratio of unity was chosen and the swept area of the rotor is therefore given by D_o^2.   This area is 50% greater than the swept area of a troposkien rotor with the same diameter and height.   From the performance data of Shankar(ref.4) for a straight blade rotor, the maximum power output of the rotor per unit of swept area is established as a function of speed ratio $R_o \Omega /V_\infty$ and solidity Nc/R_o, where V_∞ is the freestream wind speed, N is the number of blades and c is the blade chord.   As will be shown later, a solidity of 0.2 gives a desirable combination high peak output power in conjunction with a moderate power output over a range of rotational speed.

As mentioned in Section 4.1 a mean annual wind speed of 7.5 m/s was adopted for design purposes, and this in conjunction with the aerodynamic performance data gives 3660 mm as both the diameter and blade length of a rotor with a nominal 1.5 kW mechanical power output.   The design parameters are summarised in the table below.

The total wind energy available is proportional to the integration of the cube of the wind speed with time for the wind speed distribution at the site. Therefore, the total annual energy output of the wind-powered generator is greatly increased if the machine has the structural and electrical capability to operate at wind speeds greater than the mean speed.   Diesendorf(ref.10) suggests that the optimum design rated wind speed of a wind turbine, namely that which maximises energy production over a year, is twice the mean annual wind speed.   Further, he indicates that the minimum energy cost (for large wind turbines) is obtained when the design rated wind speed is 1.5 times the mean wind speed.

TABLE I.1   DARRIEUS ROTOR CHARACTERISTICS

Darrieus rotor type	straight blade, $D_o/L_o = 1$
Rotor diameter	3660 mm
Blade length	3660 mm
Number of blades	2
Aerofoil section	NACA 0012
Aerofoil chord	180 mm
Solidity (Nc/R_o)	0.2
Nominal power output at mean wind speed	1.5 kW
Nominal speed of rotation	180 r/min
Mean wind speed	7.5 m/s

I.4   Darrieus rotor performance

I.4.1   Mean power and thrust

The aerodynamic performance of the Darrieus rotor comprising two straight NACA 0012 aerofoil blades 3660 mm long situated at a radius of 1830 mm from the axis of rotation has been calculated according to the method of Shankar(ref.4).   Computations encompassed both average power, torque and forces, together with instantaneous power, torque and forces as functions of azimuthal angle ϕ.

In Shankar's analysis, the induced velocity at the rotor is assumed to be given by simple momentum theory arguments; subsequently a blade element analysis yields equations from which power, torque and thrust may be calculated.   For ease of computation, the uniform induced velocity analysis has been used here in lieu of the more accurate non-uniform induced velocity approach.   It is not proposed to reproduce full details of Shankar's analysis here; the interested reader may consult reference 4 for further information.

Using actuator disc theory (see figure I.5) and applying the equations of continuity, momentum and energy to a large control volume leads to the result:

$$\frac{V}{V_\infty} = \frac{1}{(1 + \tfrac{1}{4} C'_{T_o})}, \qquad\qquad (I.3)$$

where C'_{T_o} is the thrust coefficient based on the local wind speed V (figure I.5), and is given by

$$C'_{T_o} = \frac{T_o}{\tfrac{1}{2} \rho V^2 A_o}$$
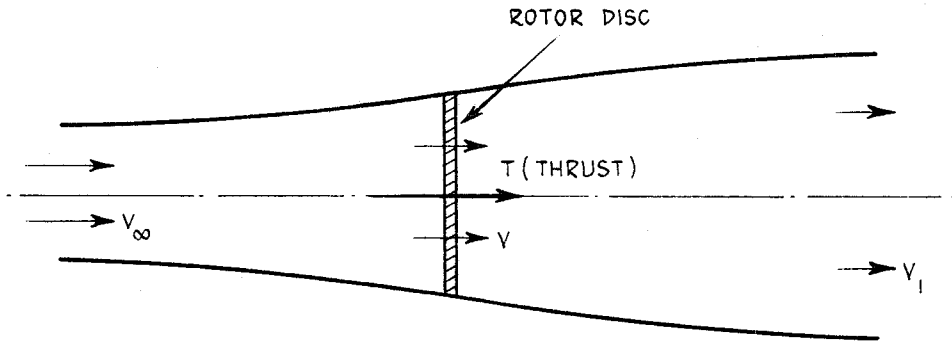
Figure I.5   Actuator disc model of rotor

In this equation A_o is the swept area of the rotor, T_o is the thrust and ρ is the air density.   By recourse to momentum theory, it is possible to show that the maximum power output is given by

$$P = k \; \tfrac{1}{2} \rho \; V_\infty^3 \; A_o,$$

where k (= 16/27) is the Betz factor and represents the fraction of the incident kinetic energy flux which is extracted from the airstream.

Definitions of solidity σ, tip speed ratio μ'_o and power coefficient C'_{P_o} based on the local speed V are as follows:

$$\sigma = \frac{Nc}{R_o},$$

$$\mu'_o = \frac{R_o \; \Omega}{V}$$

and

$$C'_{P_o} = \frac{P_o}{k \; \tfrac{1}{2} \rho \; V^3 \; A_o}.$$

For the straight blade rotor, the power and thrust equations become:

$$C'_{P_o} = \frac{1}{4\pi \; k} \int_0^{2\pi} \sigma \; \mu'_o \left(\frac{U}{V}\right)^2 c_t \; d\phi \qquad (I.4(a))$$

and

$$C'_{T_o} = \frac{1}{4\pi} \int_0^{2\pi} \sigma \left(\frac{U}{V}\right)^2 (c_n \sin\phi - c_t \cos\phi) \, d\phi, \qquad (I.4(b))$$

where

$$\left(\frac{U}{V}\right)^2 = (\mu'_o + \cos\phi)^2 + \sin^2\phi, \qquad (I.4(c))$$

$$a = \tan^{-1}\left(\frac{\sin\phi}{\mu'_o + \cos\phi}\right), \qquad (I.4(d))$$

$$c_t = c_1 \sin a - c_d \cos a \qquad (I.4(e))$$

and

$$c_n = c_1 \cos a + c_d \sin a. \qquad (I.4(f))$$

Using lift and drag data, c_1 and c_d, appropriate to the Reynolds number range of the aerofoil, numerical integration of equations (I.4(a)) and (I.4(b)) is carried out with the aid of equations (I.4(c)) to (I.4(f)) to obtain the power and thrust coefficients C'_{P_o} and C'_{T_o} which are based on local wind speed V. Now the practically useful tip speed ratio μ_o, power coefficient C_{P_o} and thrust coefficient C_{T_o} are those based on freestream wind speed V_∞. By using equation (I.3) for the induced velocity, these quantities can be related to the corresponding coefficients based on the local wind speed as follows:

$$\mu_o = \mu'_o \frac{V}{V_\infty} = \frac{\mu'_o}{(1 + \frac{1}{4} C'_{T_o})}, \qquad (I.5(a))$$

$$C_{T_o} = C'_{T_o} \left(\frac{V}{V_\infty}\right)^2 = \frac{C'_{T_o}}{(1 + \frac{1}{4} C'_{T_o})^2} \qquad (I.5(b))$$

and

$$C_{P_o} = C'_{P_o} \left(\frac{V}{V_\infty}\right)^3 = \frac{C'_{P_o}}{(1 + \frac{1}{4} C'_{T_o})^3} \qquad (I.5(c))$$

A computer program was written to obtain the results and the computational procedure was to choose a value of local speed ratio μ'_o and to compute $\left(\frac{U}{V}\right)^2$, a, c_t and c_n as functions of the azimuthal angle ϕ. The integrals

in equations (I.4(a)) and (I.4(b)) were evaluated numerically at a minimum of twenty four values of ϕ (15° intervals), and the true speed ratio μ_o, power coefficient C_{P_o} and thrust coefficient C_{T_o} were calculated from equations (I.5(a)), (I.5(b)) and (I.5(c)).

The NACA 0012 aerofoil data as tabulated by Shankar in reference 4 were used in the present computations. The data correspond to a chord Reynolds number of about 3×10^5 which falls within the range of Reynolds number encountered by the present aerofoil blades with a chord of 180 mm. The aerofoil data are summarised briefly as follows:

  (i)   lift curve slope $c_{l\alpha}(\text{rad}^{-1}) = 5.73$;

  (ii)   zero lift drag coefficient, $c_{do} = 0.010$;   and

  (iii) maximum lift coefficient, $c_{l_{max}} = 0.86$ at $\alpha = 12^o$.

It should be noted that the aerofoil data are described as section characteristics and are therefore strictly applicable to two dimensional flows only. No corrections have been made at this stage to account for three dimensional effects resulting from the finite span of the aerofoils.

Results of the present computations are shown in non-dimensional coefficient form in figures I.6 and I.7. Figure I.6 shows that, on the basis of the present analysis, the chosen solidity of 0.2 gives the highest maximum power output. The characteristic behaviour of a Darrieus rotor is evident in all the curves shown in figure I.6, namely that the power coefficient increases initially with speed ratio, reaches a maximum and then declines as speed ratio increases further.

The calculated peak power coefficient of 0.72 at a solidity of 0.2 is a measure of the aerodynamic efficiency of the Darrieus rotor, which is therefore commendably high. However, as Shankar points out, the analysis errs on the optimistic side, and lower values of C_{P_o} are expected in practice.

The thrust coefficient of a Darrieus rotor is shown as a function of speed ratio and solidity in figure I.7. For a solidity of 0.2, the thrust coefficient corresponding to the peak power condition is 0.9, which means that the thrust on the rotor is 90% of the force equivalent to the dynamic pressure of the freestream wind acting on the swept area of the rotor.

The maximum power output of the Darrieus rotor and the corresponding thrust are shown dimensionally in figure I.8 as functions of wind speed. In the absence of losses the peak power output at the mean wind speed of 7.5 m/s is 1.5 kW which occurs at a rotational speed of 180 r/min, and the corresponding thrust on the rotor is 430 N. The peak power output increases rapidly according to the cube of the wind speed as mentioned previously, and the speed of rotation at which the maximum power occurs increases in proportion to wind speed. Therefore, in the absence of other constraints such as power transmission or alternator capacity, structural limitations will determine the maximum power capability of the turbine.
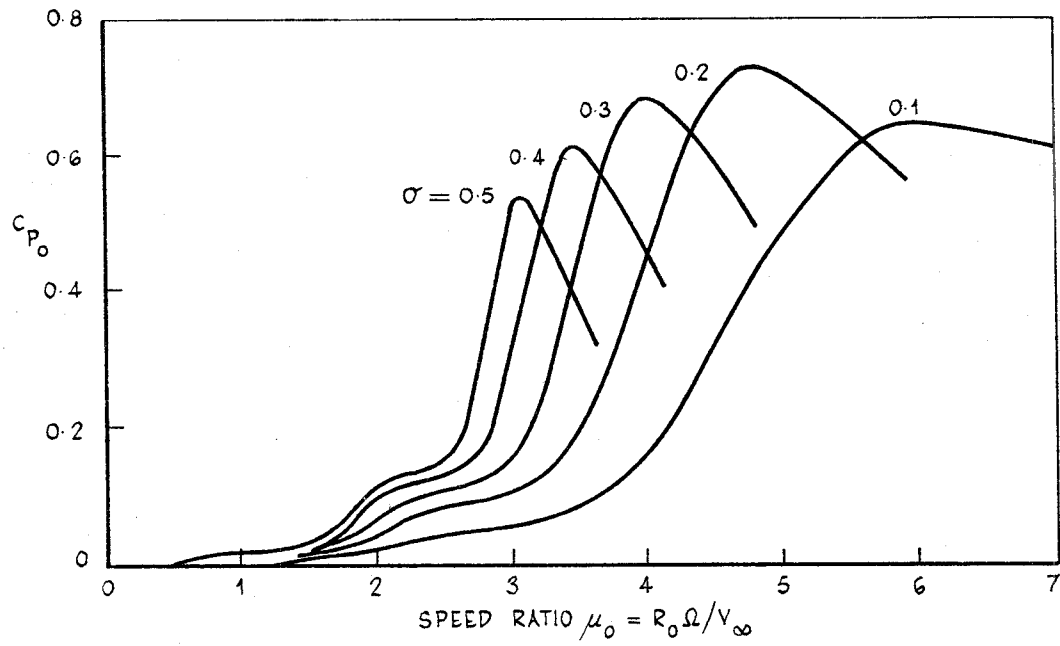
Figure I.6   Variation of power coefficient of Darrieus rotor with
solidity and speed ratio
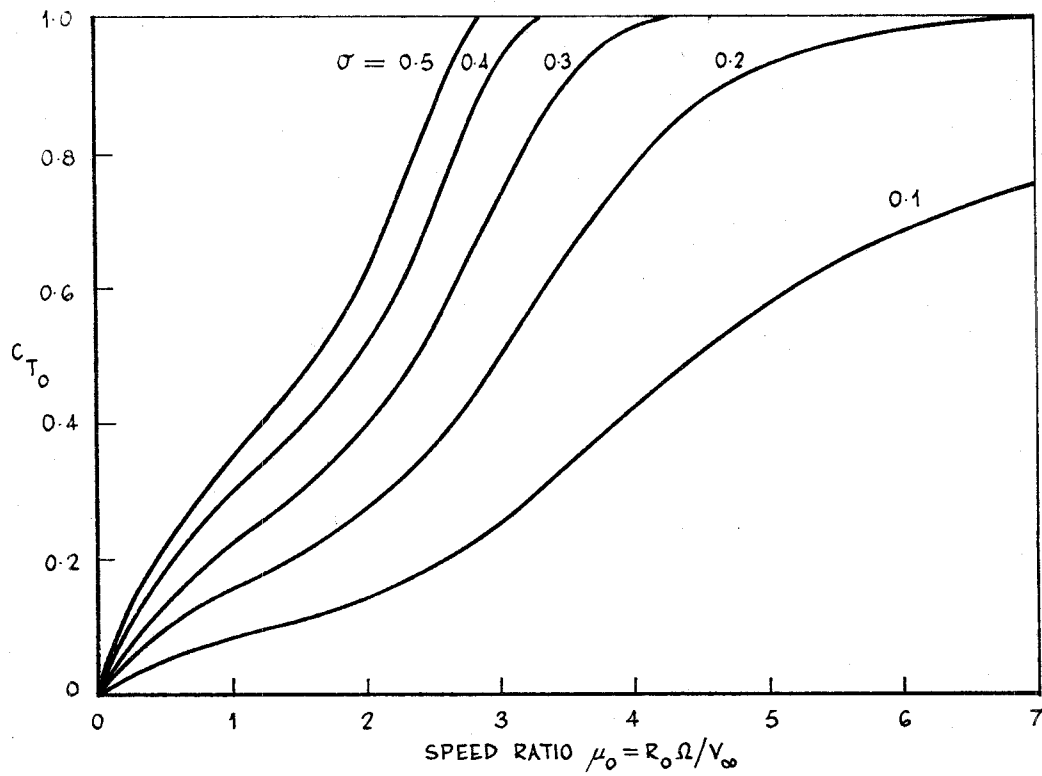
Figure I.7   Variation of thrust coefficient of Darrieus rotor with
solidity and speed ratio
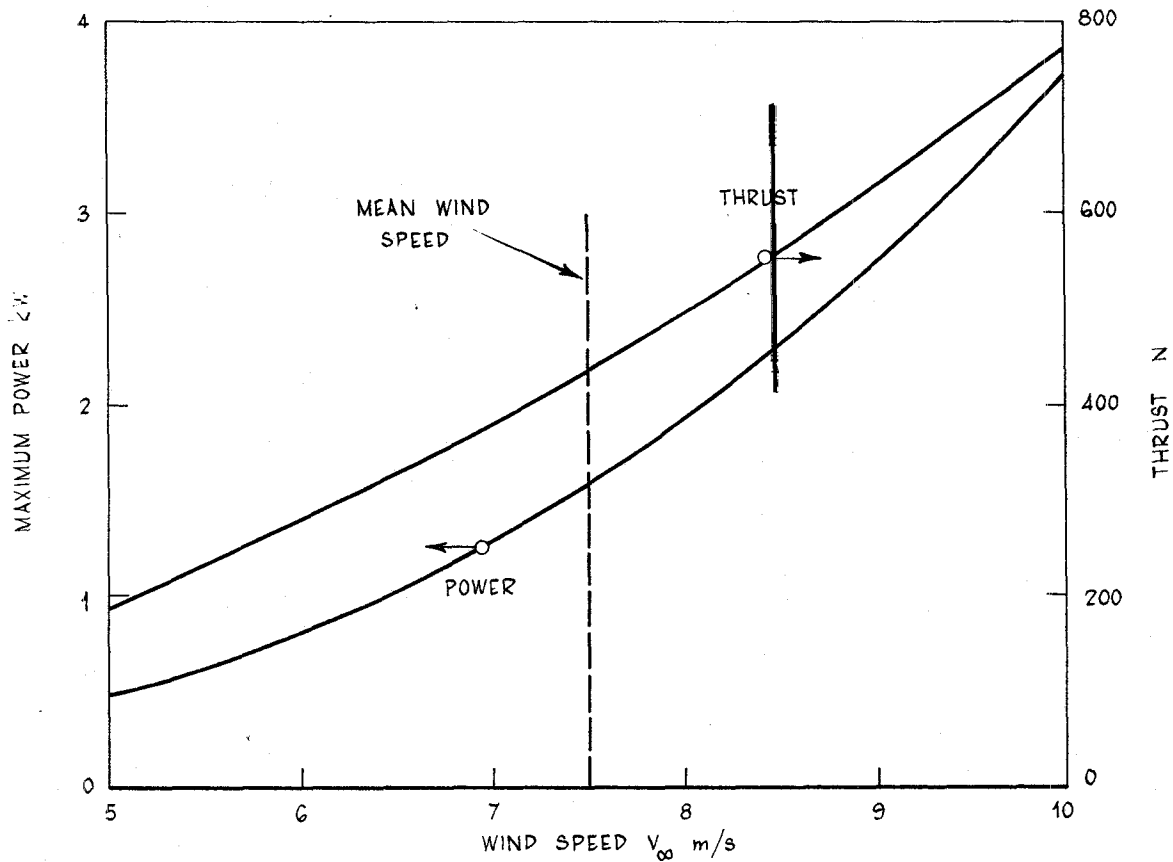
Figure I.8   Maximum power output and corresponding thrust of Darrieus rotor

I.4.2   Unsteady load analysis

In the previous Section the quantities of interest were time-averaged power output, torque and thrust.   For structural design purposes, it is necessary to establish the nature and magnitude of the loads acting on the rotor structure, and a brief outline of the analysis is given here. Defining the normal and tangential forces per unit length of aerofoil at an azimuthal angle ϕ as F_n and F_t respectively, it follows that

$$F_n = \tfrac{1}{2} \rho \, U^2 \, c \, c_n$$

and

$$F_t = \tfrac{1}{2} \rho \, U^2 \, c \, c_t.$$

Now

$$U^2 = V_\infty^2 \left(\frac{U}{V}\right)^2 \left(\frac{V}{V_\infty}\right)^2$$

$$= V_\infty^2 \left(\frac{U}{V}\right)^2 \frac{1}{(1 + \tfrac{1}{4} C'_{T_o})^2}.$$

The total blade forces over the length L_o of the blade at an azimuthal angle ϕ are therefore

$$F_N = \tfrac{1}{2}\,\rho\; V_\infty^2\; c\; c_n L_o \left(\frac{U}{V}\right)^2 \frac{1}{(1 + \tfrac{1}{4}\,C'_{T_o})^2}$$

and

$$F_T = \tfrac{1}{2}\,\rho\; V_\infty^2\; c\; c_t L_o \left(\frac{U}{V}\right)^2 \frac{1}{(1 + \tfrac{1}{4}\,C'_{T_o})^2}.$$

The quantities required to calculate the forces F_N and F_T, namely C'_{T_o}, $\left(\dfrac{U}{V}\right)^2$, c_n and c_t are given in the set of equations (I.4). Since the normal and thrust forces F_N and F_T are of most interest in the structural analysis, typical computed results are given in figures II.4 and II.5 of Appendix II.

The aerodynamic behaviour of a blade can be described in terms of the angle of attack a, the thrust coefficient c_t and the normal force efficient c_n. These quantities are shown in figures I.9 to I.11 for speed ratios μ_o of 3.3, 4.7 and 5.8. The speed ratio of 3.3 represents operation at low power at less than the optimum rotational speed, 4.7 corresponds to maximum power output and the speed ratio of 5.8 represents operation at higher than the optimum speed.

Figure I.9 shows that the angle of attack varies with ϕ in a near-sinusoidal manner, and that large excursions in angle of attack occur at low speed ratios with consequent stalling of the aerofoil. At the highest speed ratio of 5.8, the aerofoil operates over an angle of attack range which is too small to achieve the best overall lift to drag performance.

As a result of the angle of attack variations shown in figure I.9, the thrust coefficient c_t and normal force coefficient c_n vary with azimuthal angle ϕ as shown in figures I.10 and I.11. Figure I.10 shows that the thrust coefficient exhibits two broad peaks per revolution at the higher speed ratios of 4.7 and 5.8, but at the speed ratio of 3.3, four narrow thrust peaks are evident per revolution. This occurs because of stalling of the aerofoil in the range of azimuthal angles for which the angle of attack is excessive. As speed ratio increases, the magnitude of the normal force at any azimuthal angle decreases due to the reduced angle of attack levels, and the shape of the c_n versus ϕ curve becomes near-sinusoidal.

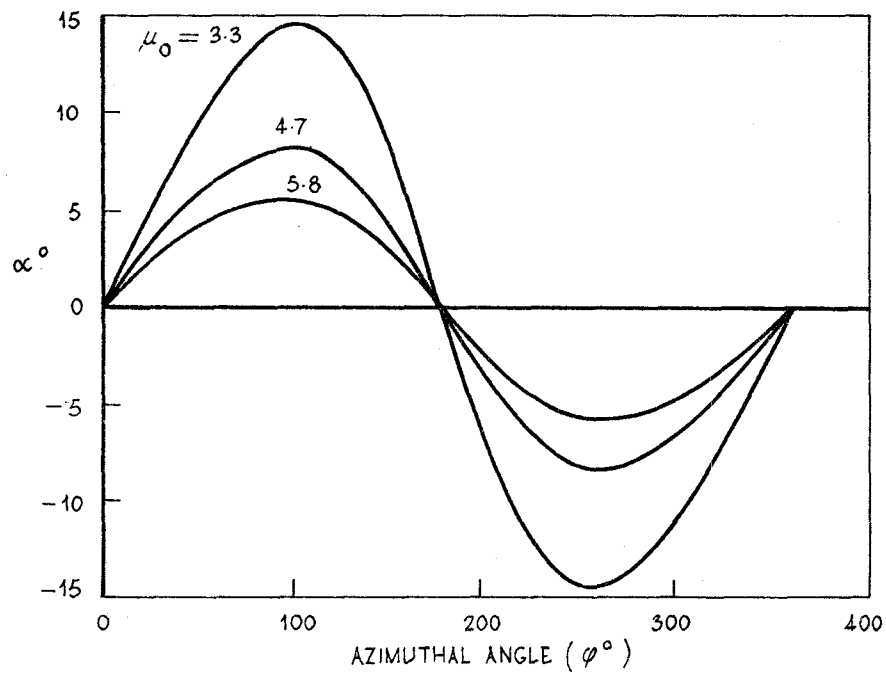Figure I.9   Variation of angle of attack with azimuthal angle and
              speed ratio
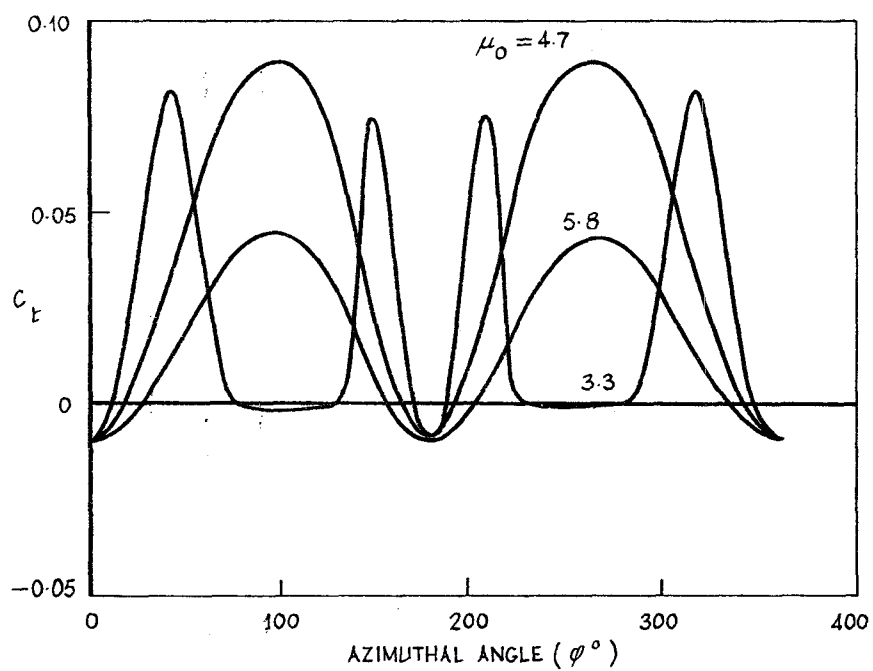

Figure I.10   Variation of blade thrust coefficient with azimuthal
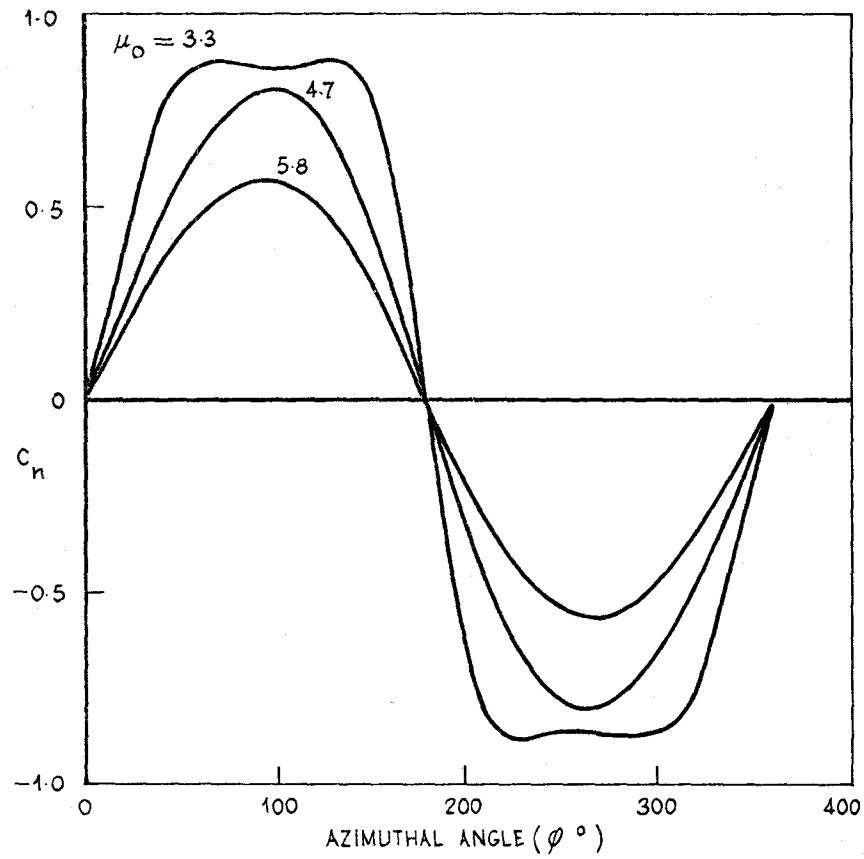   angle and speed ratio

Figure I.11   Variation of blade normal force coefficient with
               azimuthal angle and speed ratio
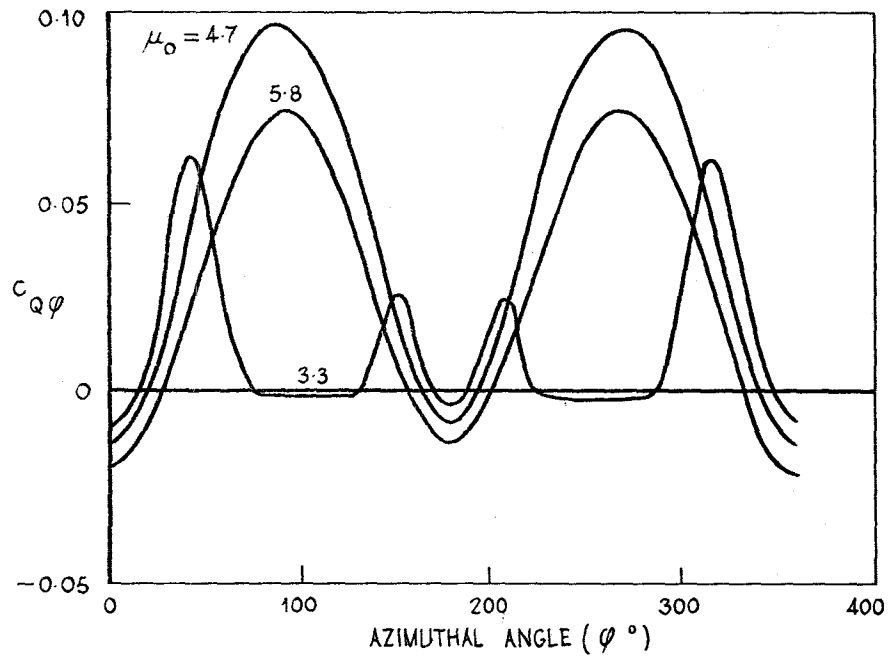
Figure I.12   Variation of blade torque coefficient with azimuthal
               angle and speed ratio

Blade torque and power coefficients are shown as functions of azimuthal
angle for speed ratios of 3.3, 4.7 and 5.8 in figures I.12 and I.13 where

$$C_{Q_\phi} = \frac{\text{torque } (\phi)}{\frac{1}{2} \rho V_\infty^2 A_o R_o}$$

and

$$C_{P_\phi} = \frac{\text{power } (\phi)}{k \frac{1}{2} \rho V_\infty^3 A_o} .$$

The torque and power in these equations are functions of azimuthal angle ϕ,
and apply to a single blade.

At the lowest speed ratio of 3.3 shown, there are four narrow torque and
power pulses on each blade per revolution, and it can be seen in the
figures that this situation will also prevail for two blades with a phase
angle of 180°.   At the higher speed ratios of 4.7 and 5.8, two relatively
broad torque and power pulses occur on each blade per revolution, and for
two blades with a phase angle of 180° the rotor will also experience two
torque and power pulses per revolution.   It is noteworthy that the peak
magnitude of the blade power coefficient namely 0.75 at $\phi = 90^o$ and
$\mu_o = 4.7$ is very nearly the same as the maximum mean power coefficient of
the Darrieus rotor, namely 0.725.   With two blades the peak rotor power
coefficient is 1.5, which is about double the mean value.

Figure I.13   Variation of blade power coefficient with azimuthal
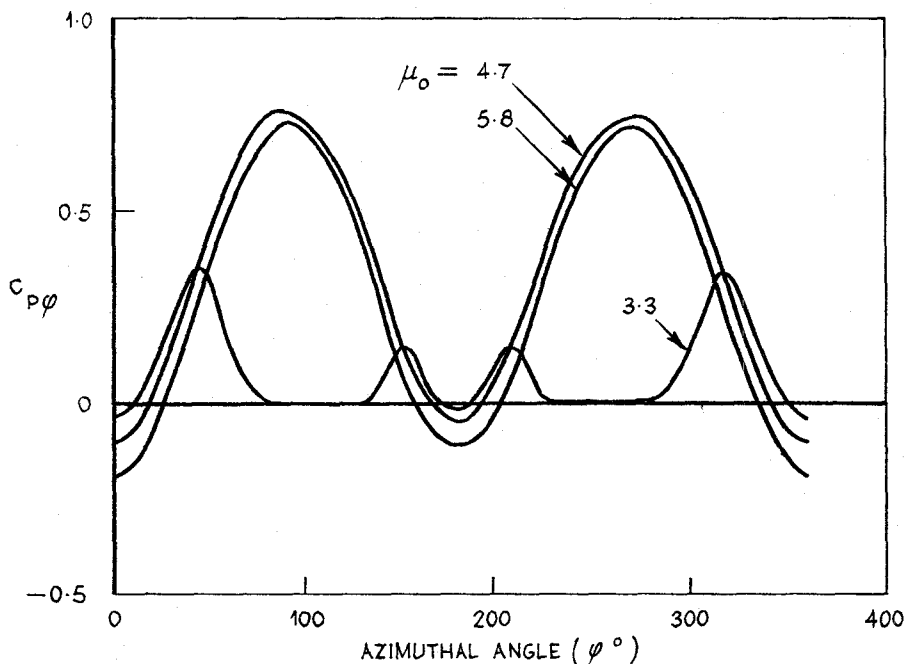   angle and speed ratio

I.5 Savonius rotor

A Savonius rotor is well suited to the task of starting a Darrieus - type
rotor because of its good torque characteristics at zero and low rotational
speeds. A Savonius rotor (figure I.14) is a vertical-axis wind machine
consisting of two semi-circular cylindrical panels which form a rough S in
plan view. The higher drag on the section momentarily concave to the wind
causes the rotor to rotate.

To simplify the structural layout, it was decided that the Savonius rotor
should be located within the horizontal spars of the Darrieus rotor, and so
the height of the rotor is limited to 896 mm. This simple and aesthetic
layout necessarily involves a performance penalty because the downwind
Darrieus rotor blade is blanketed by the Savonius rotor whilst developing
near peak instantaneous power ($\phi = 270^{o}$ in figure I.13). The preferred
aerodynamic layout is to locate the Savonius rotor (or rotors) outside the
vertical aerofoil blade extremities, but this is considered impractical in
terms of the present concept.

The preliminary aerodynamic design criteria adopted for the Savonius rotor
can be summarised as follows:

(a) The unit should provide sufficient starting torque to overcome
     windage and frictional losses and accelerate the Darrieus rotor to a
     speed ratio greater than unity within two minutes at a wind speed of
     7.5 m/s.

(b) To ensure that the unit does not interfere unduly with the flow
     through the Darrieus rotor, the swept area of the Savonius rotor A_s

     should not exceed 10% of the swept area A_o of the Darrieus rotor.

(c) To provide adequate low speed acceleration the unit should produce
     its peak power output at a Darrieus rotor speed ratio μ_o between 2 and

     2.5 and ideally should provide a positive power output over most of
     the operating range of the Darrieus rotor, namely for Darrieus speed
     ratios between 0 and 5.

The characteristics of a number of Savonius rotor designs were investigated
by Newman(ref.8), and on the basis of the power output data presented in
reference 8, the layout shown in figure I.14 was adopted as a suitable design
for the present application. The chosen design is a version of Newman's
rotor IV modified to allow for the relatively large central shaft.

The power coefficient* of Newman's rotor IV corrected for wind tunnel solid
and wake blockage is shown in figure I.15(a). However, Newman states that
magnitude of the tunnel corrections is too large for the results to be
trustworthy, a view which is supported in reference 11. In addition, the
effects of Reynolds number (scale) and length to diameter (aspect) ratio are
not easy to define precisely. In the absence of better data, Newman's
corrected results have been used to predict the characteristics of the
Savonius rotor, allowing for the fact that the Savonius rotor operates in the
induced velocity field of the Darrieus rotor. Conversely, it has been
assumed implicitly in Section I.1 that the induced velocity resulting from
the Savonius rotor has negligible effect on the Darrieus rotor.

---

* The power coefficient used herein incorporates the Betz factor and is
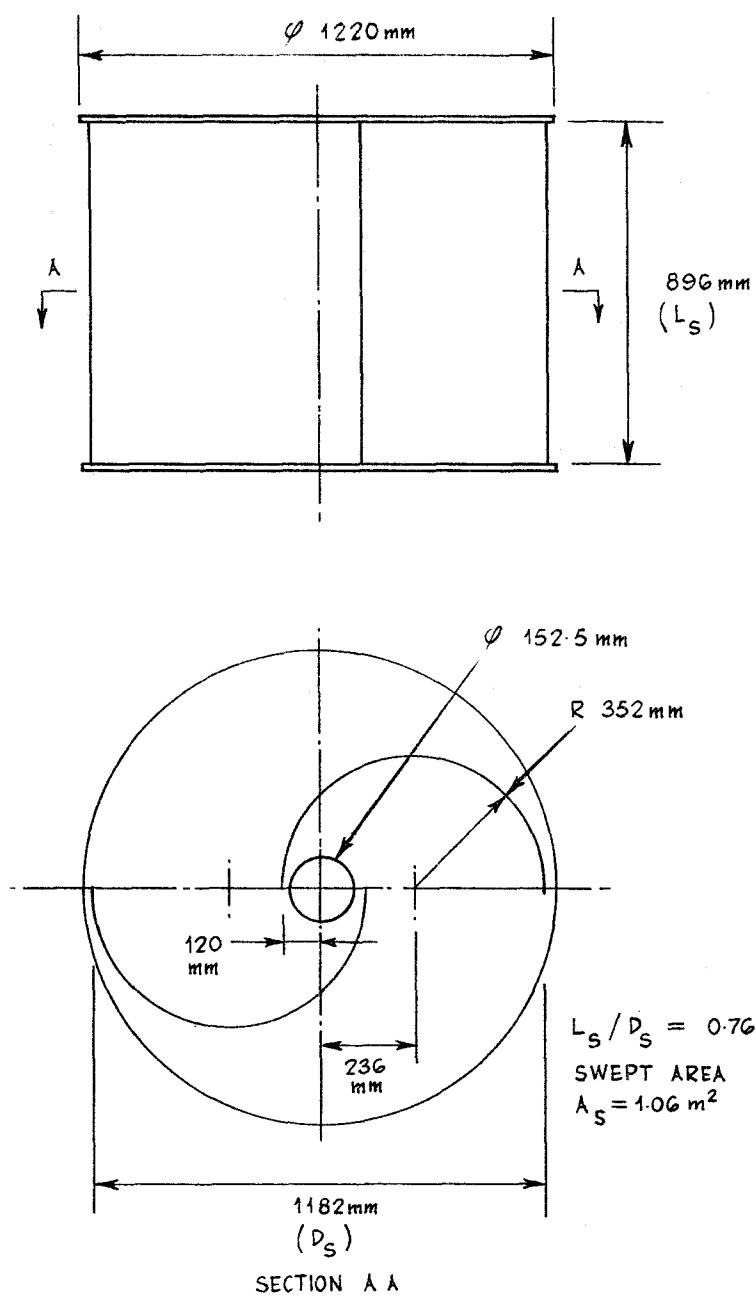 therefore (1/0.593) times the power coefficient used by Newman.
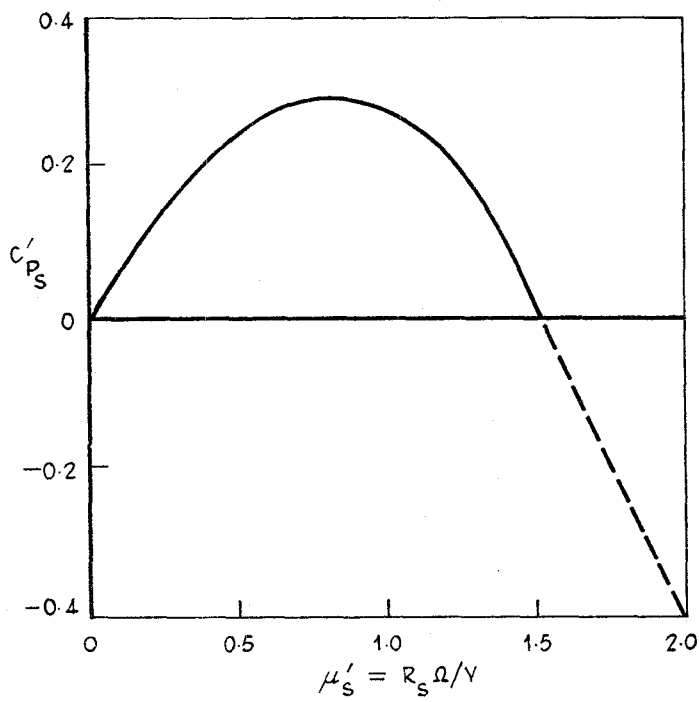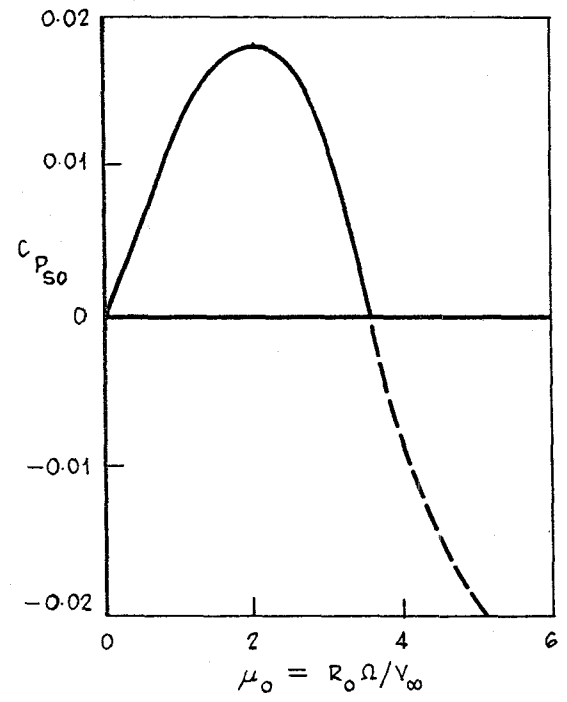
Figure I.14   Diagram of Savonius rotor
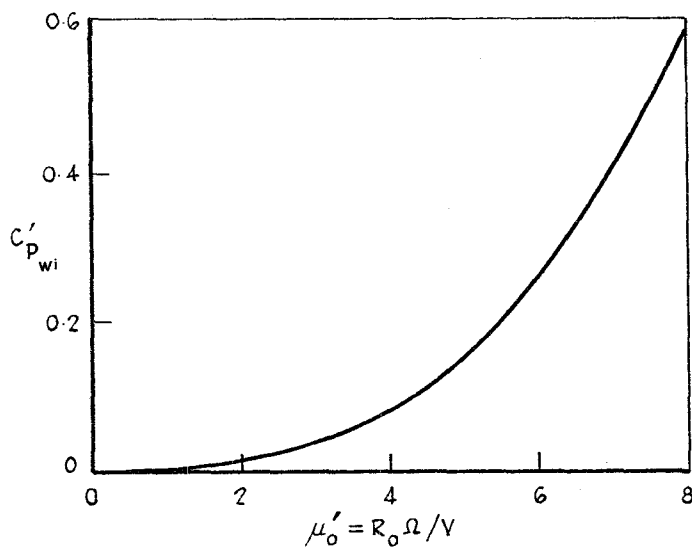
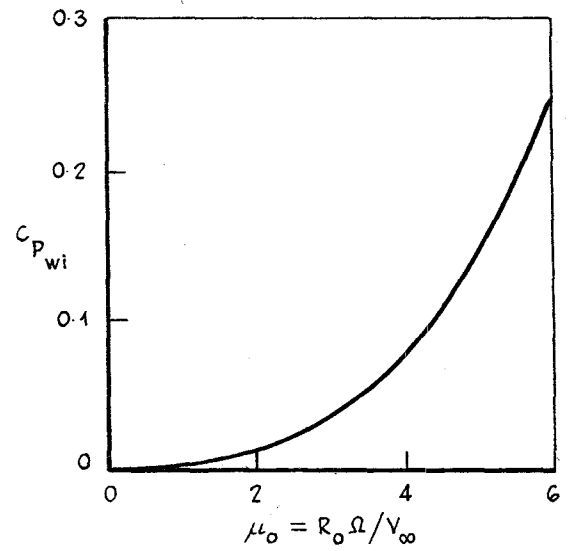(a) Local conditions, free air   (b) Modified

Figure I.15   Power coefficients of Savonius rotor

(a) Local conditions   (b) Modified

Figure I.16   Windage power loss coefficients

Designating the radius of the Savonius rotor as R_s, the local speed ratio μ'_s of the rotor is given by

$$\mu'_s = \frac{R_s \, \Omega}{V},$$

where Ω is the angular velocity and V is the local wind speed.   Defining a speed ratio based on freestream wind speed as $\mu_s = R_s \, \Omega / V_\infty$, it follows that:

$$\mu_s = \mu'_s \left(\frac{V}{V_\infty}\right) = \frac{\mu'_s}{(1 + \tfrac{1}{4} \, C'_{T_o})}, \qquad (I.6)$$

where C'_{T_o} is the local thrust coefficient of the Darrieus rotor.   In addition, the Savonius rotor power coefficient C'_{P_s} which is based on the local wind speed V is given by

$$C'_{P_s} = \frac{\text{power}}{k \, \tfrac{1}{2} \, \rho \, V^3 \, A_s}$$

and the power coefficient C_{P_s} based freestream wind speed is given by

$$C_{P_s} = C'_{P_s} \left(\frac{V}{V_\infty}\right)^3 = \frac{C'_{P_s}}{(1 + \tfrac{1}{4} \, C'_{T_o})^3}$$

From figure I.15(a) the maximum power output of the interference-free Savonius rotor occurs at a speed ratio μ'_s of 0.85.   Arbitrarily matching this condition to a Darrieus rotor speed ratio μ_o of 2.3 for which $V/V_\infty = 0.91$, $\mu_s = 0.85 \times 0.91 = 0.77$ from equation (I.6).   Since $R_s/R_o = \mu_s/\mu_o$, the chosen matching condition gives $R_s = R_o(\mu_s/\mu_o) = R_o/3$, and consequently the radius of the Savonius rotor is one third of the radius of the Darrieus rotor. Choosing a smaller radius of 591 mm, the swept area of the Savonius rotor is 1.06 m^2, which represents 7.9% of the Darrieus rotor area and is therefore within acceptable limits.

The power output of the Savonius rotor becomes negative for $\mu'_s > 1.5$ as shown in figure I.15(a), and this corresponds to a local Darrieus rotor speed ratio μ'_o of 4.5 since the rotor radii are in the approximate ratio 1:3.

According to the Darrieus rotor performance analysis in Section I.4, a value of μ'_o of 4.5 corresponds to a speed ratio μ_o of 3.5 based on freestream wind speed V_∞, and therefore the Savonius rotor absorbs power for $\mu_o > 3.5$.

A modified power coefficient $C_{P_{so}}$ which is based on the Darrieus rotor swept area rather than the Savonius rotor area is shown as a function of μ_o in figure I.15(b).   This power curve is valid only for the particular case of

the Savonius rotor operating in the induced velocity field of the Darrieus rotor.   Negative power coefficient data in the region $\mu'_s > 1.5$ were obtained by linear extrapolation of data based on local conditions.

The absorption of power by the Savonius rotor for $\mu_o > 3.5$ is undesirable but the amount of power absorbed does not appear to be excessive, and indeed the Darrieus rotor may gain some of the power absorbed since the Savonius rotor may act as an impeller, thereby increasing the local wind speed.   The power absorption problem could be eliminated by reducing the Savonius rotor diameter by about 30% but this would reduce the starting torque and low speed power contribution of the Savonius rotor.   Alternatively, an over-running clutch could be used to avoid power absorption by the Savonius rotor.

Since the low speed portion of the Savonius rotor power curve is almost linear, the slope of the curve is equivalent to the mean starting torque Q_s^i, and therefore

$$Q_s^i = \frac{\partial P_s^i}{\partial \Omega} \, ,$$

where

$$\frac{\partial P_s^i}{\partial \Omega} = \frac{\partial C_{P_{so}}^i}{\partial \mu_o} \times k \, \tfrac{1}{2} \rho \, V_\infty^2 A_o R_o \, ,$$

and the superscript 'i' denotes initial or starting conditions, namely, $\Omega = 0$.

Taking $\dfrac{\partial C_{P_{so}}^i}{\partial \mu_o} = 0.013$ from figure I.15(b), the Savonius rotor mean starting torque is 6.5 Nm at a wind speed of 7.5 m/s.   In addition, at very low rotational speeds, the Darrieus rotor contributes a mean torque equivalent to 40% of the Savonius rotor torque.

On the assumptions that wind speed is constant and that the sum of the Savonius and Darrieus rotor torques remains constant for $0 \leqslant \mu_o \leqslant 1$, the time to accelerate the wind turbine to an angular velocity Ω_1, corresponding to $\mu_o = 1$ is given by $t_1 = \Omega_1 / a^i$, where the angular acceleration a^i is given by

$$a^i = \frac{1.4 \, Q_s^i - Q_f}{I} \, ,$$

and Q_f is the average torque required to overcome windage and friction for the period under consideration.   Taking an upper limit of the sum of the friction and windage torques as 5 Nm and the moment of inertia I of the rotating parts as 85 kg m^2, $a_i = 0.048$ rad/s at a wind speed of 7.5 m/s.   A speed ratio μ_o of 1 with $V_\infty = 7.5$ m/s corresponds to an angular velocity of 4.1 rad/s or 39.1 r/min, and the time to accelerate to this rotational speed is 85 s. Therefore the Savonius rotor as designed should accelerate the wind turbine to a speed ratio μ_o greater than unity within the specified time limit of 2 min

at a wind speed of 7.5 m/s.   Operation at this wind speed is consistent with
the nominal power output of 1 kW which is achieved at a rotational speed of
180 r/min.

The minimum wind speed at which rotation can be sustained with the assumed
friction torque is 5.5 m/s.   At wind speeds in excess of this value, the
turbine is expected to start from a stationary condition except for a small
range of rotational attitudes relative to the wind direction at which the
turbine torque will be insufficient to overcome friction.

I.6 Aerodynamic losses

Aerodynamic power losses in the turbine commonly referred to as windage
occur because of the aerodynamic drag of the rotating parts.   The drag of
the Darrieus elements, namely the vertical aerofoil blades, has already been
accounted for in the Darrieus rotor performance analysis.   However, the
turbine concept as shown in figure I.1 includes, in addition, four horizontal
spars 1830 mm long of NACA 0012 aerofoil section, four MacWhyte diagonal tie
rods, and two diagonal wire braces.

The power absorbed by these components has been calculated by considering
only the normal component of velocity relative to the blades and ignoring the
spanwise velocity component.   The drag data used in the computations were
obtained from Hoerner(ref.12) where the Reynolds number is that pertaining
to the local normal velocity occurring at the maximum distance of the
component from the axis of rotation at the design condition.   This approach
is justified because the greater proportion of the power loss occurs at the
outer extremity of each spar, tie rod or brace.   In the computations it has
been assumed that each spar-aerofoil junction is well faired, and that the
interference drag of the junction is represented by an interference factor i_f
of unity.   The interference factor is defined as the length of spar,
expressed as chord lengths, which has the same drag as the interference or
additional drag of the junction.   For a poorly faired junction, Hoerner
suggests that the interference factor may reach as high as 10, which would
result in unacceptable power losses.

The average windage torque acting on a spar or tie rod rotating about a
vertical axis and sweeping out the surface of a disc or cone is given by:

$$Q_w = \frac{1}{2\pi} \, \tfrac{1}{2} \, \rho \, V^2 \, \frac{1}{\cos \beta} \int_0^{2\pi} \int_0^{R_o} c_d \, c \left(\mu_o' \, \frac{r}{R_o} + \cos \phi\right) \left| \mu_o' \, \frac{r}{R_o} + \cos \phi \right| r \, dr \, d\phi$$

where β is the angle of inclination of the component to the horizontal plane
and c_d is the drag coefficient based on the chord or reference dimension c.
Assuming that the drag coefficient c_d is independent of radius, the average
power loss is given by

$$P_w = \frac{1}{2\pi} \, \tfrac{1}{2} \, \rho \, V^2 \, \frac{1}{\cos \beta} \, \Omega \, c_d \, c \int_0^{2\pi} \int_0^{R_o} \left(\mu_o' \, \frac{r}{R_o} + \cos \phi\right) \left| \mu_o' \, \frac{r}{R_o} + \cos \phi \right| r \, dr \, d\phi,$$

which can be integrated for $\mu'_o \geqslant 1$ to give

$$P_w = \tfrac{1}{2} \rho \, V^2 \, \frac{R_o}{4 \cos \beta} \, c_d \, c(\mu'_o \, V)(\mu'^2_o + 1 - \frac{1}{8 \, \mu'^2_o}) \, .$$

A term must be added to account for the interference drag of the spar-aerofoil junction giving the result which again applies for $\mu'_o \geqslant 1$:

$$P_{wi} = \tfrac{1}{2} \rho \, V^2 \, c_d \, c(\mu'_o \, V) \left[\frac{R_o}{4 \cos \beta} (\mu'^2_o + 1 - \frac{1}{8 \, \mu'^2_o}) + i_f c(\mu'^2_o + 0.5) \right] .$$

where i_f is the interference factor. The power loss can be converted to a non-dimensional power loss coefficient as follows:

$$C'_{P_{wi}} = \frac{P_{wi}}{k \, \tfrac{1}{2} \rho \, V^3 \, A_o}$$

$$= \frac{c_d \, c}{k \, A_o} \, \mu'_o \left[\frac{R_o}{4 \cos \beta} (\mu'^2_o + 1 - \frac{1}{8 \, \mu'^2_o}) + i_f \, c(\mu'^2_o + 0.5) \right] \qquad (I.7)$$

where k is the Betz factor.

With the aid of equation (I.7) the power loss coefficient $C_{P'_{wi}}$ which is based on local velocity V has been evaluated for the spars, tie rods and braces the principal dimensions of which together with other pertinent data are given in Table I.2 below.

TABLE I.2   DATA FOR POWER LOSS COMPUTATION

Component	Number of components	Radius in horizontal plane (mm)	Chord or diameter (mm)	Inclination to horizontal (degrees)	c_d	i_f
Main spar, NACA 0012 section	4	1830	180	0	0.010	1
MacWhyte tie rod	4	1830	7.6	28.5	0.10	5
Wire brace	2	1830	1.5	26.1	1.2	5

The results of the power loss computation are shown in figure I.16(a).

By using previously established relationships between μ_o' and μ_o, and between C_p' and C_p, the power loss coefficient $C_{p_{wi}}$ which is based on freestream velocity V_∞ for the rotating parts of the turbine has been computed as a function of the speed ratio μ_o and the result is shown in figure I.16(b).

At the maximum power condition of the Darrieus rotor, namely at a speed ratio μ_o of 4.66, the power loss coefficient $C_{p_{wi}}$ is 0.115. At a wind speed of 7.5 m/s this represents a power loss of 0.25 kW due to windage, that is 16% of the predicted maximum power output of the Darrieus rotor. The four spars contribute 51% to the windage power losses, the four MacWhyte tie rods 23% and the two wire braces 26%. The relatively large losses associated with the small diameter wire braces emphasise the need to minimise the drag coefficient of the rotating parts.

The drag forces on the rotating components will contribute a thrust force on the rotor structure in addition to that imposed by the Darrieus rotor. Because the thrust force arising in this way is likely to be small compared with the Darrieus rotor thrust force, it has been ignored in the design calculations.

I.7 Spoilers

To prevent a Darrieus vertical-axis wind turbine from achieving excessive rotational speeds, some method of controlling the speed within safe limits is required. A properly matched load will achieve the desired result, but an aerodynamic backup system is considered essential in the event of failure of the load system or a breakdown in the power transmission system. A mechanical brake on the turbine shaft is an alternative means of controlling the speed, but the brake would have to be capable of dissipating a large amount of energy as heat on a continuous basis. Therefore, the aerodynamic spoiler concept, wherein spoilers are deployed by centrifugal force, offers an attractive solution to the energy absorption problem.

The spoilers when fully deployed must absorb the full power output of the wind turbine at 250 r/min. From Section 4 in the main body of the report, the maximum power output is 3.7 kW at 250 r/min and wind speed 11.2 m/s. Allowing 20% excess capacity, the spoiler system should therefore be capable of absorbing 4.5 kW at 250 r/min or 26.18 rad/s, equivalent to a torque of 172 Nm. Suppose there are two spoilers, one mounted on each Darrieus aerofoil blade, at a radius of 1830 mm from the axis of rotation as shown in figure I.1. The drag force $F_{d_{sp}}$ on each spoiler is given by

$$F_{d_{sp}} = \tfrac{1}{2}\left(\frac{\text{torque}}{\text{radius}}\right) = \tfrac{1}{2}\left(\frac{172}{1.83}\right) = 47.0 \text{ N.}$$

Assume that the drag coefficient $c_{d_{sp}}$ is based on the mean tangential speed $R_o \Omega$ and on the frontal or projected area of the spoiler in the normal (radial) direction. Designating the spanwise length of the spoiler by l_{sp} and the effective displacement of the trailing edge normal to the aerofoil chordwise axis by h_{sp}:

$$c_{d_{sp}} = \frac{F_{d_{sp}}}{\frac{1}{2}\,\rho\,(R_o\,\Omega\,)^2\,1_{sp}\,\times\,h_{sp}}$$

Substituting for $F_{d_{sp}}$ and $R_o\,\Omega$ corresponding to 250 r/min we find that

$$(c_d\,\times\,1\,\times\,h)_{sp}\ =\ 3.40\,\times\,10^{-2}\ m^2.$$

Using data given in Hoerner(ref.12) as a guide, the drag coefficient of the spoiler is expected to be about unity based on the frontal area of a surface deflected through an angle of 60° or greater. Therefore, the frontal area of each spoiler is given by:

$$(1\,\times\,h)_{sp}\ =\ 3.40\,\times\,10^{-2}\ m^2. \tag{I.8}$$

On the basis that a 75 mm chord trailing edge flap is deployed through 60°, the effective displacement h_{sp} is 75 x sin 60° = 64.95 mm.   The length of the spoiler is obtained from equation (I.8) which gives 1_{sp} = 523 mm.   The basic specification of the spoilers is summarised in Table I.3 below.

TABLE I.3. BASIC SPECIFICATION OF SPOILERS

Number of spoilers	2 (one per blade)
Chord	75 mm
Length	523 mm
Angle of deployment	60°

Flow separation ahead of the deflected spoiler may cause a reduction in drag coefficient below the estimated value of unity, and wind tunnel tests or performance tests on a centrifuge would be required to establish the drag coefficient of the spoilers with certainty.   However, it is believed that the spoilers as designed have ample capacity to absorb excess energy over the operating speed range of the wind turbine.

The design of the centrifugal deployment mechanism for the spoilers is not considered here.   However, preliminary work in this area has shown that it is possible to devise a mechanism which deploys the spoilers to 60° as the rotational speed reaches a specified limit and then retracts the spoilers as the turbine decelerates to a lower speed.   To avoid losses under normal operating conditions, each spoiler should be positively held against a stop in the retracted position so that there is minimal disturbance to the flow over the aerofoil.

APPENDIX II

ROTOR BLADE DESIGN ANALYSIS

The purpose of this paper is to investigate the effect of centrifugal (steady)
and aerodynamic (unsteady) induced loads on the blades for the rotor speed range
0 to 300 r/min and for wind speeds up to 13.5 m/s.

The figure of 13.5 m/s for maximum wind speed for operation is an arbitrary
choice.   In the case of the AEL wind turbine, it coincides with the condition
of maximum power output when turbine speed is constant at 300 r/min.

II.1 Blade section properties

Blade dimensions are shown in figure II.1.   Using the Structural Members
Users Group Ltd program BEAMSTR, reference 13, cross section properties of the
Darrieus rotor blade were computed as follows:

Area of section	845.147 mm^2
Centroid (from leading edge)	90.1 mm
Moment of inertia about chordline	40 300 mm^4
Polar moment of inertia	2 148 620 mm^4
Shear centre (from leading edge)	60.1 mm
Aerodynamic centre (0.25 chord)	45 mm

II.2 Blade material properties

The preferred blade material is extruded aluminium alloy, specification
6061 - T6 with properties:

Yield strength	241 MPa
Ultimate strength	262 MPa
Elongation	8%
Density	2.768 x 10^{-6} kg mm^{-3}

II.3 Blade mass

Blade mass = area x length x density

$\qquad\quad$ = 845.1 x 3660 x 2.768 x 10^{-6}

$\qquad\quad$ = 8.56 kg

II.4 Centrifugal induced loads in blades - steady load

The rotor configuration is shown in figure II.2.   When the rotor is in motion,
the induced normal load in the blade is given by the equation

$$F_b = m R \Omega^2$$

where F_b = total blade force (N)
$\quad\ \ m$ = mass of blade (kg)
$\quad\ \ R$ = rotor radius (m)
$\quad\ \ \Omega$ = angular velocity (rad/s)

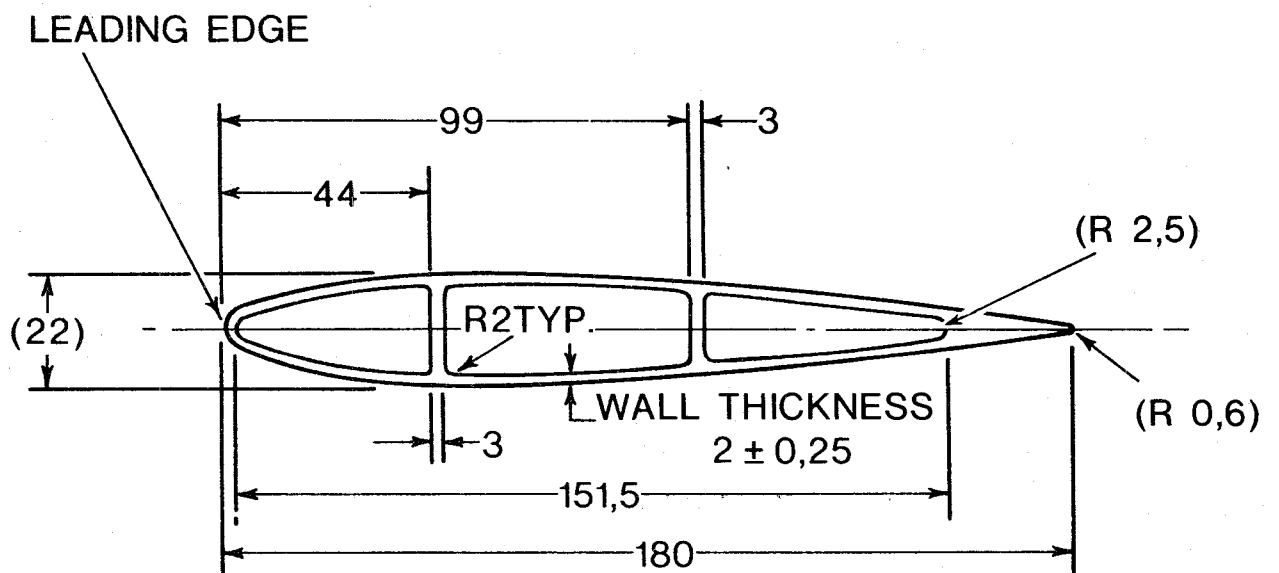Additionally, the tie rods apply an axial load to the blades.

LEADING EDGE

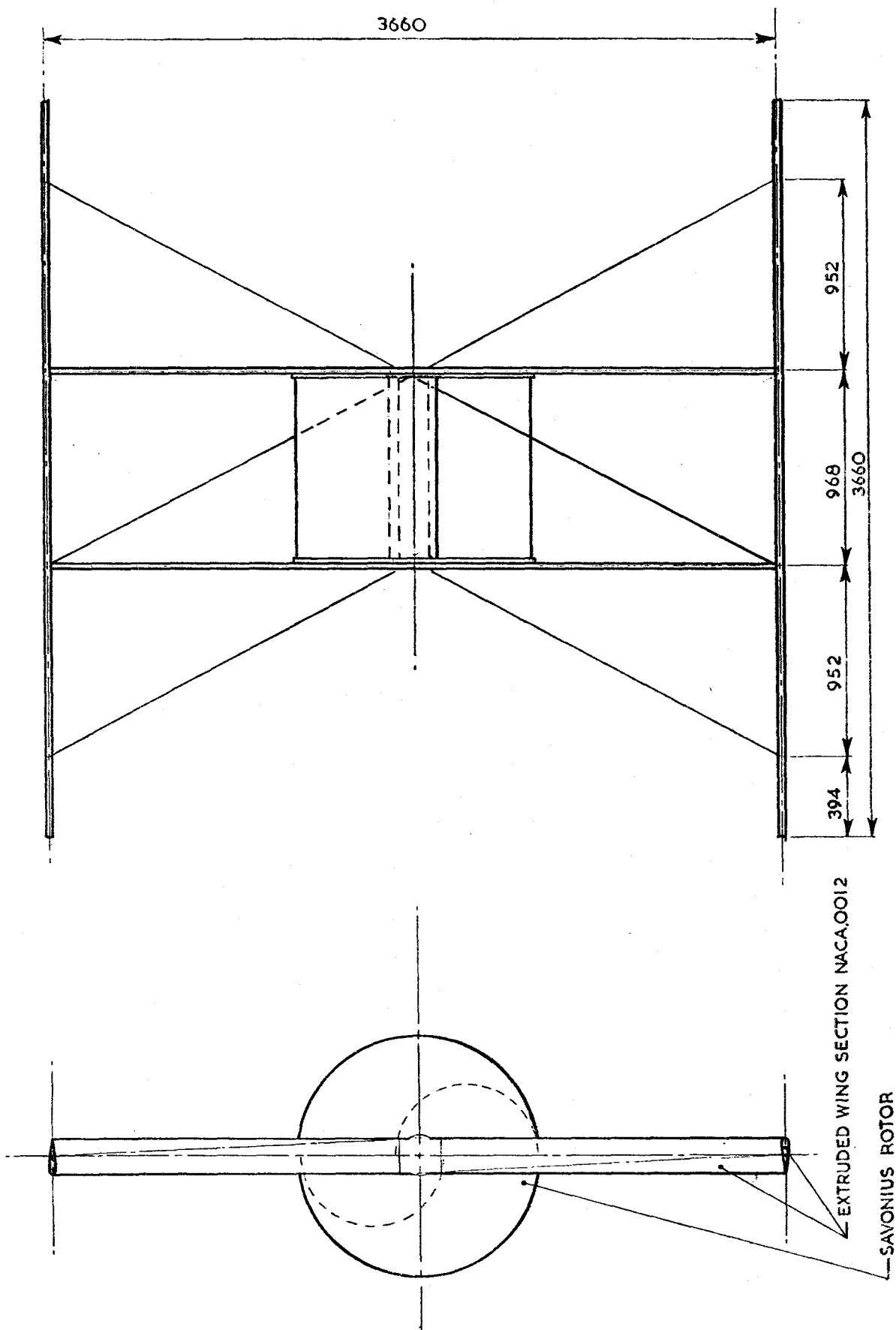Figure II.1 Darrieus rotor blade section

Figure II.2   Turbine structure

Computed values for the centrifugal induced steady load and the corresponding axial load on each blade are shown in Table II.1 for the speed range 0 to 300 r/min.   At an operating speed of 180 r/min the centrifugal load is 5595 N/blade, axial load is 754 N/blade and the induced stress is 32.5 MPa. At 225 r/min the centrifugal load is 8740 N/blade, axial load is 1180 N/blade and the induced stress is 51 MPa.   At 300 r/min, the centrifugal load is 15 540 N/blade, axial load is 2088 N/blade and the resultant induced blade stress is 90 MPa, well within the yield strength figure of 241 MPa.

TABLE II.1   STEADY LOAD/BLADE AND INDUCED STRESS

Rotor speed (r/min)	Centrifugal force (N)	End load (N)	Induced stress (MPa)
100	1727	233	10.0
150	3884	525	22.0
180	5595	754	32.5
225	8740	1180	51.0
250	10790	1455	62.0
270	12580	1694	73.0
300	15540	2088	90.0

II.5 Scale up potential

It has been shown by Feltz(ref.14) that for a linear scale up of all dimensions of the rotor, the blade bending stresses remain unaltered.   In the analysis it is assumed that linear blade velocity is a function of only the wind speed, and that blade skin thickness increases linearly as rotor size increases.

Referring to the various parameters used above and considering the effect of an increase in a characteristic length L.

(a) Moment of inertia about chordline a L^4

(b) Blade mass a L^3

(c) Centrifugal acceleration for a constant linear speed a $\frac{1}{L}$

(d) Blade force a L^2

(e) Maximum moment a L^3

then bending stress, $S_b = \frac{My}{I} = \frac{L^3 \times L}{L^4} = $ unity

ie blade bending stress remains unaltered.

The same considerations are applicable to scale down potential where a practical limit is reached in terms of wall thickness, 1.2 mm being a practical minimum figure.

II.6   Aerodynamic loads on blades - unsteady load

The average torque versus rotor revolutions per minute characteristic for the
rotor shown in figure II.3 was derived in the studies on aerodynamic
performance (Appendix I).   The analysis included the derivation of the
unsteady forces acting on the blades during a full revolution for various
rotor and wind speeds.   Figures II.4 and II.5 show instantaneous torques
and instantaneous normal forces acting on a blade during a full revolution.

Figure II.4 shows how the shape of the instantaneous torque pulse changes as
rotor speed is held constant at 300 r/min and wind speed increases.   The
change in shape from roughly sinusoidal when wind speed is 12.5 m/s to an
irregular pulse at 13.5 m/s wind speed reflects the change in blade speed
ratio from 4.66 to 4.26.   Maximum instantaneous torque/cycle delivered at
13.5 m/s wind speed is 243 Nm.   The instantaneous torque is the product of
the tangential thrust, acting through the blade chord line, and the rotor
radius.   Therefore the tangential force acting on the blade is
$\frac{243}{1.85}$ or 131 N and the resultant bending stress induced in the blade about the
longitudinal axis normal to the chordline is negligible.

Figure II.5 shows the corresponding picture for instantaneous normal forces
acting on the blade.   The force is cyclic, occurring twice in each revolution
of the rotor.   At constant rotational speed, the force increases with wind
speed.

The instantaneous normal force is applied at the aerodynamic centre of the
blade and therefore the torsional shear stress can be calculated using the
Bredt Batho formula

$$\tau = \frac{T}{2\,A_p t}$$

where τ = torsional shear stress (MPa)
      T = torque acting about the shear centre (Nm)
      A_p= enclosed area of blade mean periphery (m^2)
      t = wall thickness of blade (m)

In taking A_p as the enclosed area of the blade mean periphery, ie 2232 mm^2,
as for a single cell structure, the resultant computed stress is conservative.
At a rotor speed of 300 r/min and with a wind speed of 13.5 m/s the maximum
value of the normal instantaneous load is 1280 N, thus:

$$\tau = \frac{1280 \times (60.1 - 45) \times 10^{-3}}{2 \times 2232 \times 2 \times 10^{-9}}$$

$$= 2.2 \times 10^6 \text{ Nm}^{-2}$$
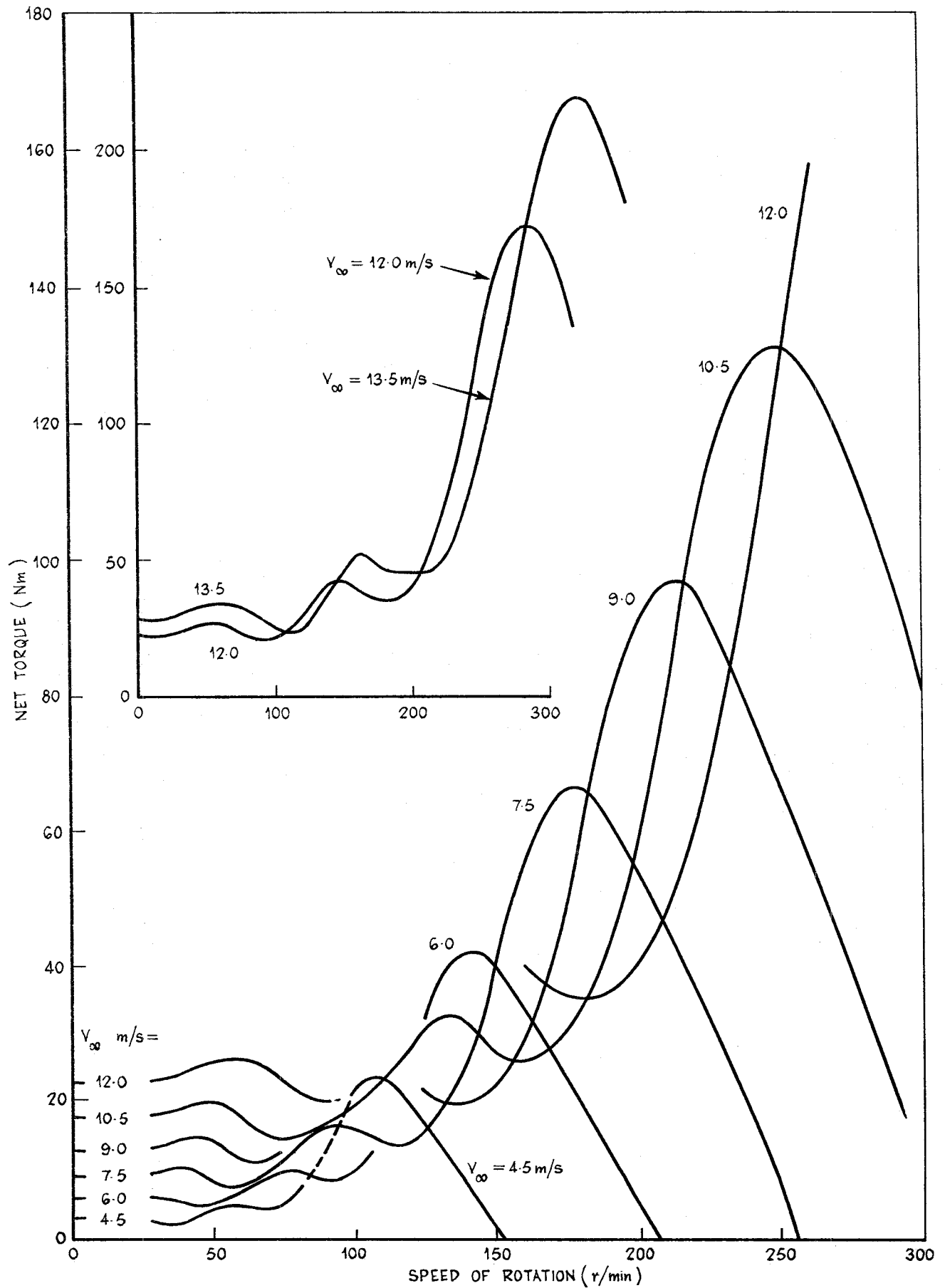
say

$$= 2.0 \text{ MPa}$$

Figure II.3   Variation of net torque of turbine with wind
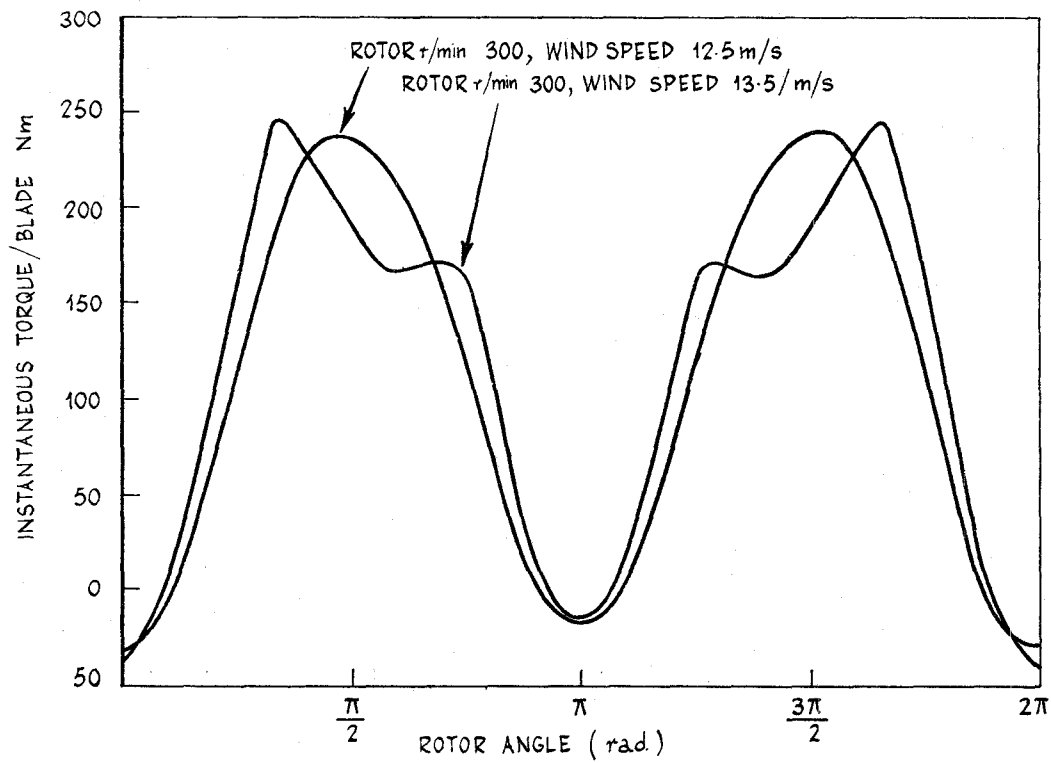speed and speed of rotation

Figure II.4   Variation of instantaneous torque output of a single blade
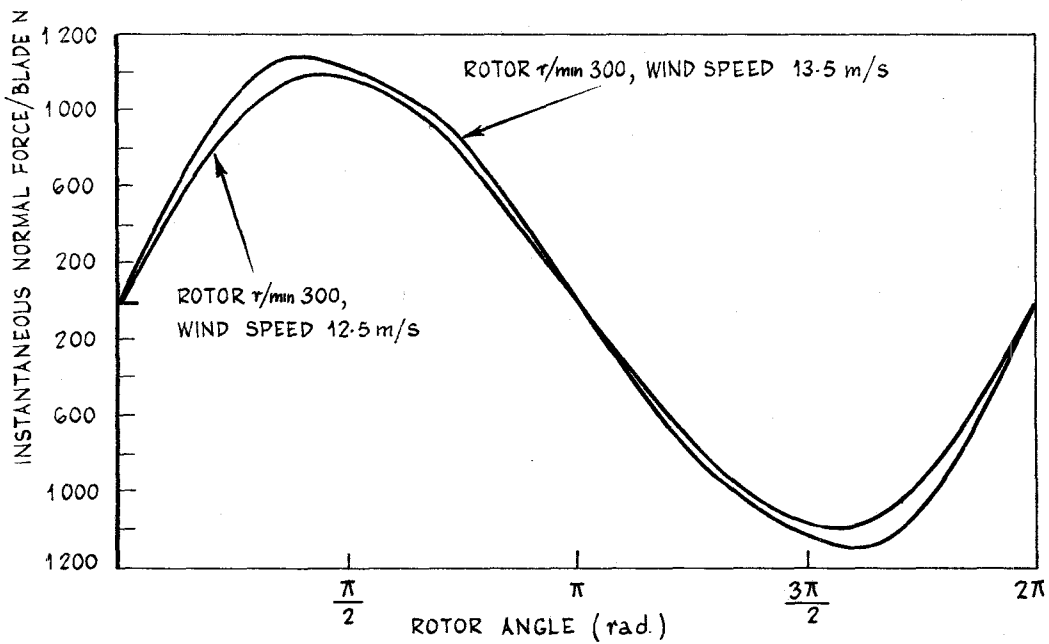with rotor angle and wind speed

Figure II.5   Variation of instantaneous normal force output of a single
blade with rotor angle and wind speed

Provided that the blade torsional natural frequency is maintained above 10 Hz, stresses due to normal aerodynamic load inputs should remain low. The unsteady torsional shear stress level 2.0 MPa is only 2% of the corresponding steady bending stress, 90 MPa (refer Table II.1).

II.7   Blade deflection - steady load

Deflection induced in the blades by centrifugal forces acting at various rotor speeds is shown in figure II.6.   Maximum deflection occurs at the blade tips. At 225 r/min rotor speed, the deflection is 2.5 mm rising towards 5 mm at 300 r/min.
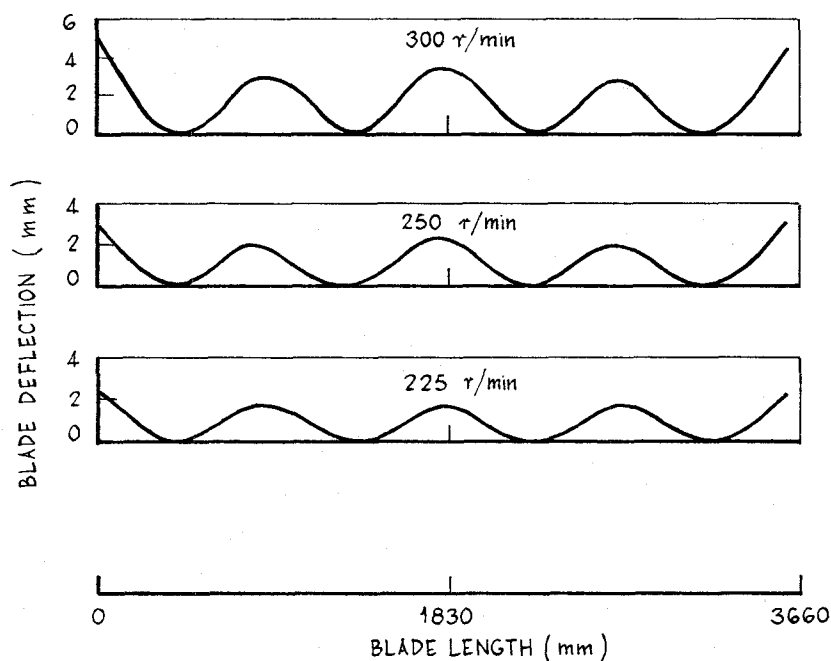

Figure II.6   Variation of blade deflection with rotor speed

II.8   Summary of results

(1)   Centrifugal (steady) induced loads are the major source of stress in the blades.

(2)   Aerodynamic (unsteady) normal induced loads produce torsional shear in the blades.   The stress induced is approximately 2% of the level due to centrifugal effects.

(3)   Aerodynamic (unsteady) torque loads produce negligible stress in the blades.

(4)   The frequency of the aerodynamic (unsteady) normal induced loads is twice the rotor speed.

(5)   The rotor blade is considered safe to operate at 300 r/min.   At this speed the factor of safety on yield point is 2.7.

APPENDIX III

TURBINE MAIN SHAFT DESIGN ANALYSIS

III.1 Introduction

The purpose of this paper is to investigate (i) the effect of loads applied to the turbine main shaft when the wind generator is (a) operational and (b) parked. The paper also includes brief notes on (ii) the main bearing selection and (iii) the emergency hydraulic brake rating.

The various normal operational modes applicable to the turbine have been defined in Section 4, constant speed and variable speed - maximum power.

For the turbine main shaft design analysis, the relevant conditions for each case have been extracted from figures III.1 and III.2:-

(a)   constant speed, for example 250 r/min: maximum mechanical power output 3.7 kW at wind speed 11.2 m/s.

(b)   variable speed - maximum power: maximum mechanical power output is 6.4 kW at wind speed 13.5 m/s. Corresponding shaft torque is 204 Nm.

When parked, the turbine may be subject to wind load effects due to winds up to 42 m/s. This figure was selected as the design limit for survival after examining the following cases(ref.3):-

(a)   wind velocities applicable to southern Australia, for a 50 year return period, in open terrain.   42 m/s

(b)   wind velocities applicable to the whole of Australia for a 25 year return period, allowing for cyclonic areas and assuming that the system is deployed inconspicuously in well wooded terrain.   40 m/s

(c)   wind velocities applicable to the whole of Australia for a 50 year return period with possible cyclone conditions and in open terrain.   63 m/s

Case (c) is considered inconsistent with the need expressed in the design guidelines (Table 1) for a light weight system and therefore the figure of 42 m/s for case (a) which also includes case (b), has been adopted for the study. However, it can be shown by calculation that the turbine blades are capable of surviving case (c) without additional restraint, when the machine is locked in the parked mode.

III.2 Turbine main shaft

(a)   Shaft properties at Section AA (figure III.3).   Cross section properties of the Darrieus rotor main shaft are as follows:

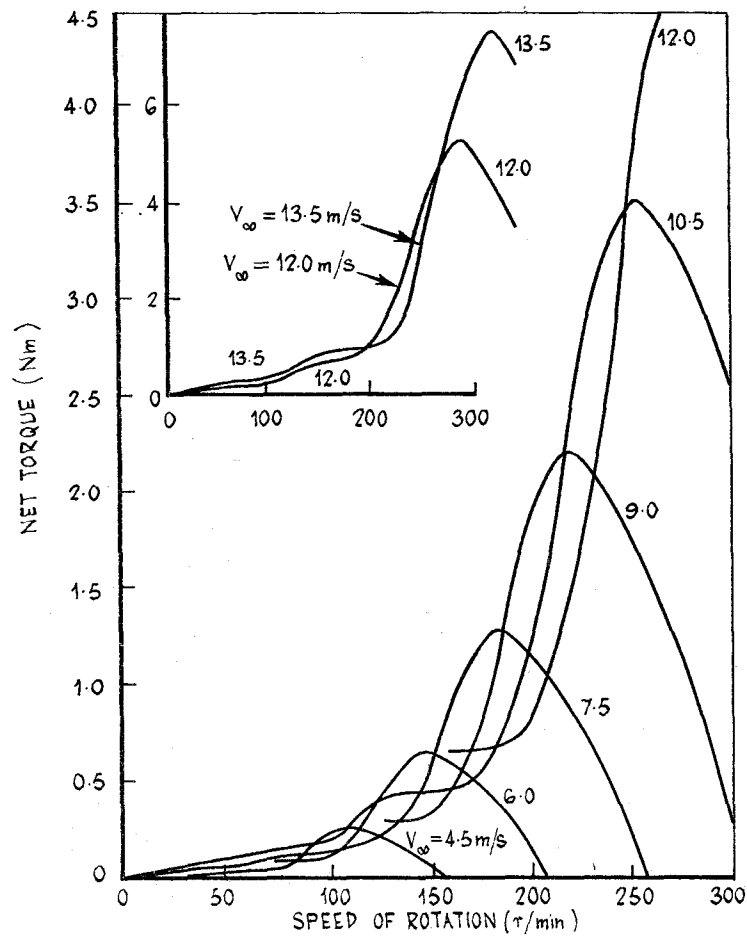|	
Outer diameter of shaft	85 mm
Inner diameter of shaft	50 mm
Area of section	3711 mm^2
Polar modulus of section	106 146 mm^3

Figure III.1   Variation of net power output of turbine with wind speed and speed of rotation
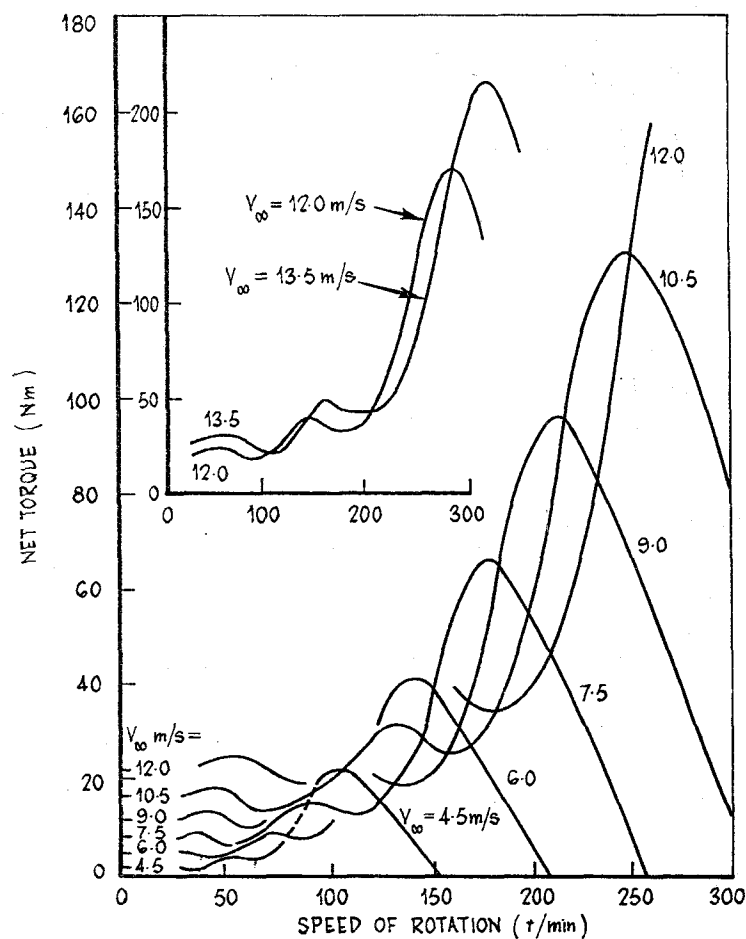

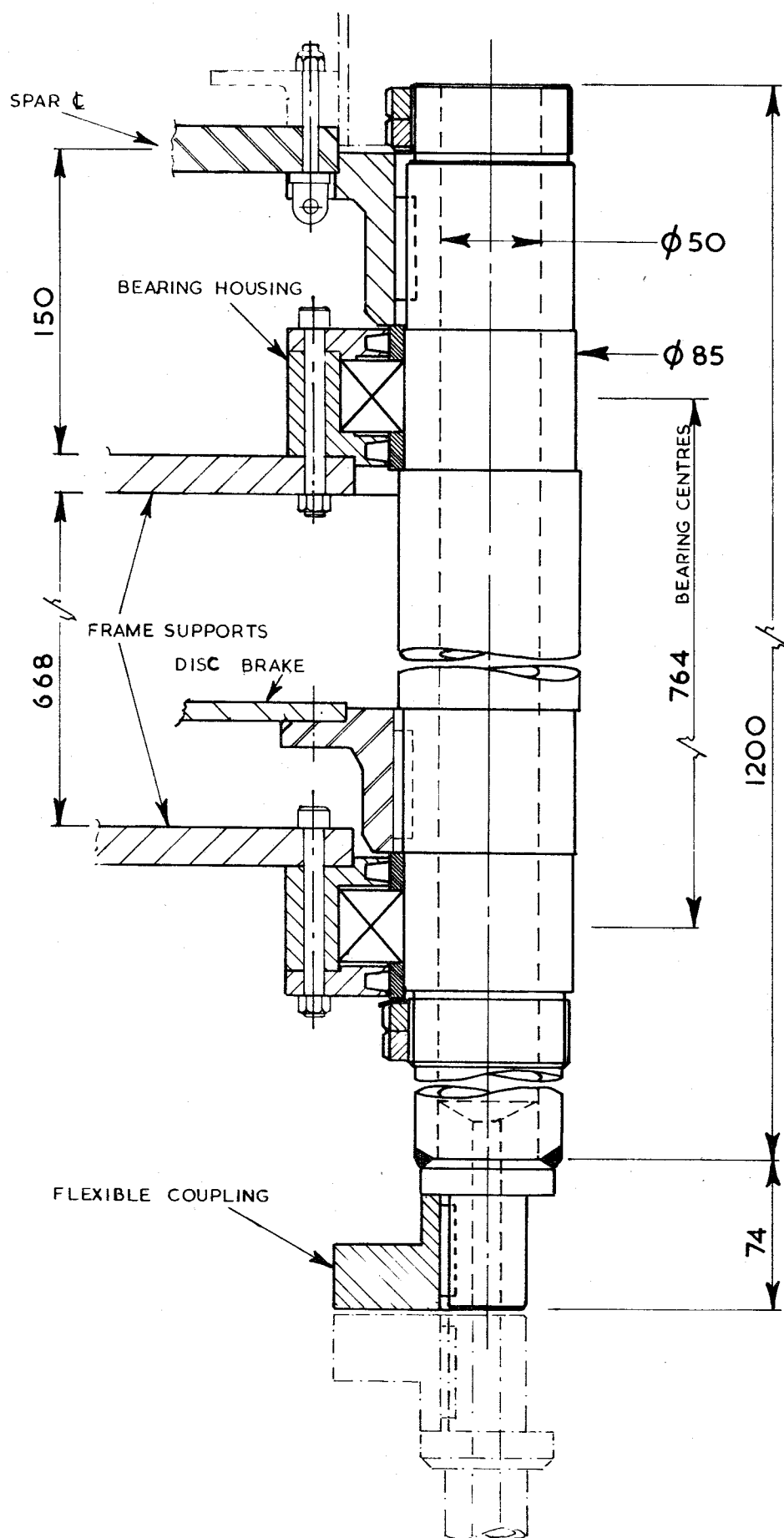Figure III.2   Variation of net torque of turbine with wind speed and speed of rotation

Figure III.3 Turbine main shaft arrangement

(b) Shaft material properties

The preferred material is carbon manganese steel, specification BS 970 120 M 28 with properties:

Yield strength	400 MPa
Ultimate strength	620 MPa
Endurance strength (assume 0.5 ultimate)	310 MPa
Elongation	16%

III.3 Loads on the shaft in the overspeed case at 300 r/min rotor speed

The main shaft is subject to loads comprising (1) a steady axial load due to the mass of the rotor, (2) the unsteady torsional and bending loads generated at the blades by the aerodynamic forces.

The worst case condition is at 300 r/min rotor speed with 13.5 m/s wind speed when the main shaft critical section is subject to the combined loads due to axial force, torque and moment.

The steady axial force = M.g, where

M is the mass of the turbine, 85 kg

(see Section 5), and

g is the gravitational constant, 9.806 ms^{-2}

thus

axial force $= 85 \times 9.806$

$= 833$ N.

Figure III.4 represents the combined instantaneous torque generated by the two rotor blades. The maximum instantaneous torque output occurs at 13.5 m/s and is 518 Nm. The corresponding average torque is 238 Nm. Thus the maximum variation in torque about the average is 518 - 238 = 280 Nm. The torque is cyclic with frequency equal to two cycles per revolution of the rotor.

Figure III.5 shows the instantaneous combined load on the rotor main shaft due to instantaneous normal forces acting on the two blades. At 13.5 m/s wind speed the maximum load on the rotor main shaft due to normal load effects on the blade is 2440 N and the average load is 870 N. Variation on the average is therefore 1570 N. Now the moment arm of this load about the rotor shaft critical section is 0.65 m. Therefore the average moment M_{av} = 870 x 0.65 = 565 Nm and the variable moment M_r = 1570 x 0.65 = 1020 Nm. The bending moment application is cyclic with the combined loads providing two pulses per revolution of the rotor main shaft at all wind speeds.
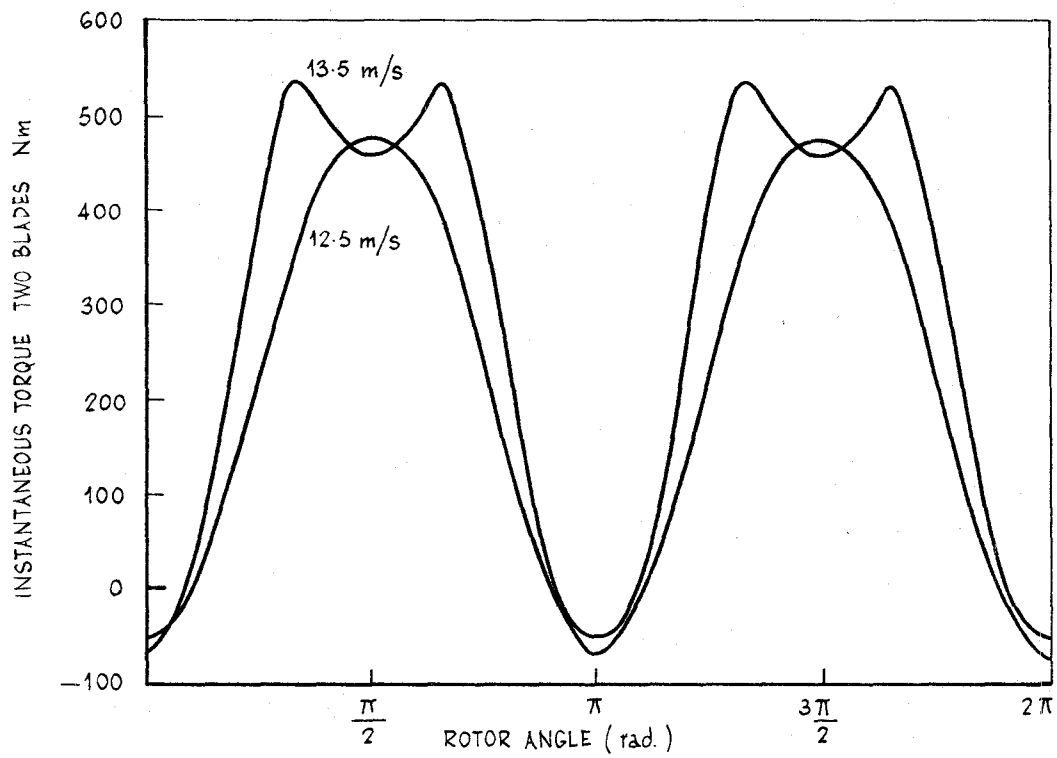
Figure III.4   Variation of combined instantaneous normal force
                 output of two blade rotor with rotor angle and
                 wind speed
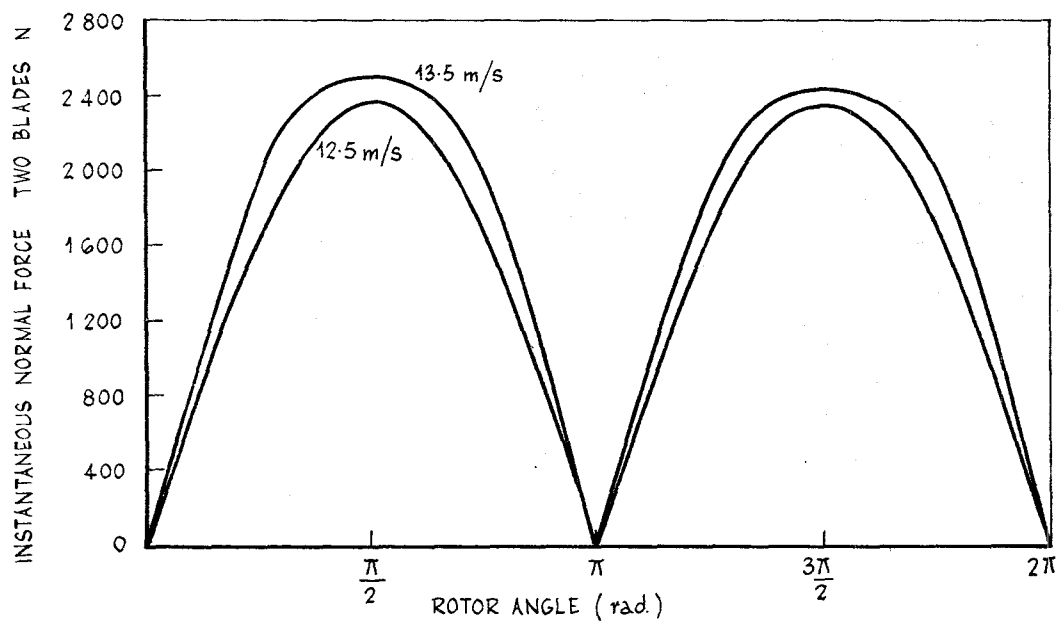

Figure III.5   Variation of combined instantaneous torque output
                 of two blade rotor with rotor angle and wind
                 speed

III.4 Stress analysis - operational condition

For ductile materials with non steady loading in bending, Soderberg's equation applies (ref.15) that is

$$S = S_{av} + K\frac{Syp}{Se} S_r$$

where S = maximum design stress allowable (MPa)

S_{av} = average value of induced stress (MPa)

K = stress concentration factor

Syp = yield stress for material (MPa)

Se = endurance stress for material (MPa)

S_r = variable stress relative to average stress (MPa)

Allowing for the axial load, the normal static stress is then:

$$S = S_{av} + S_{axial\ load} + K\frac{Syp}{Se} S_r.$$

For the unsteady torque load the equivalent static shear stress is:

$$S_s = S_{sav} + Kt \cdot \frac{Syp}{Se} S_{sr}$$

Now the value of maximum shearing stress for static loads is given by

$$S_{s_{max}} = 0.5\frac{Syp}{FS} = \sqrt{\left(\frac{S}{2}\right)^2 + S_s^2}$$

Therefore for the steady axial load and unsteady torsion and bending moment loads and allowing for the hollow section(ref.16)

$$S_{s_{max}} = 0.5\frac{Syp}{FS} = \sqrt{\frac{1}{4}\left[S_{av} + \frac{K\ Syp}{Se} S_r + S_{axial}\right]^2 + \left[S_{av} + \frac{Kt.Syp\ S_{sr}}{Se}\right]^2}$$

or

$$S_{s_{max}} = \frac{16}{\pi\ Do(1-B^4)}\sqrt{\left[M_{av} + K_m\frac{Syp}{Se} M_r + \frac{aFDo(1+B^2)}{8}\right]^2 + \left[T_{av} + \frac{Kt.Syp}{Se} T_r\right]^2}$$

where $S_{s_{max}}$ = maximum allowable static shear stress (MPa)

$$B = \frac{Di}{Do} = \frac{\text{inner diameter}}{\text{outer diameter}} = \frac{50}{85}$$

M_{av} = average bending moment (MPa)   = 565 Nm

K_m = stress concentration factor (bending)   = 1.35

S_{yp} = yield stress for material   = 400 MPa

M_r = variable component of moment   = 1020 MPa

S_e = endurance stress for material   = 310 MPa

$$a = \frac{1}{1 - 0.0044\frac{1}{K}} \qquad\qquad = 1.166$$

where 1 = distance between   = 764 mm
bearing centres

K = radius of gyration   = 23.58 mm
of shaft

F_a = axial force on shaft   = 833 N

T_{av} = average torque   = 235 Nm

K_t = stress concentration factor (torsion)   = 1.35

T_r = variable component of torque   = 280 Nm

$$S_{s_{max}} = \frac{16}{\pi\left(\frac{85}{1000}\right)^3\left(1 - \frac{50}{85}\right)^4}$$

$$\left\{\left[565 + \frac{1.35 \times 400 \times 10^6 \times 1020}{310 \times 10^6} + \frac{1.166 \times 833}{8} \times \frac{85}{1000}\left(1 + \left(\frac{50}{85}\right)^2\right)\right]^2\right.$$

$$\left. + \left[235 + \frac{1.35 \times 400 \times 10^6 \times 280}{310 \times 10^6}\right]^2\right\}^{\frac{1}{2}}$$

$$= 9423 \left[565 + 1776 + 13.88\right]^2 + \left[235 + 487\right]^2 \quad ^{\frac{1}{2}}$$

$$= 23.21 \times 10^6 \text{ Nm}^{-2}$$

$$= 23.21 \text{ MPa}$$

Now allowing for a keyway and reducing the working stress by allowing it to be 90% of the value for a shaft without a keyway:

$$S_{s_{max}} \text{ allowable } = \frac{0.9 \times 0.5 \times Syp}{FS}$$

Therefore

$$FS = \frac{0.9 \times 0.5 \times 400}{23.21}$$

$$= 7.7$$

The factor of safety is greater than 2 and more than adequate.

III.5 Loads on the shaft in the parked condition

For the parked condition the shaft may be subject to an axial force of 833 N as above, due to the mass of the turbine, together with a bending moment of 2035 Nm arising from side load of 3130 N on the turbine structure at a wind speed of 42 m/s.

III.6 Stress analysis - parked condition

Using the ASME formula for the Design of Transmission Shafting(ref.17) for a shaft subject to axial load and bending

$$S = \frac{Km\ M}{Z} + a\ \frac{F_a}{A_s}$$

where S = normal design stress = 0.6 x tensile yield stress.

$$= 0.6 \times 400$$

$$= 240 \quad MPa$$

Km = stress concentration factor = 2

M = moment = 2035 Nm

Z = polar section modulus = 106146 mm^3

a = 1.166

F_a = axial load = 833 N

A_s = area of section = 3711 mm^2

Therefore

$$S = \frac{2 \times 2035 \times 10^3 \times 10^6}{106146} + 1.166 \times \frac{833}{3711}$$

$$= 38.58 \times 10^6 \ Nm^{-2}$$

$$= 39 \ MPa$$

$$\text{Factor of Safety} = \frac{0.9 \times 240}{39}$$

$$= 5.5$$

Again the factor of safety is greater than 2 and more than adequate.

III.7 Rotor main bearing rating

The rotor main bearings are subject to a steady axial load due to the combined mass of the rotor and the shaft sub-assembly and a fluctuating radial load due to cyclic instantaneous normal loads acting on the blades. Installation is arranged so that the top bearing reacts to the axial load plus radial load while the bottom bearing reacts to radial load only.

A self aligning type of bearing was selected to allow for any minor misalignment which might occur in field aseembly or in operation due to structural deformation. The permissable maximum misalignment permitted for spherical roller bearings is 0.5°(ref.18) and this is considered practical for the pedestal design.

Assuming conditions of operation, rotor speed 300 r/min, wind speed 13.5 m/s and choosing a service life for the bearings of 10 years, the dynamic load capacity required based on standard formulae is 44480 N(ref.19).

Now the dynamic capacity of a double row self aligning roller bearing type 22217 HL with dimensions 85 mm ID x 150 mm OD x 36 mm width is 173 000 N and is therefore, in keeping with the rotor main shaft strength, more than adequate.

III.8 Emergency brake rating

The emergency brake operates as a backup to the spoiler speed control system. The brake can also be used for parking.

The maximum design speed of the rotor is 300 r/min so that the brake should be able to stop the system effectively from this speed and overcome any wind applied torques which may be present during the operation.

From rotor performance data in figures III.1 and III.2, the maximum possible torque and power output during braking is as summarised in Table III.1.

TABLE III.1   EMERGENCY BRAKE TORQUE AND POWER REQUIREMENTS

Rotor speed (r/min)	Optimum wind speed (m/s)	Torque (Nm)	Power (kW)
300	13.5	204	6.42
275	12.0	172	5.03
250	10.5	132	3.53
225	10.5	114	2.22
200	9.0	92	2.0

Preliminary measurements made on a YAMAHA 250 standard hydraulic disc caliper assembly indicate that the unit will supply 100 Nm of braking torque with 5 kg applied at the manual control lever.   A set of two disc caliper units is therefore proposed.

The brake would be fitted directly to the rotor main shaft and would be automatically applied at a preset speed.

APPENDIX IV

CONTROL SYSTEM CONCEPT

IV.1 Introduction

The family of turbine torque versus rotational speed characteristics for
various wind speeds is un-nested as shown in figure IV.1.   This means that
the turbine torque does not necessarily increase with an increase in either
rotational speed or wind speed.   To maximise the power output of a system
with un-nested characteristics a closed loop control system is needed.   Such
a system will regulate the load torque applied to the turbine by continuously
modifying the field current of an alternator driven by the turbine so that its
load characteristic is optimally matched to the torque-rotational speed curves
of the turbine for various wind speeds.   The optimal load characteristic is
shown in figure IV.1;   this curve is the locus of the points corresponding to
maximum power on each of the torque-rotational speed curves at constant wind
speed.

IV.2 Load voltage

The control system was designed on the basis of an alternator supplying a
constant voltage load.   Since the proposed load will consist of a bank of
batteries which can have a variable terminal voltage, a shunt regulator is used
to maintain constant load voltage by incrementally by-passing excessive load
current into a current sink as the batteries approach a fully charged condition.

IV.3 Operating modes

Three modes of operation are envisaged for the wind-powered system namely, a
variable speed (maximum power) mode, a constant speed mode and an idle speed
mode.   The intelligence required to activate a particular mode is obtained
by monitoring shaft speed at regular intervals, differentiating the signals
twice to determine acceleration and rate of change of accereration, and
processing the speed and rate information in a selection unit by means of
mathematically devised algorithms.   The result of this signal processing is
to activate one of the three possible operating modes wherein the alternator
field current and hence the load torque applied to the turbine are controlled
throughout the operating range.

IV.4 Variable speed mode

This mode is used in the rotational speed range from zero to the maximum value
specified for the wind-powered system.   Steady state load matching is achieved
by using programmed data on the turbine optimal load characteristic, that is the
load line at locus of maximum power, to provide the information for load
regulation.   The optimal load characteristic data would be measured in
developmental tests of the turbine and stored in a programmable read only
memory (PROM).

IV.5 Constant speed mode

When the turbine achieves the maximum normal operating speed a constant
rotational speed mode is activated.   This will only occur while the wind
speed exceeds the rated value.   In this wind speed range, the load torque is
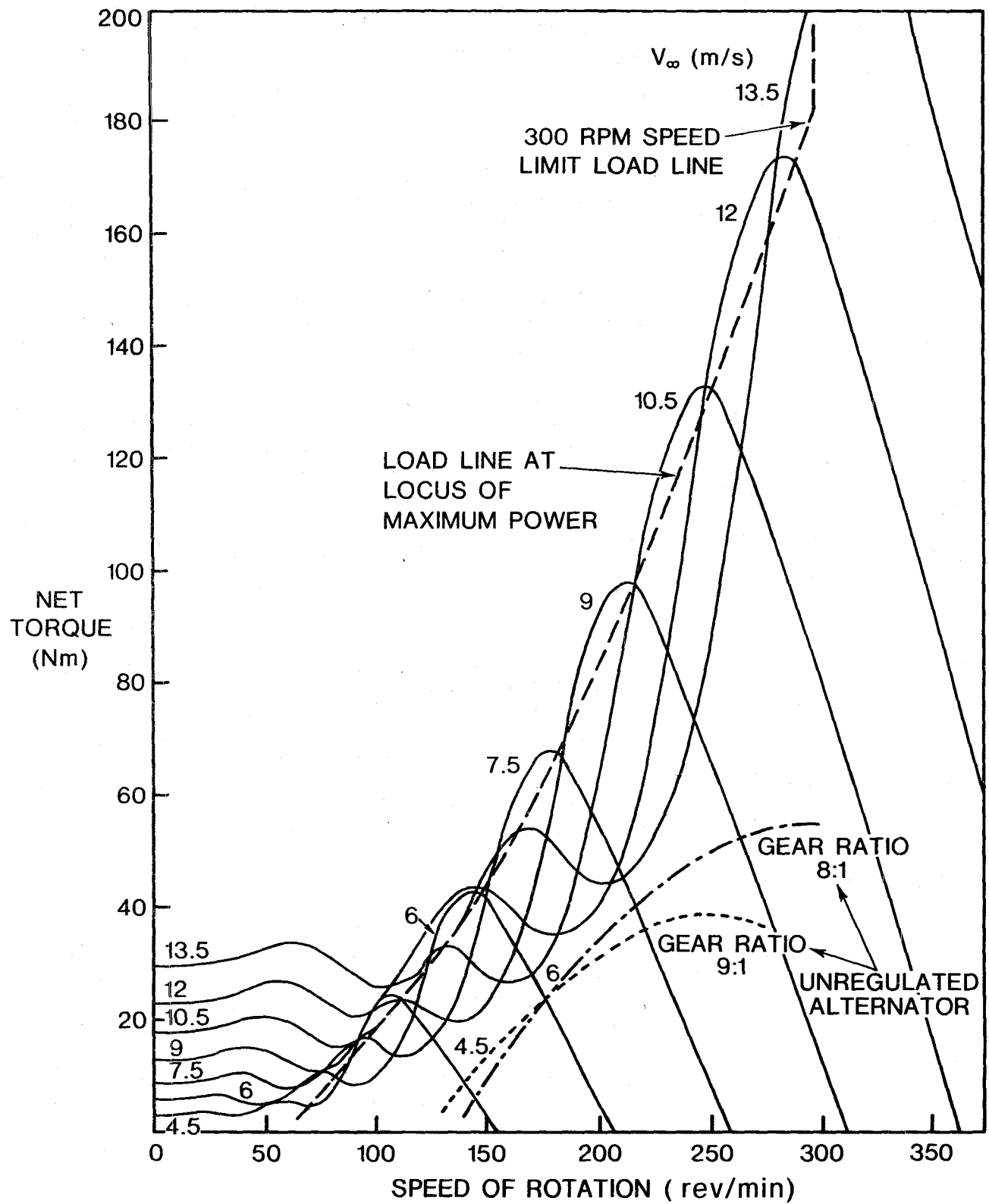automatically regulated so that a constant rotational speed is maintained.

Figure IV.1   AEL wind-powered generator - theoretical curves for
composite Savonius and Darrieus turbine torque -
speed characteristics

Operation in this mode is illustrated in figure IV.2.   Consider an initial operating point P_o at a wind speed Vo;   a change in wind speed to V_1 or V_2 will cause the operating point to shift to a new equilibrium operating point P_1 or P_2 after transients have settled.   If the wind speed continually varies the operating point will shift in a moving equilibrium condition along the path $P_oP_1P_2$.

IV.6 Idle speed mode

If the wind speed exceeds the upper design limit of the system the idle speed mode will be activated for the duration of the excess wind speeds.   Initially an excess load is applied to the turbine to cause the system to decelerate to a low speed.   The idle speed mode is actually a constant speed mode centred about a low shaft speed so as to reduce excessive thrust transients on the rotor blades resulting from excessive wind speeds in conjunction with a high shaft speed.   A dynamic equilibrium is established between load torque and input torque, except that in this region the majority of the input torque results from the Savonius rotor.

Wind speed is determined in the idle mode by monitoring the turbine torque which is implied by the alternator output.   When the wind speed again reduces to a safe level, operation is returned to either the variable speed mode or the constant speed mode.

The cyclic nature of the transfer between the three modes is shown in figure IV.3.

IV.7 Undefined transient behaviour

Consider operation at the maximum power point on a constant wind speed curve shown in figure IV.1.   Let a wind shift occur to the system such that the load torque exceeds the input torque.   This condition can occur due to a positive wind shift or negative wind shift, yet both of these wind shifts will slow down the turbine under constant load.   To achieve reliable operation, it is essential to be able to detect the direction of any wind shift that may occur with respect to the current wind speed acting on the turbine.   This task is performed by the selection unit described in paragraph IV.9.

IV.8 Selection of operating mode

A given operating point can be defined by the intersection of the generator torque-speed curve with the turbine torque-speed curve for a particular wind speed.   A common operating point for two wind speeds V_1 and V_2 is shown in figure IV.4.   The system behaviour during wind transients allows us to determine which of the two wind speeds is applicable at any given time.

The gradient of the torque-speed curve for wind speed V_1 will be negative at the operating point while the gradient for wind speed V_2 will be positive. Therefore, an indication of the direction of a wind speed shift can be deduced by continuously detecting the sign of the gradient of the torque-speed curve of the turbine at the operating point.

As mentioned earlier, there are three possible modes of operation. In the variable speed mode, or a shift to the variable speed mode, $dT/d\Omega$ will always be negative at the operating point. Similarly, in the constant speed mode, or a shift to it, $dT/d\Omega$ will always be positive. The idle mode selection depends more on torque levels rather than on gradients and hence is not concerned with torque gradient fluctuations. Detection of the sign of the torque gradient permits activation of the correct mode to ensure reliable and efficient operation of the wind turbine.

IV.9 Operating mode selection unit

Shaft speed samples (Ω) are monitored at pre-determined time intervals and referenced to a particular time t_o that advances at preset intervals.

Angular acceleration (a) and the rate of change of angular acceleration da/dt are computed and their signs are recorded with respect to values observed at t_o. By determining shaft speed with respect to a reference speed Ω ref at t_o and the signs of a and da/dt due to a step wind speed shift, the sign of the torque gradient induced by the new wind speed can be deduced and therefore the correct mode of operation can be activated.

A truth table can be drawn up that shows all possible conditions that may occur and the corresponding mode that should be activated (see Table IV.1). A '1' indicates a positive sign and a '0' indicates a negative sign for the variables ($\Omega - \Omega_{ref}$), a and da/dt.

TABLE IV.1 SWITCHING LOGIC USED IN SELECTION UNIT

$\Omega - \Omega_{ref}$	a	da/dt	Variable speed mode	Constant speed mode	$dT/d\Omega$
0	0	0		1	+ve
0	0	1	1		-ve
0	1	0	1		-ve
0	1	1	1		-ve
1	0	0		1	+ve
1	0	1	1		-ve
1	1	0	1		-ve
1	1	1		1	+ve

The sign of $dT/d\Omega$ shown above is that which occurs at the old operating point following the wind shift.

After a wind speed shift the initial value of $dT/d\Omega$ need not necessarily agree with the final value at the new operating point. This condition does occur for one particular case. It does not, however, have any ill effect on the selection logic which takes into account the possibility of such a situation occurring. The correct mode will still be activated.
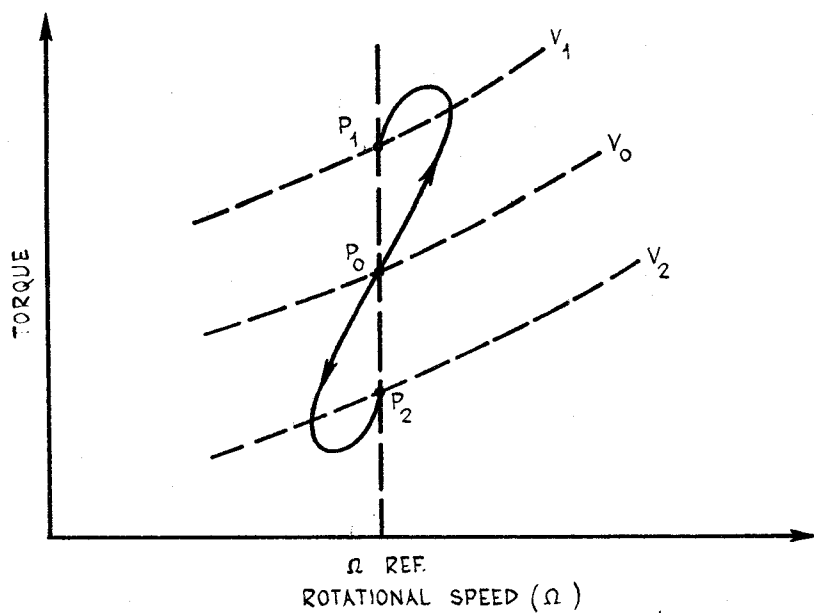
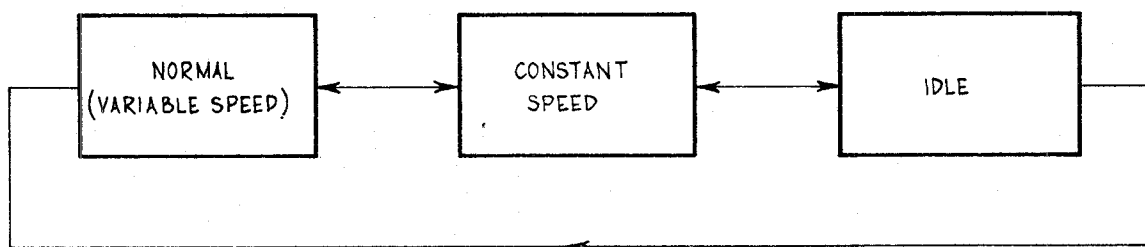Figure IV.2   Transient operating point track

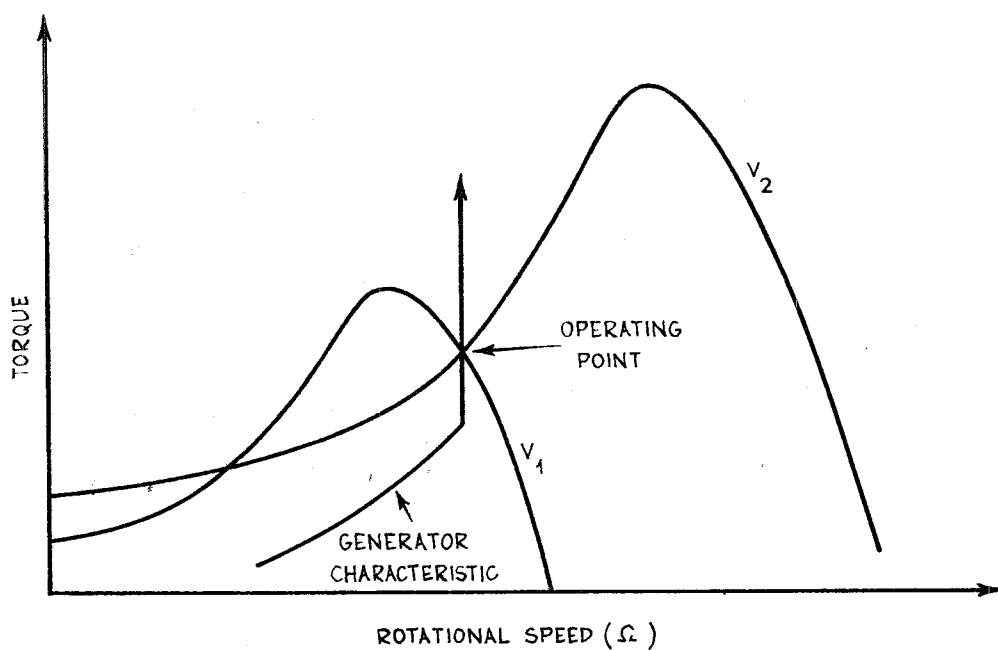Figure IV.3   Alternative operating modes

Figure IV.4   Common operating point for two wind speeds

The results shown in Table IV.1 have been justified by mathematical analysis. However, the lengthy nature of the analysis just not warrant its inclusion in this report.

IV.10 Summary remarks

IV.10.1 Use of anemometer

The use of an anemometer would simplify the amount of calculation required but it is not recommended due to the extra cost and the problems associated with isolating it from the interactive effects of the turbine. The current state of the art of electronic hardware allows the inherent characteristics of the turbine to be used for automatically controlling the system for optimum results at all wind speeds.

IV.10.2 Dissipation of excess power

Too methods of dissipating excess power from the wind turbine, when the output exceeds battery charging requirements, are available:

(a) Reduce the turbine output by means of spoilers. This allows the shaft speed to increase to the maximum allowable value and the torque is then regulated by the spoilers.

(b) Dissipate the excess power into an electrical load. This will regulate the turbine speed but requires an alternator of adequate capacity.

Both avenues are currently being investigated but for initial operations proposal (b) is being pursued.

IV.10.3 Control system

The overall control system is a closed loop multiple feed-back path system. Figure IV.5 shows a block diagram version of the main functions involved. The logical and decision making functions of the control system are carried out by a microprocessor. This minimises the hardware content of the system and provides maximum flexibility for optimisation to loads with various torque-speed characteristics.
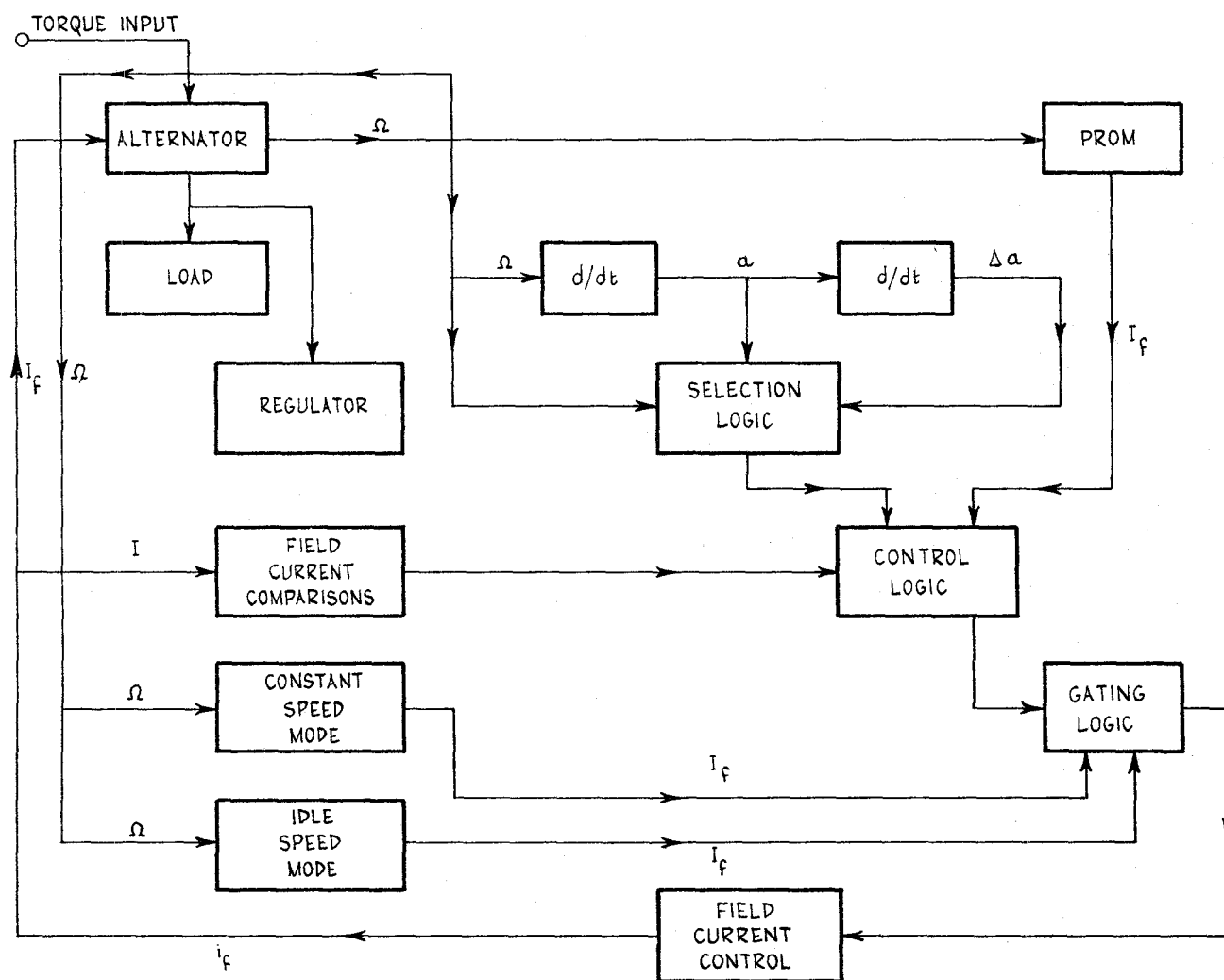
Figure IV.5   Control block diagram

DOCUMENT CONTROL DATA SHEET

Security classification of this page   UNCLASSIFIED

1	DOCUMENT NUMBERS	2	SECURITY CLASSIFICATION
AR Number: AR-001-672		a. Complete Document: Unclassified	
Series Number: AEL-0039-TR		b. Title in Isolation: Unclassified	
Other Numbers:		c. Summary in Isolation: Unclassified	

3	TITLE
	FEASIBILITY STUDY ON A LOW POWER VERTICAL AXIS WIND-POWERED GENERATOR

4	PERSONAL AUTHOR(S):	5	DOCUMENT DATE:
	W.R. Crook, T. Puust, M.L. Robinson and L.J. Vencel		September 1980
		6	6.1 TOTAL NUMBER OF PAGES 94
			6.2 NUMBER OF REFERENCES: 19

7	7.1 CORPORATE AUTHOR(S):	8	REFERENCE NUMBERS
	Advanced Engineering Laboratory		a. Task: DST/212
			b. Sponsoring Agency:
	7.2 DOCUMENT SERIES AND NUMBER Advanced Engineering Laboratory 0039-TR	9	COST CODE:

10	IMPRINT (Publishing organisation)	11	COMPUTER PROGRAM(S) (Title(s) and language(s))
	Defence Research Centre Salisbury		

12	RELEASE LIMITATIONS (of the document):
	Approved for Public Release

Security classification of this page: UNCLASSIFIED

13 | ANNOUNCEMENT LIMITATIONS (of the information on these pages):

No limitation

14 | DESCRIPTORS:

a. EJC Thesaurus
   Terms

Electric power generation
Wind power generation
Feasibility

b. Non-Thesaurus
   Terms

15 | COSATI CODES:

1001

16 | SUMMARY OR ABSTRACT:
   (if this is security classified, the announcement of this report will be similarly classified)

This paper describes investigations carried out to establish a design concept for a 1 kW wind-powered generator suitable for use as an alternative power source in isolated locations. Design criteria include high power to weight ratio, simplicity of assembly and potential for fixed, mobile or portable applications. The report proposes a suitable configuration using a Darrieus straight blade rotor with a microprocessor based control system and provides information on the power output to be expected in different wind environments.